Murine transfusion-related acute lung injury caused by anti-CD36 antibodies: mechanism and intervention

Dawei Chen

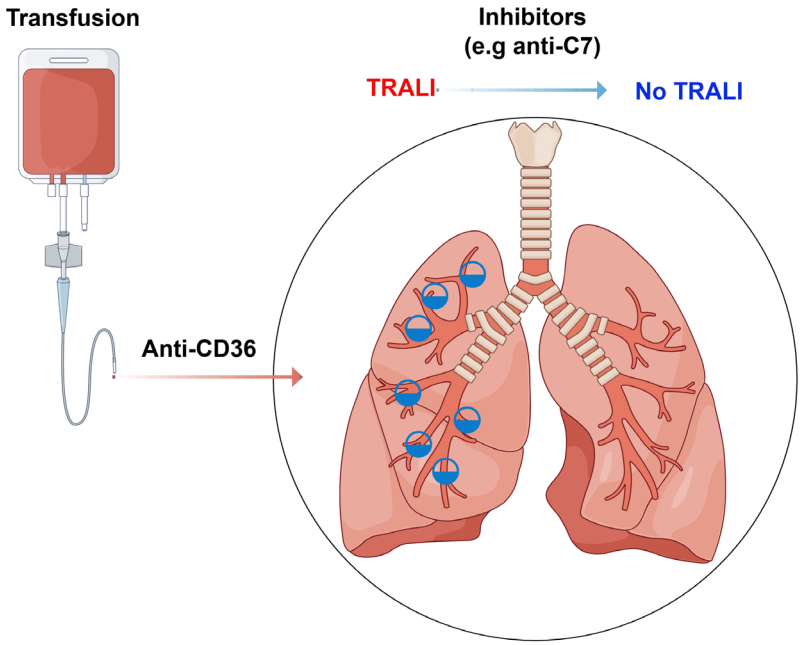

Aus dem Fachbereich Medizin der Justus-Liebig-Universität Gießen

Institut für Klinische Immunologie, Transfusionsmedizin und Hämostaseologie

Murine transfusion-related acute lung injury caused by anti-CD36 antibodies: mechanism and intervention

Dawei Chen

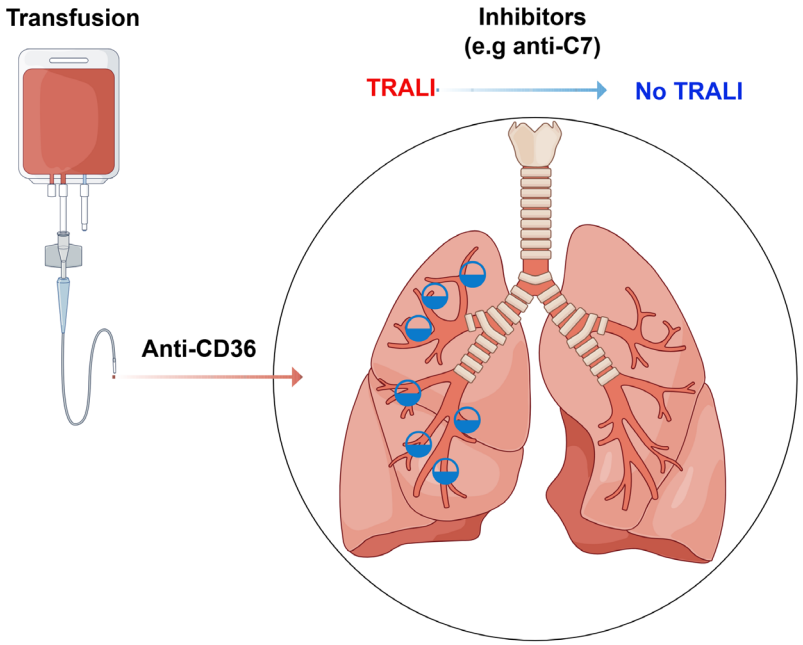

Aus dem Fachbereich Medizin der Justus-Liebig-Universität Gießen

Institut für Klinische Immunologie, Transfusionsmedizin und Hämostaseologie

Murine transfusion-related acute lung injury caused by anti-CD36 antibodies: mechanism and intervention

Inauguraldissertation

zur Erlangung des Grades eines Doktors der Humanbiologie

des Fachbereichs Medizin

der Justus-Liebig-Universität Gießen

vorgelegt von Chen, Dawei aus

Henan, China

Aus dem Fachbereich Medizin der Justus-Liebig-Universität Gießen

Institut für Klinische Immunologie, Transfusionsmedizin und

Hämostaseologie

Gutachter/in: Prof. Dr. Gregor Bein

Gutachter/in: Prof. Dr. Serge Adnot

Tag der Disputation: 2026-01-15

Gießen 2026

Table of Contents

List of Abbreviations

AABB	American Association of Blood Banks
ALI	Acute lung injury
ANOVA	Analysis of variance
APS	Ammonium persulfate
ARDS	Acute respiratory distress syndrome
ATCC	American Type Culture Collection
BALF	Bronchoalveolar lavage fluid
BSA	Bovine serum albumin
°C	Degree Celsius
C1q	Complement 1q
C5a	Complement component 5a
C5L2	C5-like receptor 2
C5aR	C5a receptor
CCC	Canadian Consensus Conference
CCL-4	Chemokine (C-C motif) ligand 4
CCL7	Chemokine (C-C motif) ligand 7
CCL21	Chemokine (C-C motif) ligand 21
cDNA	Complementary DNA
CD11b	Cluster of Differentiation 11b
CD14	Cluster of Differentiation 14
CD16	Cluster of Differentiation 16
CD32	Cluster of Differentiation 32
CD36	Cluster of Differentiation 36
CD45	Cluster of Differentiation 45
CD88	Cluster of Differentiation 88
CD115	Cluster of Differentiation 115
COX	Cyclooxygenases
CP	Classical pathway
CSF-1	Colony-stimulating factor 1

CXCL1	C-X-C Motif Chemokine Ligand 1
CXCL2	C-X-C Motif Chemokine Ligand 2
DC	Dendritic cells
DAPI	4', 6'-diamino-2-phenylindole
DHT	Dihydrotestosterone
DMEM	Dulbecco's Modified Eagle's medium
DNA	Deoxyribonucleic acid
DNase	Deoxyribonuclease
dNTPs	2'-deoxynucleoside-5'-triphosphate
DTT	Dithiothreitol
ECL	Chemiluminescence
EDTA	Ethylene diamine tetraacetic acid
EDS	Ethane dimethane sulphonate
ELISA	Enzyme-linked Immunosorbent Assay
EVs	Extracellular vesicles
FCS	Fetal calf serum
FDA	Food and Drug Administration
FFP	Fresh Frozen Plasma
FiO_2	Fraction of inspired oxygen
FNAIT	Fetal/neonatal alloimmune thrombocytopenia
GC-MS/MS	Gas Chromatography mass spectrometry
GM-CSF	Granulocyte-macrophage colony-stimulating factor
GR	Glucocorticoid receptor
GREs	GCs response elements
HLA	Human leukocyte antigens
HLMVECs	Human lung microvascular endothelial cells
HNA	Human Neutrophil Antigens
HRP	Horseradish peroxidase
HSA	Human serum albumin
HSC	Hematopoietic stem cell

HSPC	hematopoietic stem and progenitor cells
ICAM	Intercellular adhesion molecule
IF	Interstitial fluid
IFN-γ	Interferon-γ
IDO	Indolamin-2, 3-dioxygenase
IL-1β	Interleukin 1β
IL-6	Interleukin 6
IL-8	Interleukin 8
IL-10	Interleukin 10
ISBT	International Society of Blood Transfusion
IVIG	Intravenous immunoglobulin
kDa	Kilo Dalton
kg	Kilogram
KC	Keratinocyte-derived cytokine
L	Liter
LPS	Lipopolysaccharide
LC-MS/MS	Liquid chromatography–MS/MS
LDL	Low density lipoprotein
LysoPCs	Lysophosphatidylcholines
M	Molar
MAC	Membrane attack complex
MCP-1	Monocyte chemoattractant protein-1
M-CSF	Macrophage colony stimulating factor
MEM	Minimum essential medium
mg	Milligram
MHC	Major Histocompatibility Complex
MIF	Macrophage migration inhibitory factor
min	Minute
MIP-2	Macrophage inflammatory protein 2
mL	Milliliter

mM	Milimolar
MW	Molecular weight
NaCl	Sodium chloride
NF-κB	Nuclear factor-Kb
ng	Nanogram
NHSN	National Hemovigilance Safety Network
nm	Nanometer
NP-40	Nonidet P-40
OD	Optical density
PaO_2	Arterial oxygen pressure
PAGE	Polyacrylamide gel electrophoresis
PAMP	Pathogen associated molecular pattern
PBMCs	Peripheral blood mononuclear cells
PBS	Phosphate buffered saline
PCR	Polymerase chain reaction
pDCs	plasmacytoid dendritic cells
PLTs	Platelets
PMSF	Phenylmethylsulfonyl fluoride
PMN	Polymorphonuclear leukocytes
P/S	Penicillin/Streptomycin
PSGL-1	P-selectin glycoprotein ligand-1
PTR	Platelet transfusion refractoriness
PVDF	Polyvinylidene Fluoride
qRT-PCR	Quantitative real-time RT PCR
RBCs	Red blood cells
RE	Relative expression
RIP	Receptor interacting protein
RNA	Ribonucleic acid
RNase	Ribonuclease
ROS	Reactive oxygen species

RPMI	Roswell Park Memorial Institute
rpm	Revolutions per minute
RT	Room temperature
RT-PCR	Real time polymerase chain reaction
sCD40L	soluble CD40L
SDS	Sodiumdodecylsulphate
sec	Second
SHOT	Serious Hazards of Transfusion
TACO	Transfusion-associated circulatory overload
TAE	Tris acetate EDTA
TBS	Tris buffered saline
TGF-β	Transforming growth factor β
TJ	Tight junctions
TLR	Toll like receptor
TNF-α	Tumor necrosis factor alpha
TRALI	Transfusion-related acute lung injury
Tregs	T regulatory cells
Tris	Tris (hydroxymethyl) amino methane
TSP-1	Thrombospondin-1
UV	Ultraviolet
µ	Micro
µg	Microgram
µL	Microliter
µm	Micrometer
µM	Micromolar
V	Volt
VCAM	Vascular cell adhesion molecule
VLA-4	Very late antigen 4
v/v	Volume per volume
w/v	Weight per volume

1. INTRODUCTION

1.1 Transfusion-related acute lung injury (TRALI) is a fatal adverse reaction to blood transfusion

Blood transfusion is a common clinical treatment for various bleeding disorders, including surgery, trauma, and anemia correction. However, clinicians are troubled by adverse blood transfusion reactions caused by immune responses, representing the main focus of recent research in the area. TRALI is a severe, life-threatening complication that can occur during or after a blood transfusion.

1.1.1 Definition of TRALI

TRALI is a life-threatening syndrome that occurs within 6 h of blood transfusion and is characterized by acute respiratory distress and the development of non-cardiogenic pulmonary edema (1-4). From a clinical perspective, it can be challenging to differentiate between TRALI and transfusion-associated circulatory overload (TACO) as both conditions present with respiratory distress temporally related to transfusion. However, TACO is characterized by pulmonary hydrostatic (cardiogenic) edema, whereas TRALI is associated with non-cardiogenic permeability edema (1).

Non-cardiogenic pulmonary edema, which is the hallmark of TRALI, has been widely reported since the 1850s (5). However, the term “TRALI” was coined by Popovsky et al. in 1983, confirming the high similarity between TRALI and the symptoms of patients with acute lung injury (ALI) (6). In 1985, TRALI was officially acknowledged as a separate clinical entity following an analysis of a comprehensive series of 36 patients by Popovsky and Moore (7). The recognition of TRALI increased after adverse reactions to blood transfusions were first reported in the United Kingdom in 1996 in the “Serious Hazards of Blood Transfusion” (SHOT) report, which reported that TRALI as being one of the most common causes of major morbidity and mortality associated with transfusions (8). This finding has since been confirmed by hemovigilance systems in many Western countries.

The diagnostic criteria for TRALI proposed by Popovsky and Moore included (i) the occurrence of respiratory distress within 6 h of transfusion initiation; (ii) the absence of signs of circulatory

overload; and (iii) the radiographic evidence of new bilateral pulmonary infiltrates (7). These criteria became widely accepted for many years, but have since undergone two major revisions. The initial revision was made in 2004, when Canadian Blood Services called for a consensus conference (CCC) regarding TRALI (9). The CCC established a standard clarification of TRALI to aid research in its epidemiology, pathogenesis, prevention, and treatment. The CCC distinguished TRALI into two forms: TRALI and possible TRALI. Additionally, the ALI criteria for the definition of hypoxemia were expanded in the Consensus Panel definition of TRALI. In the context of clinical investigations, it is recommended that hypoxemia be defined as a ratio of the partial pressure of oxygen to the fractional inspired oxygen concentration (arterial oxygen pressure/fraction of inspired oxygen: PaO_2/FiO_2) of < 300 mm Hg or as an oxygen saturation measured by pulse oximetry of < 90% when a patient is breathing room air. However, in the context of patient care and surveillance studies, in the absence of pulse oximetry measurements on room air, alternative clinical evidence of hypoxemia may be sufficient. Possible TRALI is identified for patients who present with a clinical syndrome that satisfies the definition of TRALI but who also have risk factors for ALI to distinguish between cases caused by blood transfusion and those with risk factors for non-transfusion ALI. The outcome of the CCC was the formulation of a standardized definition of TRALI, which was designed to facilitate research on its epidemiology, pathophysiology, and risk mitigation, as well as providing a framework for decisions on appropriate case investigation and donor testing. Pulmonary specialists redefined ALI and acute respiratory distress syndrome (ARDS) during the 2012 Berlin Consensus Conference (known as the Berlin definition). A preliminary definition was put forth, which proposes three mutually exclusive categories of ARDS based on the degree of hypoxemia: mild (200 mm Hg < PaO_2/FIO_2 ≤ 300 mm Hg), moderate (100 mm Hg < PaO_2/FIO_2 ≤ 200 mm Hg), and severe (PaO_2/FIO_2 ≤ 100 mm Hg). Moreover, the term “ALI” was dropped and replaced with mild ARDS. However, the field of transfusion medicine has not yet included this information when considering TRALI (10).

In 2019, the Delphi methodology was used to establish new diagnostic criteria for the Type I (without an ARDS risk factor) and Type II (with an ARDS risk factor or with existing mild ARDS) TRALI subtypes (3). The definition of TRALI type I follows the 2004 CCC definition of TRALI. For a case to be classified as TRALI Type II, it must meet three specific conditions: (i) the case must fulfill the same clinical criteria as TRALI Type I; (ii) the onset of post-transfusion pulmonary edema must have occurred in the presence of an ARDS risk factor or mild ARDS; and (iii) the patient must have had stable pulmonary status (e.g., based on PaO_2/FiO_2 [i.e., P/F] ratio) in the 12 h before transfusion.

1.1.2 The incidence of TRALI

A new systematic review and meta-analysis of 80 studies investigated the incidence of TRALI using active surveillance. The findings revealed that the pooled TRALI estimates for active surveillance studies were 0.17/10,000, 0.31/10,000, and 3.19/10,000 for red blood cells (RBCs), platelets, and plasma, respectively (11). However, the exact incidence of TRALI is difficult to determine due to varying definitions and reporting practices across different countries.

The initial survey of TRALI incidence was 1:5000 per transfused unit (7). A study conducted by the Serious Hazards of Transfusion (SHOT) committee in the UK and the Paul-Ehrlich-Institute in Germany found that the occurrence of TRALI from fresh frozen plasma transfusions was 1:65,000-1:66,000, which is higher than that of other blood products. The fatality rate of TRALI was reported as 18 and 21% (12, 13). As a result, policies were developed in the subsequent decade to mitigate the incidence of TRALI. Since 2005, the American Association of Blood Banks (AABB) has implemented several measures to reduce the incidence of TRALI, including the formulation of a standardized definition of TRALI, preparation of high-volume plasma components from male donors or never-pregnant females, implementation of TRALI mitigation strategies for AB plasma donors, implementation of TRALI mitigation strategies for plasma and whole blood transfusable units, and implementation of TRALI mitigation strategies for apheresis platelets (14). The effect of these TRALI mitigation strategies has been remarkable, as the TRALI rate declined from 2.88 in 2007 to 0.60 in 2017 per 100,000 units, including RBCs of any type, plasma of any type, and apheresis single-donor platelets (14). In contrast, according to the SHOT, the United Kingdom implemented a policy of pure male plasma as early as 2003, and the incidence of TRALI in the United Kingdom was only 0.84% per 100,000 units in 2007 of total number of blood components (24 of 2,914,228 components), including RBCs, platelets, Fresh Frozen Plasma (FFP), and cryoprecipitate, (15). Furthermore, data from the International Hemovigilance Network database, which compiled information from 13 European countries, indicated that the incidence of TRALI was below 0.5% per 100,000 units from 2009 to 2012 (16). The U.S. Food and Drug Administration's (FDA) 2021 Annual Report shows that TRALI was still the second leading cause of death among serious adverse events related to the administration of blood components (17).

1.1.3 White blood cell antibodies associated with TRALI

According to its pathogenesis, TRALI can be divided into non-antibody mediated TRALI and antibody-mediated TRALI (18), among which antibody-mediated TRALI is more common, accounting for 65 to 90% of TRALI cases (19). Antibody-mediated TRALI was proven in a single-lung transplant case, and the development of TRALI was observed exclusively in the transplanted lung that expressed the cognate antigen, while the native lung, which did not express the cognate antigen, remained unaffected (20). Regarding transfusion risk factors, the receipt of plasma from female donors was identified as a potential risk, as demonstrated in a double-blind, crossover, randomized controlled trial conducted in Sweden in 2001 (21). The most important and common antibodies implicated in TRALI are human leukocyte antigen (HLA) and human neutrophil antigen (HNA) antibodies. In Germany, 28% of TRALI cases are caused by anti-HNA antibodies and 72% by anti-HLA antibodies, whereas in the UK, the corresponding distributions are 8 and 75%, respectively (12, 13). TRALI caused by anti-HLA-A2 and anti-HNA-3a antibodies is typically severe and fatal (12, 22, 23). The prevalence of anti-HLA antibodies in female donors with 0, 1–2, and ≥ 3 pregnancies has been documented to be 7.8, 14.6, and 26.3%, respectively (24). In China, a similar survey also found that the HLA antibody positivity rates among multiparous female blood donors who had 0, 1, 2, 3 and more deliveries were 4.9, 20.61, 23.26, and 26.67% (25). Additionally, the first reported case of TRALI caused by CD36 antibodies has been identified in Japan (26, 27).

1.1.4 Non-antibody-mediated TRALI

The infusion of cognate donor antibodies against HLA and HNA was initially identified as the causative factor of TRALI. However, antibodies are not involved in all cases that fulfill the clinical definition of TRALI (28, 29), and recipients of a product containing antibodies do not always develop TRALI, even in the presence of the cognate antigen (30). The accumulation of cell-derived substances in donor blood and storage-related changes in donor RBCs and platelets (PLTs) have been reported as the underlying causes of non-antibody mediated TRALI (28). The role of aged blood products in TRALI remains a topic of contention. In animal models, there is a clear correlation between aged PLTs and RBCs and the development of TRALI (31). The accumulation of bioactive lipids in stored transfusion products is postulated to be a causal factor in the development of TRALI in vivo and in vitro (32-37). The polar lipids that accumulate in both RBCs and PLTs have been identified as lysophosphatidylcholines (LysoPCs), which have been implicated in the development of ALI in a series of ten patients with TRALI (28). However, the role of LysoPCs and non-polar lipids in TRALI is unclear. Platelet-derived soluble CD40L

(sCD40L), which activates macrophages and induces the synthesis and secretion of numerous pro-inflammatory cytokines, has also been shown to be associated with TRALI (38). Although sCD40L is a potent mediator of inflammation, most studies have indicated that sCD40L plays a relatively minor role in TRALI pathogenesis. Recently, a study demonstrated that extracellular vesicles (EVs) from stored platelets mediate TRALI by unbalancing the sphingolipid rheostat (39).

1.1.5 Pathogenesis of TRALI

The pathogenesis of TRALI has been the focus of research, and several hypotheses have been proposed, including the 2-hit model and threshold theory (40, 41). Among these, the 2-hit model is the most widely accepted (42). The 2-hit model postulates that a "first hit" occurs in patients with clinical risk factors, such as recent surgery, active infection, or a long history of alcohol abuse. This creates a clinical environment that effectively increases susceptibility to TRALI and develops during subsequent transfusions (40, 42-44). This clinical "first hit" promotes an inflammatory environment, which in turn leads to pulmonary endothelial cell activation (increased Intercellular Adhesion Molecule-1 [ICAM-1] expression), polymorphonuclear leukocyte (PMN) induction and migration to the pulmonary vasculature, and subsequent induction of PMN adhesion to activated endothelial cells (35, 40, 42, 45). The "second hit" is induced by biological response modulators or passively transferred antibodies through blood transfusion, which lead to the release of cytokines and reactive oxygen species (ROS) from stimulated/adherent PMN, causing lung endothelial damage, capillary leakage, and lung injury (35, 40, 42, 45, 46). Both theories suggest that neutrophils are the primary effector cells of TRALI, although some studies propose that monocytes/macrophages, rather than neutrophils, are the key cells of TRALI (47, 48).

1.1.6 Complement system

The complement system is a complex network of plasma proteins that work together to protect against foreign microorganisms and maintain tissue homeostasis (49). Three pathways of complement activation have been identified: classical, lectin and alternative pathways. The classical and lectin pathways are triggered by the recognition of pathogens or altered self-cell surfaces by antibodies (classical pathway: CP) and pattern recognition molecules (e.g.,

pentraxins and complement 1q [C1q] for the CP; lectins and ficolins for the lectin pathway). The classical and lectin pathways converge on C4 cleavage, leading to the formation of the C4b/C2a C3-convertase complex on target surfaces, with subsequent proteolysis of C3 into C3a and C3b. The alternative pathway is initiated by the spontaneous low-level formation of C3b in the fluid phase (50). The CP employs C1 and is initiated by antigen–antibody immune complexes. Inactive C1 circulates in the serum as a molecular complex consisting of six C1q molecules and two each of the serine proteases C1r and C1s. Subsequent to binding to a cognate antigen, the Fc fragment of an IgG or IgM antibody interacts with the collagen-like tail of C1q. This interaction instigates a conformational change, which in turn leads to the sequential activation of C1r and C1s.Subsequent to this, the activated C1s then cleaves C4 and C2 into small inactive fragments (C4a and C2b) and larger active fragments (C4b and C2a) (51). C4b binds to the sugar moieties of cell surface glycoproteins and noncovalently to C2a, generating the CP C3 convertase C4bC2a. C4bC2a is an enzymatic complex that cleaves C3, the central component of the complement cascade, into the anaphylatoxin C3a and C3b. In addition to activation by IgG and IgM immune complexes, C1q can also be activated by apoptotic and necrotic cells as well as acute phase proteins such as C-reactive protein (52). The integration of C3b into C3 convertases leads to the formation of the C5 convertases. These C5 convertases split C5 into complement components 5a (C5a) and C5b, eventually giving rise to the multimeric complement membrane attack complex (MAC, C5b-9) (53). C5a, a powerful, pro-inflammatory anaphylatoxin synthesized after cleavage of complement component C5, exerts its biological action by binding to its specific receptor C5aR1, also known as CD88, expressed on macrophages, neutrophils, monocytes, keratinocytes, and human plasmacytoid dendritic cells (pDCs) (54-56). A second receptor of C5a, C5-like receptor 2 (C5L2), was identified as a negative regulator of C5a-dependent signaling (57).

1.1.7 Complement is involved in the development of TRALI

An increasing number of studies have shown that complement is involved in the development of TRALI. In relation to human TRALI studies, one case report on the activation of complement was an anti-HLA class II-mediated TRALI case (58). Intriguingly, complement was found to be activated in the product transfused during the onset of TRALI symptoms, suggesting that the activated complement components present in the transfusion product contributed to the

occurrence of TRALI (58). Another study reported that complement-fixing anti-HNA-1a IgM antibodies from a female donor were associated with a TRALI case (59).

In recent years, several animal experiments have been conducted to study the role of complement in TRALI. However, the conclusions on this particular issue have been somewhat divergent. In one study, anti-major histocompatibility complex I (MHC class I) antibody induced TRALI in BALB/c male mice, which was protected in C3, C5, and C5a receptor (C5aR)-deficient mice indicating the important role of C5a in murine TRALI (47). However, another study found that C5aR-deficient BALB/c mice still induced TRALI, suggesting that C5a is dispensable in murine TRALI mediated by anti-MHC class I antibody (60). Additionally, another study revealed that complement activation was correlated with increased macrophage trafficking from the lungs to the blood in a fragment crystallizable region (Fc)-dependent manner which was dependent on C5 (61). Cleary et al. found that complement activation on the endothelium initiated anti-MHC class I-mediated TRALI by conditionally removing MHC class I antigen from endothelial cells (62), and anti-MHC class I IgG hexamerization initiated complement activation (63). Although many studies have confirmed that complement is involved in the occurrence of TRALI, whether complement acts through C5a after activation is still inconclusive.

1.2 Anti-CD36 antibodies associated with TRALI

1.2.1 CD36

CD36, a platelet integral membrane glycoprotein (glycoprotein IV), is a receptor for thrombospondin-1 (TSP-1), which is present in extracellular matrices and platelet alpha granules. CD36 is involved in cell attachment, motility, and proliferation, as well as the modulation of protease activity, transforming growth factor beta (TGF-β) activation, neurite outgrowth, and angiogenesis (64). CD36 belongs to the class B scavenger receptor family, which can recognize modified low density lipoprotein (LDL) related to macrophage foam cell formation and the pathogenesis of atherosclerosis (65). CD36 expression is widespread and found on the microvascular endothelium, adipocytes, skeletal muscle, dendritic cells, retina, breast, intestinal epithelia, smooth muscle cells, and hematopoietic cells, including erythroid precursors, platelets, monocytes/macrophages, and megakaryocytes (64). Moreover, a well-defined human blood group polymorphism, Nak^a, is carried by platelet CD36 (66). CD36 (Nak^a)

deficiency can be classified into two types: type I, which involves a deficiency in platelets and monocytes, and type II, which involves a deficiency in platelets only (67). Individuals lacking CD36 on platelets and monocytes (type I deficiency) generate anti-CD36 Abs (anti-Nak^a, hereafter referred to as anti-CD36) due to immunization after blood transfusion or during pregnancy (67, 68). Type I CD36 deficiency is extremely rare in White individuals but is found at a relatively high frequency among Asians (> 0.5%) (69). In Asians, anti-CD36 antibodies play a critical role in the pathological mechanism of platelet transfusion refractoriness (PTR) and fetal/neonatal alloimmune thrombocytopenia (FNAIT) (69-72).

1.2.2 Anti-CD36 antibodies induce TRALI

Anti-CD36 antibody-induced TRALI was reported for the first time in Japan (26, 27). In two patients with TRALI, only anti-Nak^a (CD36) antibodies, but not anti-HLA and other anti-HNA antibodies, were found in the transfused blood products of the donor. Incubation of monocytes with plasma derived from the donor resulted in the production of the proinflammatory mediators LTB_4 and TNF-α. This reaction was dependent on the presence of human lung microvascular endothelial cells (HLMVECs), indicating the role of cellular crosstalk between monocytes and lung endothelial cells (26). Nevertheless, the exact mechanism of anti-CD36-mediated TRALI remains unknown.

Although TRALI is a leading cause of transfusion-related death, specific treatments are currently unavailable (1, 73). Hence, supportive measures remain the mainstay for patients with TRALI (42). In recent years, animal models have been established to study the mechanism of TRALI and to evaluate specific treatments. Some drugs, including aspirin, intravenous immunoglobulin (IVIG), anti-osteopontin antibody, and IL-10, have been shown to prevent TRALI in a mouse model of anti-MHC class I-mediated TRALI (74-77). However, no promising preclinical approaches have been reported for anti-CD36 antibody-induced TRALI

1.3 Aim of the study

In this study, we investigated two major aspects of anti-CD36 antibody-mediated TRALI. First, we established a mouse TRALI model using an anti-CD36 monoclonal antibody. Based on this model, we conducted a thorough investigation into the role of blood components, such as neutrophils, monocytes, platelets, and complement, before testing possible drugs to prevent and cure TRALI induced by anti-CD36 antibodies.

2. MATERIALS AND METHODS

2.1 Materials

2.1.1 Equipments

Animal automatic hematology analyzer BC-5000 Vet	Mindray, Shenzhen, China
Biology microscope CX31	Olympus, Nishishinjuku, Japan
Cell culture CO_2 incubator	Thermo Fisher Scientific, Waltham, USA
Desktop centrifuge	Thermo Fisher Scientific, Waltham, USA
Digital thermometer	Yuyan, Shanghai, China
Electronic balance	Sartorius, Beijing, China
FluorChem FC2 System	Proteinsimple, San Jose, USA
Fluorescent plate reader FLX800	Bio-Tek, Winooski, USA
Inverted microscope	Leica DMI3000 B
Fast Real-Time PCR System 7500	Thermo Fisher Scientific, Waltham, USA
Multiskan FC	Thermo Fisher Scientific, Waltham, USA
Flow cytometer Canto II	BD Biosciences, Erembodegem, Belgium
FlowJo software version 10	Tree Star, Ashland, USA
ChemiDoc™ Touch Imaging System	Bio-Rad, California, USA
Horizontal mini electrophoresis system	Bio-Rad, California, USA
Microwave oven	Midea, Foshan, China
Mini centrifuge Galaxy	VWR International, Darmstadt, Germany
Mini-rocker shaker MR-1	PEQLAB, Erlangen, Germany
NanoDrop ND 2000	Thermo Fisher Scientific, Waltham, USA
NanoZoomer S360 Digital slide scanner	Hamamatsu Photonics, Hamamatsu, Japan

PCR thermocycler	Thermo Fisher Scientific, Waltham, USA
Power supply units	Bio-Rad, California, USA
Protein chromatography system	Senhui, Suzhou, China
SDS gel electrophoresis chambers	Bio-Rad, California, USA
Tanon 5200 Chemiluminescent Imaging System	Tanon, Shanghai, China
Shaker	Allsheng, Hangzhou, China
Ultrasonic homogenizer Bandelin Sonopuls	Bandelin, Berlin, Germany
UV visible spectrophotometer Ultrospec 2100	Biochrom, Cambridge, UK
Vortex Mixers & Shakers	Scientific industries, New York, USA

2.1.2 Chemicals

4% Paraformaldehyde	Sigma-Aldrich, Beijing, China
37% Formaldehyde solution	Sigma-Aldrich, Steinheim, Germany
Acrylamide 30% (w/v)	Roth, Karlsruhe, Germany
Agarose	Invitrogen, Karlsruhe, Germany
Avertin	Sigma-Aldrich, ON, Canada
Bromophenol blue sodium salt	Sigma-Aldrich, Steinheim, Germany
Calcium chloride	Merck, Darmstadt, Germany
Clodronate-liposomes	Liposoma BV, Amsterdam, the Netherlands
Dimethylsulfoxide	Merck, Darmstadt, Germany
Dithiothreitol (DTT)	Sangon Biotech, Shanghai, China
DNA ladder	Solarbio, Beijing, China
Eosin staining solution	Sigma Aldrich, ON, Canada
Ethanol	Sigma-Aldrich, Steinheim, Germany

Ethidium bromide	Roth, Karlsruhe, Germany
Ethylene diaminetetraacetic acid disodium salt	Merck, Darmstadt, Germany
Enhanced chemiluminescence (ECL) reagents	Bio-Rad, California, Germany
Formamide	Merck, Darmstadt, Germany
Glycerol	Merck, Darmstadt, Germany
Glycine	Sigma-Aldrich, Steinheim, Germany
Hematoxylin staining solution	Baso, Zhuhai, China
Igepal CA-630 (NP-40)	Sigma-Aldrich, Steinheim, Germany
Lipopolysaccharide (LPS)	Sigma-Aldrich, Darmstadt, Germany
Magnesium chloride	Merck, DarmstadtSigma, Germany
β-Mercaptoethanol	Sangon Biotech, Shanghai, China
Methanol	Sangon Biotech, Shanghai, China
Non-fat dry milk	Sangon Biotech, Shanghai, China
N, N, N', N'-Tetramethylethylenediamin (TEMED)	Roth, Karlsruhe, Germany
Phenylmethylsulfonyl fluoride (PMSF)	Sigma, Steinheim, Germany
PMX-53	MCE, Shanghai, China
Proteinase inhibitor cocktail	Sigma-Aldrich, Steinheim, Germany
Protein loading buffer (reducing)	Ncmbio, Suzhou, China
Sodium chloride	Sangon Biotech, Shanghai, China
Sodium dodecyl sulfate (SDS)	Merck, Darmstadt, Germany
Sodium pentobarbital	Yuyan, Shanghai, China
Tris (hydroxymethyl) aminomethane	Roth, Karlsruhe, Germany
Triton X-100	Sigma-Aldrich, Steinheim, Germany
Tween-20	Roth, Karlsruhe, Germany

2.1.3 Cell culture reagents

Bovine serum albumin (endotoxin free)	Invitrogen, Karlsruhe, Germany
Ca-Mg-free HBSS (1x) medium	Invitrogen, Karlsruhe, Germany
Fetal bovine serum (FBS)	Gibco, South America
Fetal calf serum (FCS)	Gibco, Australia
Penicillin/Streptomycin (100×)	Gibco, Darmstadt, Germany
Dulbecco's phosphate buffer saline (DPBS)	Gibco, Beijing, China
RPMI 1640 medium	Gibco, Beijing, China
Trypsin/EDTA	Gibco, Darmstadt, Germany
Dulbecco's modified eagle medium (DMEM)	Gibco, Suzhou, China
HAT supplement	Gibco, Beijing, China
PFHM-II protein-free hybridoma medium	Thermo Fisher Scientific, Rockford, USA

2.1.4 Kits

Mouse Rapid Antibody Isotyping	Thermo Fisher Scientific, Rockford, USA
Melon Gel IgG Purification	Thermo Fisher Scientific, Rockford, USA
Zeba™ Desalt Spin Column	Thermo Fisher Scientific, Rockford, USA
Pierce™ BCA Protein Assay	Thermo Fisher Scientific, Rockford, USA
Mouse Complement C3 ELISA	Sangon Biotech, Shanghai, China
Mouse Complement C5 ELISA	Abcam, Cambridge, UK
Mouse Complement C5a ELISA	Sangon Biotech, Shanghai, China
Mouse Soluble C5b-9 ELISA	Sangon Biotech, Shanghai, China
Pierce F(ab')2 Preparation	Thermo Fisher Scientific, Rockford, USA

Human TNF-alpha DuoSet ELISA	R&D Systems, Minneapolis, USA
Direct-Zol RNA Miniprep	Zymo Research, Irvine, USA
Transcriptor First Strand cDNA Synthesis	Roche, Carlsbad, USA
EasySep Human Monocyte Isolation	Stemcell Technologies, Vancouver, Canada
Mouse CXCL2/MIP-2 Quantikine ELISA	R&D Systems, Minneapolis, USA
Mouse CXCL1/KC Quantikine ELISA	R&D Systems, Minneapolis, USA
Mouse TNF-α Quantikine ELISA	R&D Systems, Minneapolis, USA
Small tissue DNA extraction	Findrop, Guangzhou, China

2.1.5 Miscellaneous

2x High-Fidelity PCR Master Mix (with Dye)	MCE, Shanghai, China
4', 6-diamidino-2-phenylindole (DAPI)	Vector Laboratories, Burlingame, USA
70-µm cell strainer	BD Bioscience, Heidelberg, Germany
Acid citrate dextrose (ACD) tube	Vacutainer, BD, USA
Cell culture plate (6/12/24/96 well)	Corning, Kennebunk, USA
Collagenase A	Roche, Münich, Germany
DAB substrate	Maxim, Fuzhou, China
Disposable pipette	Jetbiofil, Guangzhou, China
Falcon tube (15 ml)	Greiner Bio-One, Frickenhausen, Germany
Fixation/Permeabilisation Solution	eBioscience, San Diego, USA
Filter (0.22/0.45 µM)	Jetbiofil, Guangzhou, China
Fibronectin	Sigma-Aldrich, Steinheim, Germany
Ficoll-Paque PLUS gradient	GE Healthcare, Uppsala, Sweden
FITC-labelled albumin	Thermo Fisher Scientific, Rockford, USA

Heparin	Ratiopharm, Ulm, Germany
Human TNF-α	Novoprotein, Beijing, China
i-STAT CG4+ cartridge	Abbott, Illinois, USA
Goat serum	Boster, Wuhan, China
PVDF membrane	Millipore, Darmstadt, Germany
May Grünwald	Sigma-Aldrich, Steinheim, Germany
Microendothelial cell medium	ScienCell Research Laboratories, Carlsbad, USA
NatureTips	Bioer, Hangzhou, China
Neubauer counting chamber	LaborOptik, Marienfeld, Germany
Pharm Lyse™ Lysing Buffer	BD Biosciences, Shanghai, China
Primary HLMVECs	ScienCell Research Laboratories, Carlsbad, USA
rProtein G Beads 4FF	Smart-lifesciences, Changzhou, China
Radio-Immunoprecipitation Assay (RIPA) buffer	Thermo Fisher Scientific, Rockford, USA
SP2/0-Ag14 mouse myeloma cells	ATCC, Manassas, VA, USA
Syringe	BD Bioscience, Heidelberg, Germany
Sterile deionized water	Solarbio, Beijing, China
TRIzol reagent	Thermo Fisher Scientific, Rockford, USA
Trypan blue	Gibco, Darmstadt, Germany

2.1.6 Antibodies

Table 1： Primary antibodies used in Western blotting (WB) analysis

Primary antibody	Manufacturer	Catalogue No.	Dilution (application)
Rabbit anti-C5b-9	Sigma-Aldrich, San Diego, USA	2204903	1:1000 (IHC)
Normal rabbit IgG	Sigma-Aldrich, San Diego, USA	12-370	1:1000 (IHC)
Mouse anti-CD14	Abcam, Cambridge, UK	Ab181470	1:1000 (WB)
Rabbit anti-CD36	Cell Signaling Technology, Danvers, USA	114347	1:1000 (WB)
Mouse anti β-actin	Cell Signaling Technology, Danvers, USA	3700	1:1000 (WB)

Table 2: List of secondary antibodies for Western blot (WB) analysis.

Secondary antibody	Manufacturer	Catalogue No.	Dilution (application)
Goat anti rabbit IgG-HRP	Cell Signaling Technology, Danvers, USA	7074S	1:3000 (WB)
Donkey anti mouse IgG-HRP	Jackson ImmunoResearch, West Grove, USA	715-035-150	1:3000 (WB)

HRP: Horseradish peroxidase

Table 3: Antibodies for flow cytometric (FACS) staining

Antibodies against	Fluorochrome	Manufacturer	Clone	Catalog Number
CD45	PE-Cy7	BD Pharmingen, San Diego, USA	30F11	552848
CD11b	FITC	BD Pharmingen, San Diego, USA	M1/70	557396
CD115	PE	BD Pharmingen, San Diego, USA	T38-320	565249
F4-80	APC	Biogems, Westlake Village, USA	M8.1	200205
CD45	V450	BD Pharmingen, San Diego, USA	HI30	60018
CD14	PE	BD Pharmingen, San Diego, USA	M5E2	60004

2.1.7 Primers

All primer pairs were obtained according to the literature (78) and purchased from Sangon Biotech (Sangon Biotech, Shanghai, China). The sequences of primer pairs are shown in Table 4. Primers were diluted in RNA-free water.

Genes	Primer sequence (5'->3')
Cd36-fw	TGTAACCCAGGACGCTGAGG
Cd36-rv	GAAGGTTCGAAGATGGCACC
β-actin-fw	CCTCACCCTGAAGTACCCCA
β-actin -rv	TGCCAGATTTTCTCCATGTCG

Table 4: Sequences of forward (fw) and reverse (rv) primers used in quantitative real-time PCR (RT-PCR)

.2.2 Methods

2.2.1 Animals

All wild-type *Cd36*$^{+/+}$ C57BL/6J mice (8–10 weeks; later termed "wild-type mice") were purchased from the Laboratory Animal Centre of Sun Yat-Sen University (Guangzhou, China) and Guangdong Province Medical Experimental Animal Center and kept under standard conditions (22°C, 12/12 h light/dark cycle) with pelleted food and water provided ad-libitum. Homozygote *Cd36*$^{-/-}$ C57BL/6J (*B6.129S1-Cd36*^{tm1Mfe}*/J*) mice were purchased from Jackson Laboratory (Bar Harbor, Maine, USA). Heterozygous *Hc*$^{-/-}$ C57BL/6J（*C5*$^{-/-}$, *C57BL/6JGpt-Hc*^{em3Cd2040}*/Gpt*) mice and heterozygous *C5aR1*$^{-/-}$ C57BL/6J (*C57BL/6JGpt-C5ar1*^{em3Cd3133}*/Gpt*) mice were obtained from GemPharmatech (Nanjing, China) and back-crossed to obtain homozygous *C5* and *C5aR1*-deficient mice. All transgenic mice were bred in the Laboratory Animal Centre of Sun Yat-Sen University and Huateng BioScience company, where a specific pathogen-free (SPF)-level laboratory has been authorized by the Guangdong provincial government. All mice were housed under conditions of controlled humidity (50–60%) and maintained under controlled light (12/12 h light/dark cycle) with free access to water and rodent chow. This study was conducted in strict accordance with the recommendations in the Guide for the Care and Use of Laboratory Animals of the Chinese law of animal welfare. The experiments were performed according to the guidelines of the local authority (The Animal Care Committee of Sun Yat-Sen University and Huateng BioScience company, Guangzhou, China) and conformed to the Code of Practice for the Care and Use of Animals for Experimental Purposes (study approval: SYSU-IACUC-2020-000185 and HTSW-IACUC-2021-211123). The mice were euthanized by anesthesia, with every effort made to minimize suffering.

2.2.2 Immunization of *Cd36*$^{-/-}$ mice with wild-type platelets and detection of anti-CD36 antibodies

Mice were exsanguinated and whole blood was collected in 1:8 acid citrate dextrose (ACD) (Vacutainer, BD, USA). Briefly, 2 ml of Dulbecco's phosphate buffered saline (DPBS, Gibco, Beijing, China) was added to each 1 ml of whole blood in a 15-ml conical tube; samples were mixed through gentle inversion and centrifuged at 80 ×*g* for 10 min. PRP was collected, mixed by gentle inversion, and re-centrifuged for 10 min. After counting using an

animal automatic hematology analyzer (BC-5000 Vet, Mindray, Shenzhen, China), the PLT concentration was normalized to 2 × 10^8 PLT/ml by pelleting for 10 min and resuspending in DPBS. *Cd36*$^{-/-}$ female mice were immunized intraperitoneally 3 times with 10^8 WT platelets at weekly intervals. After immunization, 5 μL of serum was collected from the tail, incubated with 100 mL of EDTA blood (1:100) from WT mice for 30 min, and washed with phosphate-buffered saline containing 1% bovine serum albumin (PBS/BSA, Sangon Biotech, Shanghai, China). Then, 50 μL of fluorescein isothiocyanate–conjugated anti-mouse IgG (1:200; Jackson ImmunoResearch Laboratories, West Grove, USA) was added and incubated for 30 min. After RBC lysis (BD Biosciences, Shanghai, China) at room temperature in the dark for 15 min, the cells were suspended in 0.5 mL PBS/BSA and then analyzed by flow cytometry (FACS Canto II; BD Biosciences, Erembodegem, Belgium).

2.2.3 Generation and characterization of monoclonal antibodies against CD36

After immunization of *Cd36*$^{-/-}$ mice as described above, splenocytes were harvested and fused with SP2/0-Ag14 mouse myeloma cells (American Type Culture Collection [ATCC], Manassas, VA, USA) with polyethylene glycol using a standard protocol (79). Hybridomas were screened using mouse platelets (*Cd36*$^{+/+}$ and *Cd36*$^{-/-}$ mouse platelets) by flow cytometry. Clones producing anti-CD36 antibodies bound to *Cd36*$^{+/+}$ but not to *Cd36*$^{-/-}$ platelets were defined as positive hybridoma clones. The IgG subclasses of the hybridomas were determined using a Pierce Rapid Isotyping Kit (Thermo Fisher Scientific, Waltham, USA) according to the manufacturer's instructions. In total, 17 hybridoma clones producing anti-CD36 antibodies were generated and characterized. One clone (named GZ1, isotype: IgG2a) that produced a high-affinity IgG antibody was selected for further research. Fluorescence labeling of the detection antibodies against CD36 (mAb, GZ1) was performed with an Alexa Fluor^{TM} 647 Antibody Labeling Kit following the manufacturer's protocols. APC-conjugated anti-CD36 (GZ1) antibodies were utilized to detect the monocytes from *Cd36*$^{+/+}$ and *Cd36*$^{-/-}$ mice.

2.2.4 1- and 2-hit models of anti-CD36 induced TRALI

Male and female wild-type C57BL/6J mice (*Cd36*$^{+/+}$) and *Cd36*$^{-/-}$ male C57BL/6J mice were untreated (1-hit model) or pre-treated (2-hit model) with lipopolysaccharide (LPS, *Escherichia coli O111:B4*, 0.1 mg/kg, Sigma-Aldrich, Darmstadt, Germany) intraperitoneally (i.p.) 24 h

before intravenous injection (i.v.) with 400 µL of anti-CD36 mAbs (GZ1, 0.4 mg/kg) or the antibody's F(ab')$_2$ fragments (GZ1 F(ab')$_2$, 0.8 mg/kg) (48). IgG2a isotype (0.4 mg/kg, i.v., clone C1.18.4, Bio X cell, Lebanon, USA) was used as a control. In some experiments, 400 µL of purified IgG (5.6 mg) isolated from human sera was administered. Rectal temperatures were measured 30 min after antibody injection using a digital thermometer (Yuyan, Shanghai, China). Mice were euthanized by i.p. injection of sodium pentobarbital at 2 h after anti-CD36 administration (60). The lungs were harvested and the lung wet (W)-to-dry (D) weight ratios were determined.

2.2.5 Partial oxygen pressure and oxygen saturation measurements

The partial oxygen pressure (Pao_2) and oxygen saturation (Sao_2) were measured in blood drawn into a syringe containing heparin anticoagulant (50 U/mL) from the abdominal aortas of the anesthetized mice 10 min after anti-CD36 injection, using an i-STAT CG4+ cartridge by a handheld blood analyzer (i-STAT 1, Abbott, Illinois, USA) following the manufacturer's protocols.

2.2.6 Analysis of bronchoalveolar lavage fluid (BALF)

BALF was isolated as described previously with minor modifications (60). Thirty minutes after administration of anti-CD36 or isotype control, the tracheas of sacrificed mice were exposed and cannulated and 1 mL of sterile PBS solution was injected into the lung three times. The BALF was centrifuged at 13,000 ×*g* for 5 min at 4°C and the supernatants were stored at −80°C. The protein content of the BALF was quantified using a BCA assay with BSA as a standard.

2.2.7 Measurement of lung Wet/Dry weight ratios

The ratio between the net wet weight (W) and net dry weight (D) of lung mice was defined as a parameter of pulmonary edema. Two hours post-anti-CD36 infusion, the mice were anesthetized with Avertin (2% final in PBS, Sigma-Aldrich, ON, Canada) via i.p. injection and the chest cavity was exposed. The whole lung was removed, weighed (W), dried in an oven at 60°C for 72 h, and then reweighed (D). The lung Wet/Dry weight ratio was calculated using the following formula: net wet weight/net dry weight.

2.2.8 Histology of lung tissue

Two hours after TRALI induction with anti-CD36, the mouse lung was removed and fixed overnight with 4% paraformaldehyde (PFA, Sigma-Aldrich, Beijing, China). The fixed lung tissue was dehydrated in a step-by-step manner from low- to high-concentration alcohol. The dehydrated lung tissue was embedded with paraffin wax with a melting point of 52–60°C. A blade was used to trim the excess paraffin wax around the tissue block. The thickness of the tissue section was 8 μm. Paraffin sections were dewaxed in xylene. After washing, hematoxylin staining solution (Harris, Baso, Zhuhai, China) was added for 3–5 min. After washing, eosin staining solution (alcohol-soluble, Sigma Aldrich, ON, Canada) was added for 1–2 s, and anhydrous ethanol was added for 1–2 min, before finally sealing with xylene. The stained lung tissue was examined under a Leica DMI3000 B inverted microscope (Leica, Wetzlar, Germany).

2.2.9 In vivo depletion of monocyte, neutrophil, platelet, and complement

2.2.9.1 Monocyte depletion

Monocytes were depleted using clodronate-liposomes as described previously (48). Clodronate-liposomes or PBS-encapsulated liposomes (clodronate 5 mg/mL, 50 mg/kg, body weight, Liposoma BV, Amsterdam, the Netherlands) were administered via tail vein injection (i.v.) for 6 h. The rate of monocyte depletion in the blood was examined before (pre-) and after (post-) depletion by flow cytometry using FITC-conjugated CD11b (clone M1/70, BD Pharmingen, San Diego, USA) and APC-conjugated F4/80 (clone M8.1, Biogems, Westlake Village, USA) markers as recommended (80). Next, 100 μL of whole blood was taken from the tail vein, combined with antibody coupled with corresponding fluorescent dye, and incubated at room temperature for 30 min, before adding 2 mL BD Pharm Lyse™ Lysing Buffer (BD Bioscience, San Diego, USA) for red cell lysis. Subsequently, the samples were incubated at room temperature for 15 min, centrifuged at 200 ×*g* for 5 min, washed once with PBS/BSA, and centrifuged again. After adding 500 μL of PBS/BSA re-selected cells, flow cytometry was used for analysis.

2.2.9.2 Neutrophil depletion

Neutrophils were depleted by i.p. injection of 20 mg of hydroxyurea (Sigma-Aldrich, Saint Louis, USA) for 7 days and subsequently by i.v. injection of anti-Ly6G mAb (clone 1A8, 5 mg/kg, Bio X cell, Lebanon, USA) 48 and 24 h before TRALI induction, respectively (47). Neutrophil depletion was monitored by an animal automatic hematology analyzer (BC-5000 Vet, Mindray, Shenzhen, China) and verified by flow cytometry using PE-Cy7-conjugated CD45 (clone 30-F11, BD Pharmingen, San Diego, USA), FITC-conjugated CD11b (clone M1/70, BD Pharmingen, San Diego, USA), and PE-conjugated CD115 (clone T38-320, BD Pharmingen, San Diego, USA) markers as described previously (48).

2.2.9.3 Platelet depletion

Platelets were depleted by i.v. administration of anti-GPIbα antibodies (R300, 2 mg/kg, Emfret Analytics, Würzburg, Germany) 24 h before TRALI induction as described previously (81). Isotype IgG (C301, 2 mg/kg, Emfret Analytics, Würzburg, Germany) was used as a control. The platelet count was measured using an animal automatic hematology analyzer.

2.2.9.4 Complement depletion

Complement was depleted by i.p. injection of cobra venom factor from the Naja kaouthia snake (0.4 mg/kg i.p., 233552, Millipore, Darmstadt, Germany) or PBS as a control 24 h before TRALI induction (62). The complement factor levels were detected using C5 ELISA to verify the efficiency of complement depletion.

2.2.10 Detection of mouse complement by ELISA

Whole blood was collected from mice 2 h after infusion with mAb GZ1 or LPS-treated control. Naïve mice were treated as controls. Sera were isolated after blood coagulation on ice for 2 h and stored at −80°C until use. ELISAs for mouse C3 (D721061, Sangon Biotech, Shanghai, China), C5 (ab264609, Abcam, Cambridge, UK), and mouse C5a (D721063, Sangon Biotech, Shanghai, China) were used according to the manufacturers' instructions.

2.2.11 Plasma transfer

Plasma transfusion was performed as described previously with minor modification (47). Blood was drawn from the tail veins of male mice into 3.2% sodium citrate–containing tubes (1:10 dilution) at 4°C. Plasma was separated, pooled, and stored at −80°C. Heat-inactivated pooled plasma (56°C for 30 min) was used as a control. Mab GZ1 or isotype control (0.4 mg/kg) was diluted in 300 µL of the pooled plasma and used for TRALI induction as described above.

2.2.12 Preparation of F(ab')$_2$ fragments

The F(ab')$_2$ fragment of IgG was generated using the Pierce F(ab')$_2$ Preparation Kit (Thermo Fisher Scientific, Rockford, USA) (80). Briefly, 0.5 mL of the mAb GZ1 IgG was added into a spin column containing Immobilized Pepsin for 6 h at 37°C. After centrifugation at 5000 g for 1 min, the resin was washed with 0.5 mL of PBS and centrifuged at 5000 ×*g* for 1 min. Undigested IgG was removed using Protein A. The purity of the GZ1 F(ab')$_2$ fragment was determined by silver staining of proteins in sodium dodecyl sulphate polyacrylamide gel electrophoresis (SDS-PAGE) and confirmed by flow cytometry. For silver staining, 500 ng of purified IgG and F(ab')$_2$ fragments for mAb GZ1 were run on 7.5% SDS-PAGE gels under nonreducing (NR) and reducing (R) conditions. The concentration of purified GZ1 F(ab')$_2$ fragment was then determined using the Thermo Scientific™ BCA Protein Assay. F(ab')$_2$ fragment of mAb 73D1 (anti-C7) was prepared as above.

2.2.13 Detection of mAb GZ1 and human serum containing anti-CD36 antibodies reacting with mouse platelets by flow cytometry

Mouse and human anti-CD36 antibodies were assessed by flow cytometry with platelets from *Cd36*$^{+/+}$ or *Cd36*$^{-/-}$ mice as described previously (69). MAb GZ1 (0.25 µg) and human anti-CD36 serum #1, #2, and #3 (dilution 1:16) were incubated with 100 µL of EDTA-treated blood (1:100) from *Cd36*$^{+/+}$ or *Cd36*$^{-/-}$ mice for 30 min at room temperature and washed with PBS/BSA. IgG2a isotype control and normal human AB serum were treated as negative controls. Next, 50 µL of fluorescein isothiocyanate–conjugated anti-mouse IgG or anti-human IgG (1:200, Jackson ImmunoResearch) was added for 30 min. After RBC lysis with lysing buffer (BD Biosciences), cells were resuspended in 0.5 mL PBS/BSA and analyzed by flow cytometry (FACS Canto II, BD Biosciences).

To further confirm the purity of our IgG and F(ab')$_2$ preparations, 0.25 µg of GZ1 IgG or

$F(ab')_2$ fragment was incubated with platelets from wild-type mice for 30 min at RT. After washing, bound antibodies were detected with Fc-specific FITC conjugated goat anti-mouse IgG (1:200, Jackson ImmunoResearch) or heavy and light chain (H+L) specific Alexa Fluor 488 labeled donkey anti-mouse IgG (1:200, Thermo Fisher Scientific).

2.2.14 Measurement of cytokine secretion in vitro

Peripheral blood mononuclear cells (PBMC) were isolated from healthy CD36 (+) blood donors using Ficoll-Paque premium (Cytiva, Uppsala, Sweden) at 400 ×*g* for 30 min without a break. PBMC were primed with anti-CD36 antibodies, and the culture supernatant was analyzed for cytokine secretion as described in initial studies (82). Briefly, human anti-CD36 #3 sera (20%, vol/vol) were incubated with 5×10^5 *Cd36*$^{+/+}$ PBMC for 20 h at 37°C in a 96-well microplate (Corning, Kennebunk, USA), before collecting the culture supernatant, centrifuging at 13,000 ×*g*, and storing at −80°C until use. AB serum from healthy individuals was used as a control. The concentration of TNF-α in the supernatant was measured by a Human TNF-alpha DuoSet ELISA (DY210, R&D Systems, Minneapolis, USA) according to the requirements of the reagent manufacturer.

2.2.15 Endothelial permeability assay

A permeability assay was performed as described previously with minor modifications (83). Primary human lung microvascular endothelial cells (HLMVECs, No. 3000, Sciencell, Carlsbad, USA) were maintained in an endothelial cell medium (ECM, Sciencell). Endothelial cells at passage 5 were then plated onto Transwell plates (diameter 6.5 mm, pore size 0.4 mm, Corning) at a density of 10^5 cells/insert pre-coated with 50 µg/mL fibronectin (Sigma-Aldrich) for 1 h at 37°C. HLMVECs were cultured for 2 days to achieve a monolayer and then treated with PBMC supernatant diluted (1:1) with culture medium containing 0.25 U/mL heparin (Ratiopharm, Ulm, Germany) for 6 h. The endothelial permeability was measured by the migration of FITC-labeled albumin (400 µg/mL, 66 kDa, Thermo Fisher Scientific) for 2 h using a fluorescent plate reader (FLX800, Bio-Tek, Winooski, USA) at an excitation wavelength of 485 nm and emission wavelength of 538 nm.

2.2.16 cDNA synthesis and quantitative real-time PCR

2.2.16.1 RNA isolation

Monocytes and HLMVECs were incubated with medium alone or in medium containing TNF-α (10 ng/mL) for 4 h in a 12-well plate as described previously (78). PBMC were isolated from healthy CD36 (+) blood donors using Ficoll solution as described above. The monocytes were isolated from the PBMC via adhesion for 2 h onto microtiter wells. Monocytes were incubated with RPMI 1640 medium (Gibco, Beijing, China) alone or with medium containing TNF-α (10 ng/mL, Novoprotein, Beijing, China). HLMVECs were maintained in an endothelial cell medium. RNA from each sample (TNF-α treated monocytes or monocytes alone, TNF-α treated HLMVECs or HLMVECs alone) was extracted by using a the Direct-Zol RNA miniprep kit (Zymo Research, Irvine, USA) according to the manufacturer' instructions. The RNA concentration was measured using a NanoDrop spectrophotometer (Thermo Fisher Scientific, Waltham, USA).

2.2.16.2 Reverse transcription

The purified RNA was reverse transcribed using a Transcriptor First Strand cDNA Synthesis kit (Roche, Carlsbad, USA). For each sample, 1 µg of RNA was mixed with 2 µL of random primer and water (PCR Grade) (total volume: 13 µL), before denaturating at 65°C for 10 min and snap chilling on ice. The RT mix was prepared by adding 4 µL 5 × Transcriptor Reverse Transcriptase Reaction Buffer, 0.5 µL Protector RNase Inhibitor (40 U/µL), 2 µL Deoxynucleotide Mix, and 0.5 µL Transcriptor Reverse Transcriptase (20 U/µL) to mix with the denatured RNA samples (total volume: 20 µL). The reaction mixture was incubated at 25°C for 10 min and then heated at 55°C for 30 min to inactivate the reverse transcriptase. Transcriptor Reverse Transcriptase was inactivated by heating to 85°C for 5 min and chilling on ice. The cDNA samples were stored at −80°C untill use.

2.2.16.3 Quantitative real-time RT PCR (qRT-PCR)

To measure CD36 expression in monocytes and HLMVECs, primer pairs were designed according to the literature (78) and synthesized by Sangon Biotech (Table 4). The appropriate annealing temperatures were determined using gradient PCR. A typical 20 µL qRT-PCR reaction mix contained 2 µl cDNA, 10 µl 2x SYBR® Premix Ex Taq II (Tli RNaseH Plus) 1.6 µl forward and reverse primer mix (10 pM/µl), 6µl DNase/RNase-free water, 0.4 µl ROX

Reference Dye II (50X). Real-time PCR was performed in a triple experiment to measure the expression of target genes using the 7500 Fast Real-Time PCR System (Applied Biosystems, Thermo Fisher Scientific) under the following conditions; initial denaturation (95°C, 30 s; cycling stage 95°C, 5 s and 60°C 34 s (40 cycles); melt curve stage 95°C, 15 s, 60°C 1 min and 95°C 15 s.

The melting curve was examined to confirm the specificity of the PCR product. The real-time RT-PCR results were analyzed using the delta-delta Ct method, also known as the $2^{-\Delta\Delta Ct}$ method using β-actin as an internal standard to normalize the amount of mRNA. Data were analyzed using Microsoft Excel software and are presented as relative expression (RE).

2.2.17. Endothelial-monocyte co-culture assay

HLMVECs were co-cultured with monocytes was performed as described previously (84). Monocytes (purity > 90%) were isolated from PBMC using the EasySep Human Monocyte Isolation Kit (Stemcell Technologies, Vancouver, Canada) according to the manufacturer' instructions. The isolated monocytes were assayed for purity using CD45-V450 (BD Biosciences) and CD14-PE (BD Biosciences) by flow cytometry. HLMVECs were maintained in a 6-well plate (Corning) to be a monolayer containing TNF-α (10 ng/mL) or not for 4 h. Monocytes (10^6 cells) were then added to untreated or TNF-α treated HLMVECs for 4 h at 37°C. Cells were solubilized using RIPA buffer (Thermo Fisher Scientific) and analyzed by immunoblotting as described previously (85).

2.2.18 Immunoblotting

Cells were washed twice with cold PBS and lysed in fresh RIPA lysis buffer (85). Cell extracts were obtained by vortexing at 5 min intervals for 30 min. Cell debris was removed via centrifugation at 13000 ×*g* at 4°C for 30 min. The protein concentrations in cell lysates were determined by the BCA Protein Assay (Thermo Fisher Scientific). Next, 15 µg protein of each sample was separated on 10% SDS-PAGE under reducing conditions, and the separated proteins were transferred onto a PVDF membrane (Millipore, Darmstadt, Germany) using a Bio-Rad Electrophoresis Chambers and Power Supplies (Bio-Rad Laboratories, Hercules, USA). The membranes were washed with TBS-T buffer and blocked in blocking buffer (5% non-fat milk in TBS-T buffer) for 1 h before incubating with the primary

antibody (Table 1) diluted in 5% BSA/TBS-T overnight at 4°C. After washing three times with TBS-T, the membranes were incubated with HRP-conjugated goat anti-rabbit antibodies (dilution 1:3000, Cell Signaling Technology) or donkey anti-mouse antibodies (dilution 1:3000, Jackson ImmunoResearch) (Table 2) for 1 h at room temperature. Subsequently, the membranes were rinsed three times. Bound antibodies were detected using chemiluminescence substrates (ECL, Bio-Rad). CD36, CD14, and β-actin bands were quantified using Volume Box Tools (Image Lab software, Bio-Rad).

2.2.19 Administration of FcγR inhibitor and intravenous immunoglobulin (IVIG)

Rat anti-FcγRII/III mAb (clone 2.4G2, IgG2b; Bio X cell) or human IVIG (Boya Bio-Pharmaceutical, Fuzhou, China) was administered i.p into the mice at a dose of 25 mg/kg or 2 g/kg, 24 or 18 h, respectively before TRALI induction. Rat IgG2b isotype control (clone LTF-2, Bio X cell) and human serum albumin (HSA, Sigma-Aldrich) were injected as controls.

2.2.20 Therapeutic intervention of TRALI induced by anti-CD36 antibody

Five different inhibitors including mAb GZ1 $F(ab')_2$ fragment (80), the antioxidant N-acetylcysteine (NAC, Sigma-Aldrich) (47), the neutralizing mAb BB5.1 against mouse C5 complement (86), the neutralizing mAb 73D1 against mouse C7 complement IgG and $F(ab')_2$ fragments were applied in this study (87). Precisely, 200 µL of mAb GZ1 $F(ab')_2$ (5 mg/kg in PBS), 200 µL of BB5.1 (1 mg/200 µL in PBS), 200 µL of 73D1 (1 mg/200 µL in PBS), 200 µL of 73D1 $F(ab')_2$ (1 mg/200 µL in PBS), or 200 µL of NAC solution (10 mg in saline, Sigma) was administered 30 or 5 min pre-TRALI (prophylactic treatment). Additionally, each inhibitor was injected at the same dose post-TRALI (therapeutic treatment), 3 min after the rectal temperature dropped by 0.5°C, which we considered the significant onset of TRALI. For treatment with NAC, besides injection of NAC solution, aerosolized NAC was administered for 20 min after NAC injection in an inhalation chamber besides injection of NAC solution. The nebulizer (NE-C25S, Omron) in the inhalation chamber was operated under the following conditions: air flow ≥ 8 L/pm, nebulization rate ≥ 0.2 mL/min, and nebulizer flow 4 L/min. The aerosolized NAC solution (100 mg/mL) was

obtained from Shuyaqi (Guorun Pharma) and was spray-dried (aerodynamic diameter < 5.0 μm).

2.2.21 ELISA for mouse BALF

2.2.21.1 CXCL2/MIP-2, TNF-α, and CXCL1/KC ELISAs

Mouse BALF was isolated 30 min after administration of anti-CD36 antibodies or isotype control as described previously (60). The concentrations of CXCL2/MIP-2, TNF-α, and CXCL1/KC in mouse BALF were measured using ELISA (Quantikine ELISA Kit, R&D Systems) according to the manufacturers' instructions.

2.2.21.2 Soluble C5b-9 ELISA

The soluble C5b-9 concentration in BALF was measured by ELISA (Sangon Biotech; Shanghai, China) according to the manufacturer' instructions.

2.2.22 Immunohistochemistry of C5b-9 deposition

Immunohistochemistry was performed as described previously (88). The mouse lungs were removed 2 h after TRALI induction and then fixed with 4% paraformaldehyde (Sigma-Aldrich) at 4°C overnight. Lung tissue sections (5 μm) were prepared according to the heat-induced epitope retrieval method (HIER), treated with 10% normal goat serum (Boster, Wuhan, China) in PBS for 1 h at 37°C, and then incubated with rabbit C5b-9 antibody (1:1000 dilution) overnight at 4°C. Normal rabbit IgG was used as the control. After washing, the sections were labeled with peroxidase-labeled goat anti-rabbit IgG (Abcam, Boston, USA) for 45 min at 37°C, followed by staining with DAB substrate (Maxim, Fuzhou, China) for 10 min. After counterstaining with hematoxylin and eosin for 2 min, lung sections were examined using a NanoZoomer S360 Digital slide scanner (Hamamatsu Photonics, Hamamatsu, Japan).

2.2.23 Isolation of human anti-CD36 IgG from serum

Human anti-CD36 sera were collected from FNAIT (71), PTR (70), and TRALI (26) cases

(anti-CD36 #1, 2, 3, respectively). Anti-CD36 #1 and #2 were characterized in the Guangzhou Blood Centre in Guangzhou, and anti-CD36 #3 was a kind gift from the Japanese Red Cross in Tokyo. IgG was purified using Melon Gel IgG Purification Kits (Thermo Fisher Scientific, Rockford, USA). Anti-CD36 serum was set into correct buffer using a Zeba™ Desalt Spin Column (Thermo Fisher Scientific, Rockford, USA) and IgG Spin Purification column. Subsequently, the column was incubated for 5 min at room temperature with end-over-end mixing and centrifuged for 1 min to collect the purified antibody. The anti-CD36 IgG concentration was measured using a Pierce™ BCA Protein Assay Kit (Thermo Fisher Scientific, Rockford, USA) according to the manufacturer's instructions.

Statistical analysis

Data are presented in this study as the mean ± standard deviation and were analyzed using GraphPad Prism 6.0. Comparisons between the two groups were assessed using an unpaired Student's *t*-test (two-tailed). Statistical analysis was performed with 1-way ANOVA with Bonferroni's correction for multiple comparisons. Kaplan–Meier methods were used to estimate survival durations, while a comparison between the two subgroups was performed using a log-rank test. *P* values < 0.05 were considered significant.

3. RESULTS

3.1 Generation and characterization of mAbs against CD36

MAbs against mouse CD36 were generated to develop a murine model of TRALI. For this purpose, *Cd36*$^{-/-}$ mice were immunized with platelets from *Cd36*$^{+/+}$ mice four times per month, once a week. Splenocytes were fused with SP2/0-Ag14 mouse myeloma cells according to a standard protocol. The IgG2a clone GZ1, which produces a high-affinity IgG antibody against CD36, was selected to establish murine TRALI. **Figure 1** shows the reactivity of mAb GZ1 with monocytes from *Cd36*$^{+/+}$ and *Cd36*$^{-/-}$ mice by flow cytometry. Positive reactions were only observed in monocytes from *Cd36*$^{+/+}$ mice, but not from *Cd36*$^{-/-}$ mice.

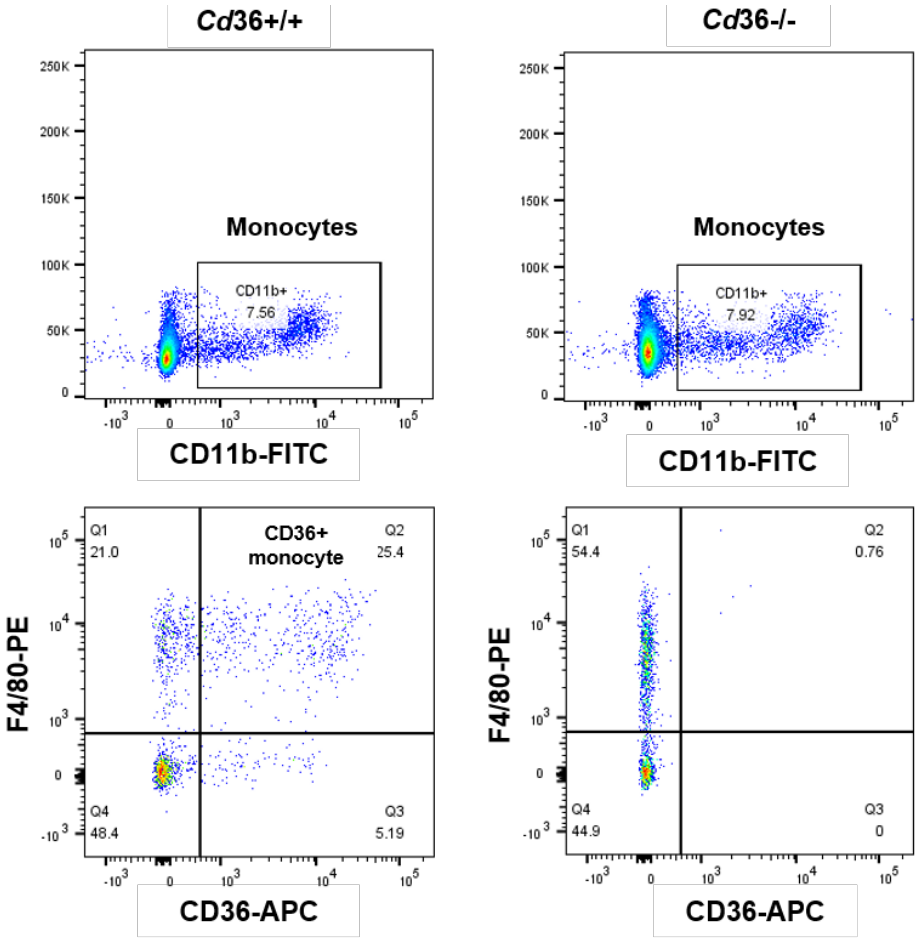

Figure 1. Binding analysis of mAb GZ1 with mouse monocytes by flow cytometry. Peripheral blood from *Cd36*$^{+/+}$ or *Cd36*$^{-/-}$ male mice was incubated with FITC-labeled anti-CD11b, PE-labeled anti-F4/80, and APC-conjugated anti-CD36 (GZ1).

3.2 Anti-CD36 antibodies induce TRALI in mice

3.2.1 Anti-CD36 treatment induced TRALI in the 2-hit, but not 1-hit model

In general, 8–10-week-old *Cd36*$^{+/+}$ C57BL/6J male mice were used in this study. To prove that anti-CD36 antibodies could induce TRALI reactions, the GZ1 mAb (0.4 mg/kg) was injected intravenously into naïve mice and LPS-pretreated mice. Without LPS pretreatment, no significant decrease in rectal temperature (37.30 ± 1.15 vs. 38.00 ± 0.32°C, $P > 0.05$; **Figure 2A**) or lung wet/dry weight ratios (4.41 ± 0.12 vs. 4.40 ± 0.13, $P > 0.05$; **Figure 2B**) were observed in GZ1 mAb treated mice compared to naïve mice.

In contrast, after GZ1 mAb administration, LPS-pretreated mice (0.1 mg/kg, i.p) developed dyspnea and decreased rectal temperature (32.12 ± 0.89 vs. 38.16 ± 0.47°C, $P < 0.0001$; **Figure 2A**), decreased Pao_2 (65.20 ± 9.73 vs. 104.60 ± 5.77 mmHg, $P < 0.0001$; **Figure 2C**), and Sao_2 (84.80 ± 6.30 vs. 97.60 ± 0.55%, $P < 0.0001$; **Figure 2D**) compared to the isotype control. Two hours after injection of the GZ1 mAb, the mice were anesthetized and sacrificed. The lung tissue was dissected, and the lung wet/dry weight ratio of the mice was analyzed. Compared to the isotype control, the TRALI mice' lung wet/dry weight ratio increased significantly (8.10 ± 1.00 vs. 4.50 ± 0.08, $P < 0.0001$; **Figure 2B**). This effect was not observed in *Cd36*$^{-/-}$ male mice. In the control experiment, administration of LPS alone did not increase the lung wet/dry weight ratio.

Furthermore, analysis of BALF showed increased protein concentrations in TRALI mice compared to the control group (5175.84 ± 654.12 vs. 357.82 ± 40.70 μg/mL, $P < 0.0001$; **Figure 2E**). Similar results were obtained for the chemokines KC and MIP-2 (KC: 151.51 ± 86.39 vs. 10.44 ± 3.43 pg/mL, $P < 0.001$; MIP-2: 19.45 ± 13.00 vs. 1.52 ± 0.79 pg/mL, $P < 0.015$, respectively), and the cytokine TNF-α (10.10 ± 2.00 vs. 5.13 ± 1.27 pg/mL, $P < 0.01$) (**Figures 2F, G and H**). These results demonstrated that anti-CD36 antibodies could only induce TRALI in the 2-hit but not the 1-hit model.

Overall, unless otherwise mentioned, murine TRALI was always induced in 8–10-week-old *Cd36*$^{+/+}$ C57BL/6J male mice with GZ1 mAb (0.4 mg/kg) pretreated with low-dose LPS (0.1 mg/kg).

3.2.2 F(ab')$_2$ fragment of anti-CD36 antibodies did not induce TRALI

To test the role of the Fc part in the mechanism of TRALI, the F(ab')$_2$ fragment of mAb GZ1 was generated. **Figure 3A** shows the molecular weight of the GZ1 F(ab')$_2$ fragment (110 KDa), which differs from that of IgG (150 KDa). This result was confirmed by flow cytometry. When IgG and F(ab')$_2$ fragments of mAb GZ1 were analyzed with platelets by flow cytometry using Alexa Fluor 488-labeled secondary antibodies against mouse heavy and light chain (H+L), positive reactions were obtained with both antibodies, as IgG as well as F(ab')$_2$ fragment. In contrast, a positive reaction was only observed with IgG when FITC conjugated secondary against mouse Fc was applied (**Figure 3B**).

Interestingly, injection of the mAb GZ1 F(ab')$_2$ fragment did not cause TRALI in our model. Significant changes in rectal temperature (38.68 ± 0.25 vs. 38.16 ± 0.47°C, $P > 0.05$; **Figure 2A**) and lung wet/dry weight ratio (4.45 ± 0.16 vs. 4.50 ± 0.08, $P > 0.05$; **Figure 2B**) were not observed compared to the isotype control. These results suggest that the interaction between the Fc-part with FcγR expressed on target cells is required for TRALI development.

3.2.3 Anti-CD36 antibodies reduced the survival rate (SR) of TRALI mice

Kaplan–Meier curves were used to analyze the SR of TRALI mice. The results showed that more than 50% of the mice died 2 h after TRALI induction with GZ1 mAb IgG. In contrast, all mice receiving the isotype control or GZ1 mAb F(ab')$_2$ fragment survived (SR: 100 vs. 45%, $P < 0.01$; **Figure 2I**). Pathological analysis of the lungs revealed pulmonary edema and alveolar septal thickening in mice treated with GZ1 mAb IgG, but not in those treated with F(ab')$_2$ fragment. Furthermore, no pathological changes were observed in *Cd36*$^{-/-}$ male mice (**Figure 2J**).

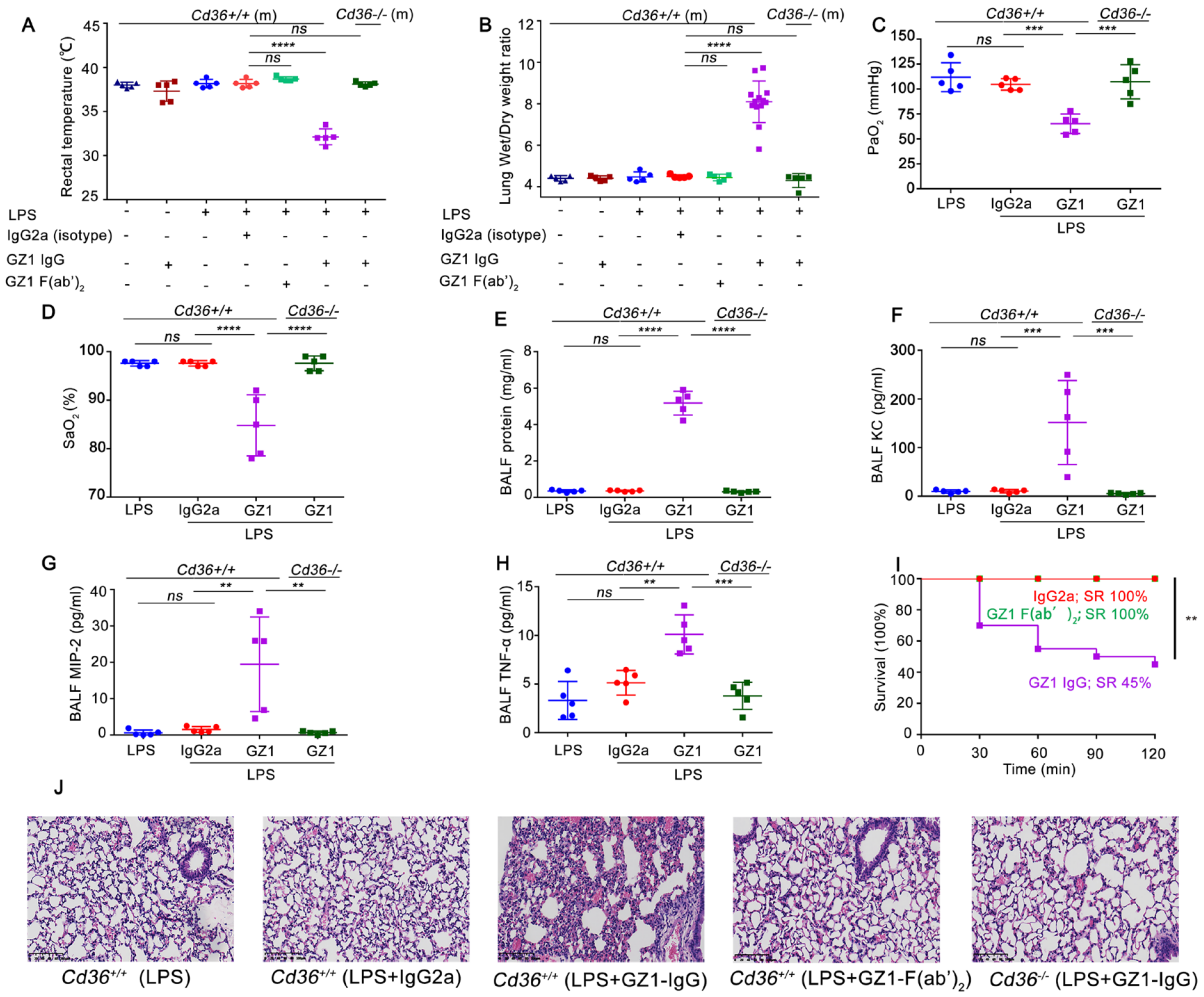

Figure 2. MAb GZ1 against CD36 induced TRALI in *Cd36*$^{+/+}$ male mice but not in *Cd36*$^{-/-}$ male mice.

(A) Rectal temperatures (n = 5 in each group) and (B) lung Wet/Dry weight ratios of mice first untreated (–) or treated (+) with LPS, then mAb GZ1 IgG, mAb GZ1 F(ab')$_2$, or IgG2a isotype control were administered (n = 5 in each group; n = 13 in LPS pre-treated *Cd36*$^{+/+}$ male with GZ1 injection). (C) Partial pressure of arterial oxygen (PaO_2) (n = 5), (D) percentage of arterial oxygen (SaO_2%) (n = 5) and concentration of (E) protein (n = 5), (F) Keratinocyte-derived Chemokine (KC) (n = 5), (G) Macrophage Inflammatory Protein 2 (MIP-2) (n = 5) and (H) Tumor Necrosis Factor Alpha (TNF-α) (n = 5) in bronchoalveolar lavage of LPS pre-treated *Cd36*$^{+/+}$ male mice were administered as described above. (I) Survival ratios of LPS-pre-treated *Cd36*$^{+/+}$ male mice injected with mAb GZ1 IgG (n = 20), mAb GZ1 F(ab')$_2$ (n = 10) or IgG2a isotype control (n = 10) were analysed. (J) Histology performed on lung tissue from the indicated mouse groups. *Cd36*$^{-/-}$ male mice treated with mAb GZ1 were used as controls. Lung tissue sections were stained with hematoxylin and eosin (*H&E*) and images were taken at 20x magnification. Representative images from each indicated group are shown. Scale bars

represent 100 µm. Statistical analysis was performed with 1-way ANOVA with Bonferroni's correction for multiple comparisons (A - H) or with log-rank test (I). Each dot represents one mouse and error bars represent the SD. ****$P < 0.0001$, **$P < 0.01$, ns: non-significant.

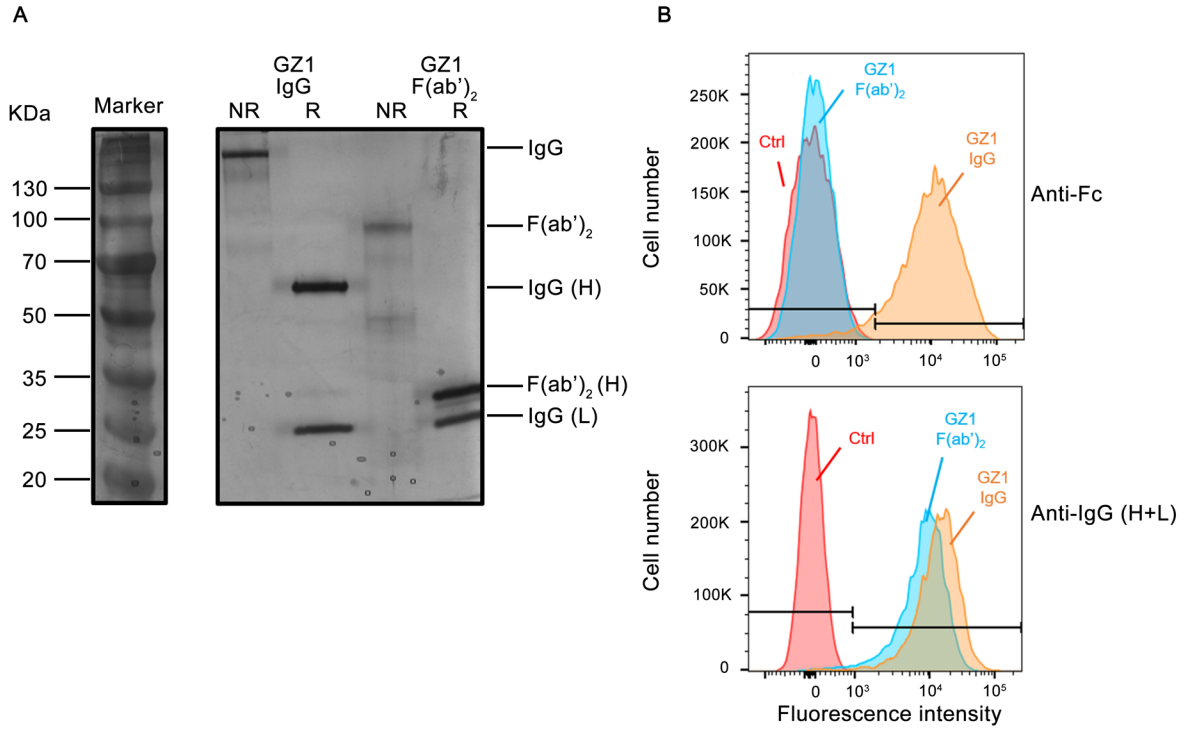

Figure 3. Analysis of F(ab')$_2$ fragments of mAb GZ1 by silver staining and flow cytometry. (A): purified IgG and F(ab')$_2$ fragments for mAb GZ1 were run on 7.5% SDS-PAGE under nonreducing (NR) and reducing (R) conditions. Separated proteins were visualized by silver staining. (B): Mouse platelets were incubated with purified IgG or F(ab')$_2$ fragment of mAb GZ1. After washing, bound antibodies were detected with Fc-specific FITC conjugated goat anti-mouse IgG or H+L specific Alexa Fluor 488 labeled donkey anti-mouse IgG.

3.3 Human anti-CD36 antibodies induced TRALI in mice

Human and mouse CD36 have high homology (approximately 85%) (89). Therefore, in theory, it is possible that human anti-CD36 antibodies could react with mouse CD36 and cause TRALI in our mouse model. When we tested sera from three immunized individuals (anti-CD36 #1, #2, and #3) for their ability to bind to mouse platelets using flow cytometry, antibody binding was observed with *Cd36*$^{+/+}$ mouse platelets, but not with *Cd36*$^{-/-}$ mouse platelets, which is consistent with the results obtained with the mAb GZ1 (**Figure 4A**). Administration of purified IgG from anti-CD36 sera samples #1 and #2 into *Cd36*$^{+/+}$ mice, decreases in rectal temperatures

(anti-CD36 #1 vs IgG control: 32.63 ± 0.48 vs. 38.00 ± 0.45°C, $P < 0.0001$; anti-CD36 #2 vs IgG control: 32.90 ± 1.72 vs. 38.00 ± 0.45°C, $P < 0.0001$; **Figure 4B**) and increases in lung Wet/Dry weight ratios (anti-CD36 #1 vs IgG control: 7.47 ± 0.25 vs. 4.30 ± 0.28, $P < 0.0001$; anti-CD36 #2 vs IgG control: 6.84 ± 1.24 vs. 4.30 ± 0.28, $P < 0.0001$; **Figure 4C**) were obtained. These reactions were not observed in *Cd36*$^{-/-}$ mice. Unfortunately, anti-CD36 #3 serum could not be tested in this model, due to limited materials.

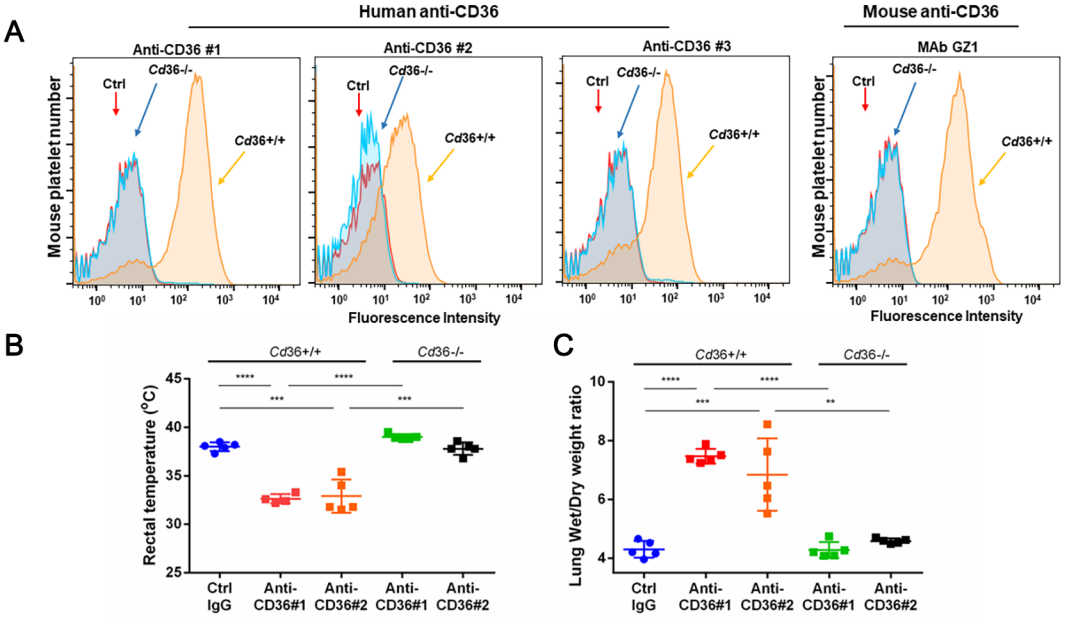

Figure 4. Human anti-CD36 antibodies induce TRALI in *Cd36*$^{+/+}$ mice but not in *Cd36*$^{-/-}$ male mice.

(A) Flow cytometric analysis of mAb GZ1 and human anti-CD36 serum asmples #1, #2, and #3 incubated with platelets from *Cd36*$^{+/+}$ and *Cd36*$^{-/-}$ male mice as indicated (arrows). (B) Rectal temperatures and (C) lung Wet/Dry weight ratios of LPS pre-treated *Cd36*$^{+/+}$ or *Cd36*$^{-/-}$ male mice that recieved either purified anti-CD36 IgG isolated from donor #1 and donor #2 or control IgG derived from normal donor. Statistical analysis was performed using1-way ANOVA with Bonferroni's correction for multiple comparisons (B–C). Each dot represents one mouse (n = 5 in each group; n = 4 in rectal temperatures from anti-CD36 #1, one mouse died in 27 min) and error bars represent the SD. ****$P < 0.0001$.

3.4 Monocytes play a significant role in the pathomechanism of anti-CD36-induced TRALI

To assess the contributions of different blood cell types to the mechanism of anti-CD36-mediated TRALI, neutrophils, platelets and monocytes were depleted *in vivo* before TRALI induction with mAb GZ1.

3.4.1 Neutrophil depletion did not prevent TRALI in mice

In a mouse model of TRALI induced by anti-MHC class I antibodies, neutrophils were identified as the primary effector cells responsible for endothelial cell damage and ultimately TRALI (90). Although neutrophils do not express CD36 (91), they may indirectly contribute to the mechanism of anti-CD36 antibody-mediated TRALI. To answer this question, we removed neutrophils from the mouse blood circulation via peritoneal injection of hydroxyurea and caudal injection of anti-ly6G. Flow cytometry revealed a removal rate of > 90% (**Figure 5B**), which was confirmed by peripheral blood examination (**Figure 5C**). Even in the absence of neutrophils, mice that received mAb GZ1 still developed TRALI as shown by a significant decrease in rectal temperature (31.46 ± 1.03 vs. 38.16 ± 0.47°C, $P < 0.0001$; **Figure 5F**), and a significant increase in lung Wet/Dry weight ratios (7.49 ± 0.98 vs. 4.50 ± 0.08, $P < 0.0001$; **Figure 5G**), compared to the isotype control. In contrast, neutrophil-depleted mice did not exhibit significantly lower mortality (65% vs. 45%, $P > 0.05$; refer to **Figure 5H**) than TRALI mice. However, the pathological slides of lung tissue showed protein deposits and edema (refer to **Figure 5I**).

3.4.2 Platelet depletion aggravated TRALI severity

To investigate the role of platelets in anti-CD36 mediated TRALI, platelets were depleted from the blood circulation with anti-GPIbα antibody. **Figure 5D** shows the platelet counts before and after GPIbα-treatment (before vs. after, 667 ± 153 vs. 34 ± 11 x10^6/mL, $P < 0.0001$). After TRALI induction with mAb GZ1, platelet-depleted mice showed a lower rectal temperature (33.78 ± 1.23 vs. 38.16 ± 0.47°C, $P < 0.0001$; **Figure 5F**) and higher lung Wet/Dry weight ratios (7.06 ± 0.54 vs. 4.50 ± 0.08, respectively, $P < 0.0001$; **Figure 5G**), compared to the isotype control. Furthermore, a more severe reaction was observed in the platelet-depleted mice compared to the non-depleted mice, leading to a significantly higher mortality rate (SR: 10%

vs. 45%, $P < 0.01$; **Figure 5H**). The autopsy findings revealed bleeding symptoms in the nasal cavity and a significant bleeding in the lung tissues of the mice (**Figure 5I**).

3.4.3 Monocyte depletion protects mice against TRALI

To evaluate the impact of monocytes on TRALI development, we removed monocytes from the blood circulation using clodronate liposomes. The liposomes were administered 18 hours after LPS injection, i.e. 6 h before anti-CD36 administration. Flow cytometry analysis confirmed total depletion of peripheral monocytes by this procedure (**Figure 5A**). In the absence of monocytes, mAb GZ1 did not trigger the TRALI reaction. Neither a decrease in rectal temperature (38.24 ± 0.61 vs. 38.16 ± 0.47°C, $P > 0.05$; **Figure 5F**) nor an increase in lung Wet/Dry weight ratio (4.36 ± 0.28 vs. 4.50 ± 0.08, $P > 0.05$; **Figure 5G**) was observed when compared to the isotype control. All mice survived anti-CD36 administration (SR: 100%, **Figure 5H**), and no interstitial edema was observed on histological preparations (**Figure 5I**).

3.4.4 Monocytes activated by anti-CD36 antibodies cause endothelial disturbance

To further study the impact of anti-CD36 bound to monocytes on the TRALI reaction (26), we isolated human monocytes from CD36(+) blood donors and incubated them with anti-CD36 serum (anti-CD36 #3) derived from TRALI cases. We found an elevated level of TNF-α (260.13 ± 68.63 vs. 41.79 ± 303.94 pg/mL, $P < 0.0001$; **Figure 6A**) and IL-1β (348.95 ± 72.14 vs. 22.14 ± 2.16 pg/mL, $P < 0.0001$; **Figure 6B**) compared to monocytes treated with control serum. Additionally, mAb GZ1 bound to monocytes resulted in ROS generation, which was prevented by the antioxidant N-acetyl cysteine (NAC) (92) (**Figure 6C**). When HLMVECs were treated with the supernatant of GZ1 mAb-primed monocytes, increased endothelial permeability was detected, as demonstrated by a higher influx of fluorescently labeled BSA through the HLMVEC monolayer in the Transwell assay compared to HLMVECs treated with control supernatant (MFI: 227.67 ± 8.69 vs. 177.67 ± 13.22, $p < 0.0001$; **Figure 6D**). However, this effect was not observed when HLMVECs were treated directly with anti-CD36 #3 serum, which TRALI-caused anti-CD36 antibody positive serum was a gift from the Japanese Red Cross.

Interestingly, the expression of CD36 in monocytes but not HLMVECs was significantly downregulated after TNF-α treatment (**Figure 6E**). Nevertheless, real-time qPCR revealed that

monocytes expressed significantly higher CD36 levels than HLMVECs (Ct values: 22.22 vs. 26.30, $P < 0.0001$; **Figure 6F**). However, when monocytes were co-cultured with TNF-α-treated HLMVECs, CD36 expression on monocytes was significantly upregulated compared to monocytes that adhered to untreated HLMVECs, as shown by immunoblotting (CD36/β-actin: 0.97 ± 0.05 vs. 0.63 ± 0.07, $P < 0.01$; **Figure 6G**). In the control experiment, no significant change in monocyte CD14 expression was observed (CD14/β-actin: 1.33 ± 0.05 vs. 1.33 ± 0.10, $P > 0.05$; **Figure 6G**). This suggests that endothelial cells treated with cytokines such as TNF-α up-regulate monocyte CD36 expression, which may increase the combination of the two and ultimately aggravate the severity of TRALI.

These results indicated that monocytes could be activated by anti-CD36 antibodies, leading to the production of TNF-α and IL-1β, and the generation of ROS, leading to increased endothelial permeability. This process could be accelerated by monocyte adhesion onto TNF-α activated endothelial cells.

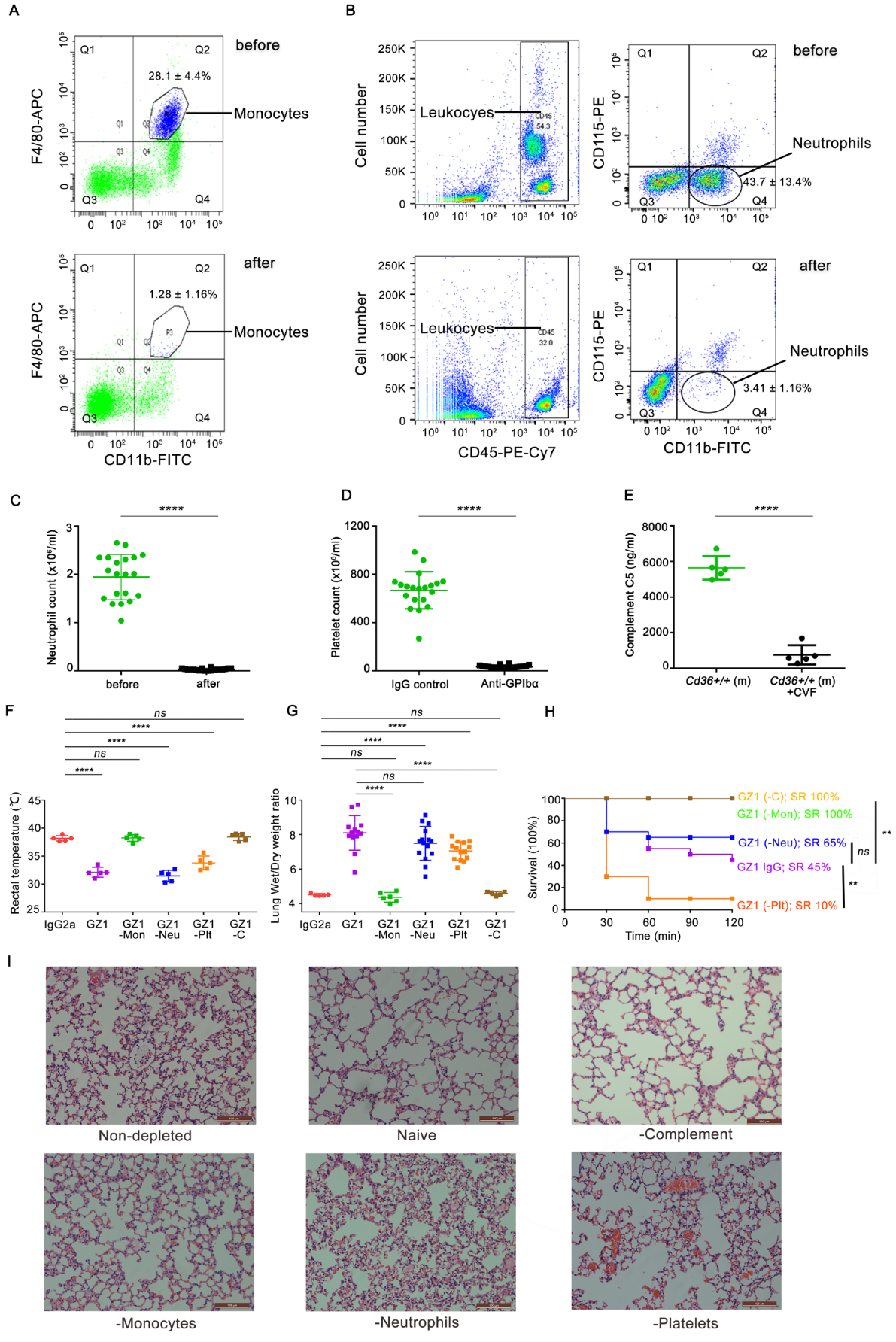

Figure 5. Monocyte and complement depletion prevents TRALI induced by mAb GZ1 against

CD36.

(A) Representative flow cytometric analysis of peripheral blood monocytes before and after depletion with clodronate-liposomes. Monocytes were stained with mAbs against CD11b (FITC) and F4/80 (APC). (B and C) Analysis of neutrophils depletion efficiency. Analysis of the neutrophil population before and after depletion with hydroxyurea and mAb anti-ly6G (1A8) treatment. Neutrophils were stained with mAbs against CD45 (PE-Cy7), CD11b (FITC), and CD115 (PE) by flow cytometry test (B, n = 5) and counted using an animal automatic hematology analyzer (C, n = 20). (D) Analysis of the platelet depletion efficiency. The platelet count was determined using an animal automatic hematology analyzer before and after depletion with a mAb against GPIbα (n = 20). (E) Analysis of the complement depletion efficiency. The concentration of C5 in male mice was measured without or with treatment of cobra venom factor (CVF) (n = 5). (F) Rectal temperatures (n = 5 in each group) and (G) lung Wet/Dry weight ratios of LPS pre-treated *Cd36*$^{+/+}$ male mice were injected with mAb GZ1 after depletion of monocytes (-Mon, n = 6), neutrophils (-Neu, n = 15), platelets (-Plt, n = 14) and complement (-C, n = 5). (H) Survival ratios of depleted mice injected with mAb GZ1 (n = 10 in monocytes and complement depletion group; n = 20 in neutrophils and platelets depletion group). (I) Histology was performed on lung tissue from the indicated mouse groups. Lung tissue sections were stained with hematoxylin and eosin (*H&E*) and images were taken at 20x magnification. Representative images from each indicated group are shown. Scale bars represent 100 μm. Statistical analysis was performed with a two-tailed unpaired Student's *t*-test (C–E) or 1-way ANOVA with Bonferroni's correction for multiple comparisons (F–G) or with a log-rank test (H). Each dot represents one mouse and error bars represent the SD. ****$P < 0.0001$, **$P < 0.01$, ns: non-significant.

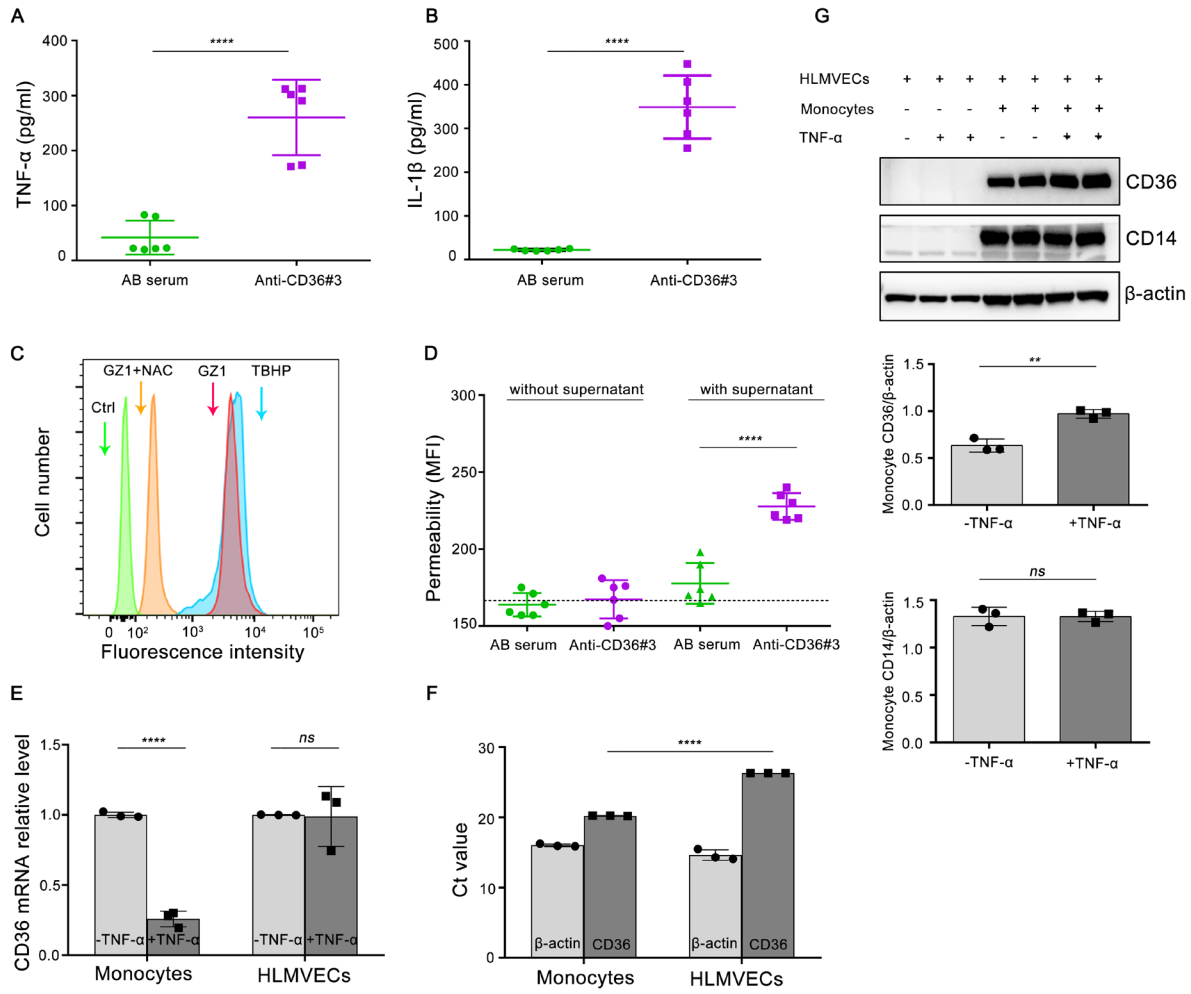

Figure 6. Cytokines derived from PBMC treated with anti-CD36 antibodies increase HLMVECs permeability.

Concentrations of TNF-α (A) and IL-1β (B) in cell supernatants derived from PBMC incubated with anti-CD36 #3 or AB serum. (C) Flow cytometric analysis of mAb GZ1 induced ROS generation in monocytes. Tert-butyl hydroperoxide (TBHP) and PBS-treated monocytes (Ctrl) were used as positive and negative controls, respectively. Monocytes were gated using the SSC vs. FSC plot and analyzed by flow cytometry. A representative result of four independent experiments is presented. (D) Cytokines derived from PBMC treated with anti-CD36 #3 increased HLMVECs permeability. Results are expressed as mean ± SD of duplicates from three independent experiments. The dotted line indicates the fluorescence intensity of HLMEVC monolayers incubated with a culture medium. (E) TNF-α decreased CD36 mRNA expression in monocytes but not in HLMVECs. CD36 mRNA expression was quantified using RT-PCR and normalized to β-actin. Data represent the mean ± SD of the relative quantification of CD36 mRNA expression measured in three experiments. (F) Ct values of untreated monocyte and HLMVECs in RT-PCR and β-actin were run as a control. Data represent the mean ± SD of

three experiments. (G) Western blots showed the upregulation of CD36 expression in monocytes adherent to TNF-α treated HLMVECs. CD36, CD14, and β-actin bands were quantified using Image Lab software and are represented as CD36/β-actin and CD14/β-actin. Representative images from three independent experiments are presented. Statistical analysis was performed with a two-tailed unpaired Student's *t*-test (A, B, E, and G), or with 1-way ANOVA with Bonferroni's correction for multiple comparisons (D and F). ****$P < 0.0001$, **$P < 0.01$, ns: non-significant.

3.5 Complement *C5* plays an important role in anti-CD36-mediated TRALI

To study the contribution of complement to the development of anti-CD36 mediated TRALI, complement was removed from the blood circulation using cobra venom factor (CVF). As shown in **Figure 5E**, the level of C5 complement in mice was significantly reduced after depletion (743.03 ± 546.36 ng/mL) compared to the initial level (5637.58 ± 658.78 ng/mL) ($P < 0.0001$). When TRALI was induced in male mice treated with mAb GZ1, no reactions were observed. The rectal temperature of the mice remained stable (38.42 ± 0.63 vs. 38.16 ± 0.47°C, $P > 0.05$; **Figure 5F**), and the mice lung Wet/Dry weight ratios did not show a significant increase (4.58 ± 0.11 vs. 4.50 ± 0.08, $P > 0.05$; **Figure 5G**) compared to the isotype control. In addition, no histological signs of acute lung injury were observed in complement-depleted mice, while the lung histology resembled that of naive mice (**Figure 5I**).

Surprisingly, female mice did not develop TRALI under this condition. No abnormalities were observed in female mice treated with or without LPS, isotype control, or anti-CD36. Compared to the isotype control, injection of anti-CD36 into the female mice did not result in a decrease in rectal temperature (38.06 ± 0.42 vs. 37.80 ± 0.21°C, $P > 0.05$; **Figure 7A**) or a change in the female mice's lung Wet/Dry weight ratios (5.02 ± 0.22 vs. 4.86 ± 0.06, $P > 0.05$; **Figure 7B**). Male and female mice exhibit different levels of complement (93). When we tested the complement concentrations in the serum of male and female mice by ELISA, similar plasma C3 levels were detected (1,196.92 ± 73.15 vs. 1,243.72 ± 39.71 μg/mL, $P > 0.05$; **Figure 7C**). In contrast, female mice had significantly lower plasma C5 levels than male mice (3,415.55 ± 259.86 vs. 5,637.58 ± 658.78 ng/mL, $P < 0.001$; **Figure 7D**). To demonstrate that a certain level of complement C5 is necessary for the development of TRALI, female mice were transfused with 300 μL plasma from male mice. After administration of mAb GZ1, female mice that

received plasma developed TRALI as shown by a significant decrease in rectal temperature (32.34 ± 0.33 vs. 38.00 ± 0.42°C, $P < 0.0001$; **Figure 7A**) and an increase in lung Wet/Dry weight ratio (6.40 ± 1.07 vs. 4.71 ± 0.11, $P < 0.01$; **Figure 7B**). However, TRALI did not occur in non-transfused female mice or in female mice that received heat-inactivated male plasma (**Figures 7A and B**). The concentration of protein in the BALF of female mice with TRALI was significantly higher than that of female mice without plasma infusion (1855.56 ± 384.00 vs. 341.26 ± 58.91 μg/mL, $P < 0.0001$; **Figure 7E**). Additionally, lung tissue sections from TRALI female mice exhibited endothelial cell injury, cell infiltration, and fibrin deposition (**Figure 7F**).

To further strengthen our findings, we analyzed the development of TRALI in complement C5 gene-deficient mice ($C5^{-/-}$). TRALI was induced in $C5^{-/-}$ male mice by administration of mAb GZ1 in 2-hit model as described previously. As expected, $C5^{-/-}$ male did not exhibit a decrease in rectal temperature (37.68 ± 0.43 vs. 38.20 ± 0.31°C, $P > 0.05$; **Figure 8A**) or an increase in lung Wet/Dry weight ratio (4.80 ± 0.11 vs. 4.68 ± 0.15, $P > 0.05$; **Figure 8B**), compared to the isotype control.

3.6 Complement *C5a* plays a minor role in anti-CD36-mediated TRALI

Complement C5a is a pro-inflammatory anaphylatoxin that is synthesized after the cleavage of complement component C5. Its biological action is exerted by binding to its specific receptor C5aR1, also known as CD88 (54-56). A previous study indicated the contribution of complement C5a to anti-MHC class I-mediated TRALI (47). However, it is currently unknown whether anti-CD36-induced-TRALI also depends on complement C5a. To answer this question we injected complement C5a into $C5^{-/-}$ male mice and provoked TRALI with mAb GZ1. Surprisingly, the mice did not develop TRALI, as evidenced by a lack of a decrease in rectal temperature (37.88 ± 0.33 vs. 38.20 ± 0.31°C, $P > 0.05$; **Figure 8A**) nor an increase in lung Wet/Dry weight ratio (4.86 ± 0.09 vs. 4.68 ± 0.15, $P > 0.05$; **Figure 8B**). These results indicate that the C5a complement does not significantly contribute to the development of anti-CD36-induced TRALI.

To further verify our observations, we tested C5a receptor-1 deficient ($C5aR1^{-/-}$) male mice. As shown in **Figure 8**, the administration of mAb GZ1 in these mice led to the development of TRALI. Similar to wild-type mice ($C5aR1^{+/+}$), $C5aR1^{-/-}$ male mice exhibited a decrease in rectal temperature (31.94 ± 1.04 vs. 39.70 ± 0.19°C, $p < 0.0001$; **Figure 8C**) and an increase in

the lung weight Wet/Dry ratio (7.81 ± 0.65 vs. 4.78 ± 0.10, $p < 0.0001$; **Figure 8D**) compared to isotype control.

Recent studies have demonstrated that mice not only express C5aR1 but also the C5aR2 receptor (94). To dissect the possibility that the C5a receptor may be involved in the mechanism of anti-CD36-mediated TRALI, we performed inhibition experiments using a non-competitive antagonist of complement C5aR1 (PMX53) (95) and a C5aR2 selective functional ligand (P32) (96). However, infusion of both inhibitors did not prevent mice from developing anti-CD36 antibody-mediated TRALI. Compared to normal TRALI mice, PMX53 did not improve the degree of rectal temperature reduction (GZ1+PMX53 vs. GZ1: 31.87 ± 0.06 vs. 31.72 ± 0.71°C, $P > 0.05$; **Figure 8E**) and lung Wet/Dry weight ratio increase (GZ1+PMX53 vs. GZ1: 9.03 ± 1.10 vs. 8.24 ± 0.75, $P > 0.05$; **Figure 8F**). Compared to mice treated with GZ1 alone, P32 administration diminished TRALI, as shown by increased rectal temperature (GZ1 vs. GZ1+P32: 31.71 ± 0.71 vs. 33.24 ± 1.15°C; $P < 0.01$) and decreased lung wet/dry weight ratio (GZ1+P32 vs. GZ1: 8.24 ± 0.75 vs. 6.36 ± 1.41; $P < 0.01$) (**Figures 8E and F**). Compared to isotype-treated mice, there was no complete reduction in the lung wet/dry weight ratio in P32-treated mice (GZ1+P32 vs. isotype alone: 6.36 ± 1.41 vs. 4.49 ± 0.08, $P < 0.05$; **Figure 8F**). Although P32 did not prevent the occurrence of TRALI, it did reduce its severity, suggesting that C5aR2 may play a role in this process, which requires further investigation, especially in the C5aR2 knockout mouse model.

Activation of complement via classical, lectin, or alternative pathways triggers enzymatic cascade reactions that result in the formation of C3-cleaving enzymes (convertases) and subsequently C5 convertases. C5 convertases cleave C5 into C5a, a potent anaphylatoxin, and C5b, which nucleates formation of membrane attack complex (MAC) by sequentially binding C6 and C7. The C5b67 complex binds membranes and sequentially recruits C8 and C9 to complete the MAC (97). Our previous findings suggest that complement C5 activation is essential and C5a plays a very limited role. Therefore, C5b is important for anti-CD36-mediated TRALI, suggesting that C5b-induced MAC may be important for anti-CD36-induced TRALI.

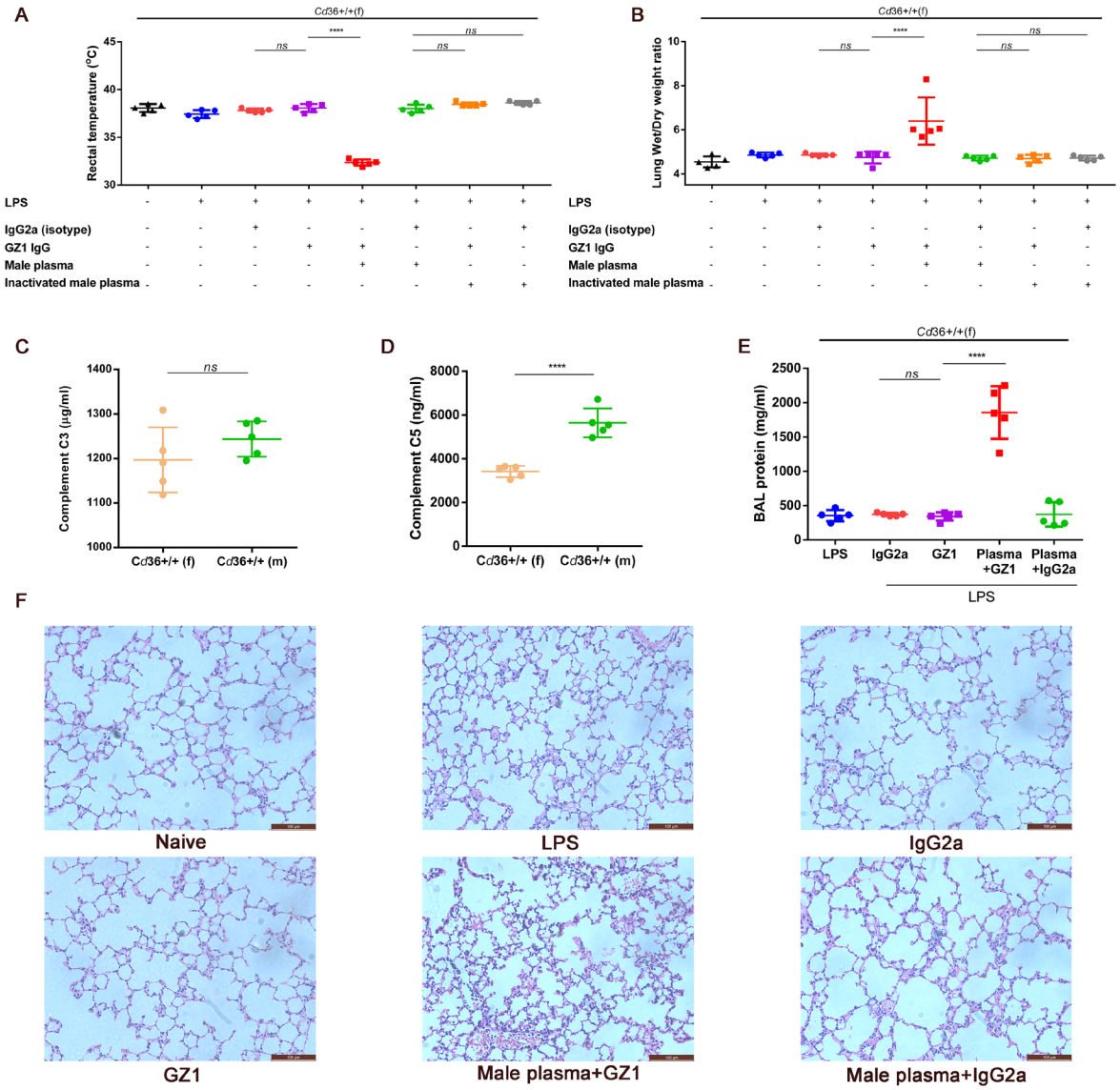

Figure 7. Female mice transfused with plasma from male mice induced TRALI by anti-CD36 administration.

(A) Rectal temperatures and (B) lung Wet/Dry weight ratios of female mice first untreated (–) or treated (+) with LPS, or then transfused with pooled male plasma or inactivated plasma for TRALI induction with mAb GZ1. The IgG2a isotype was used as control. The concentration of C3 (C) and C5 (D) in the serum of untreated *Cd36*$^{+/+}$ female and male mice. (E) Concentration of protein in the bronchoalveolar lavage of LPS pre-treated *Cd36*$^{+/+}$ female mice untreated or treated with plasma from male mice diluted with mAb GZ1. The IgG2a isotype were treated as control. (F) Histology performed on lung tissue from the indicated female mouse groups. Lung tissue sections were stained with hematoxylin and eosin (*H&E*), and images were taken at 20× magnification. Representative images of each indicated group are shown. Scale bars represent 100 μm. Statistical analysis was performed with 1-way ANOVA with Bonferroni's correction

for multiple comparisons (A, B, and E) or with a two-tailed unpaired Student's *t*-test (C and D). Each dot represents one mouse (n = 5 mice in each group), and error bars represent the SD. ****$P < 0.0001$, ns: Non-significant.

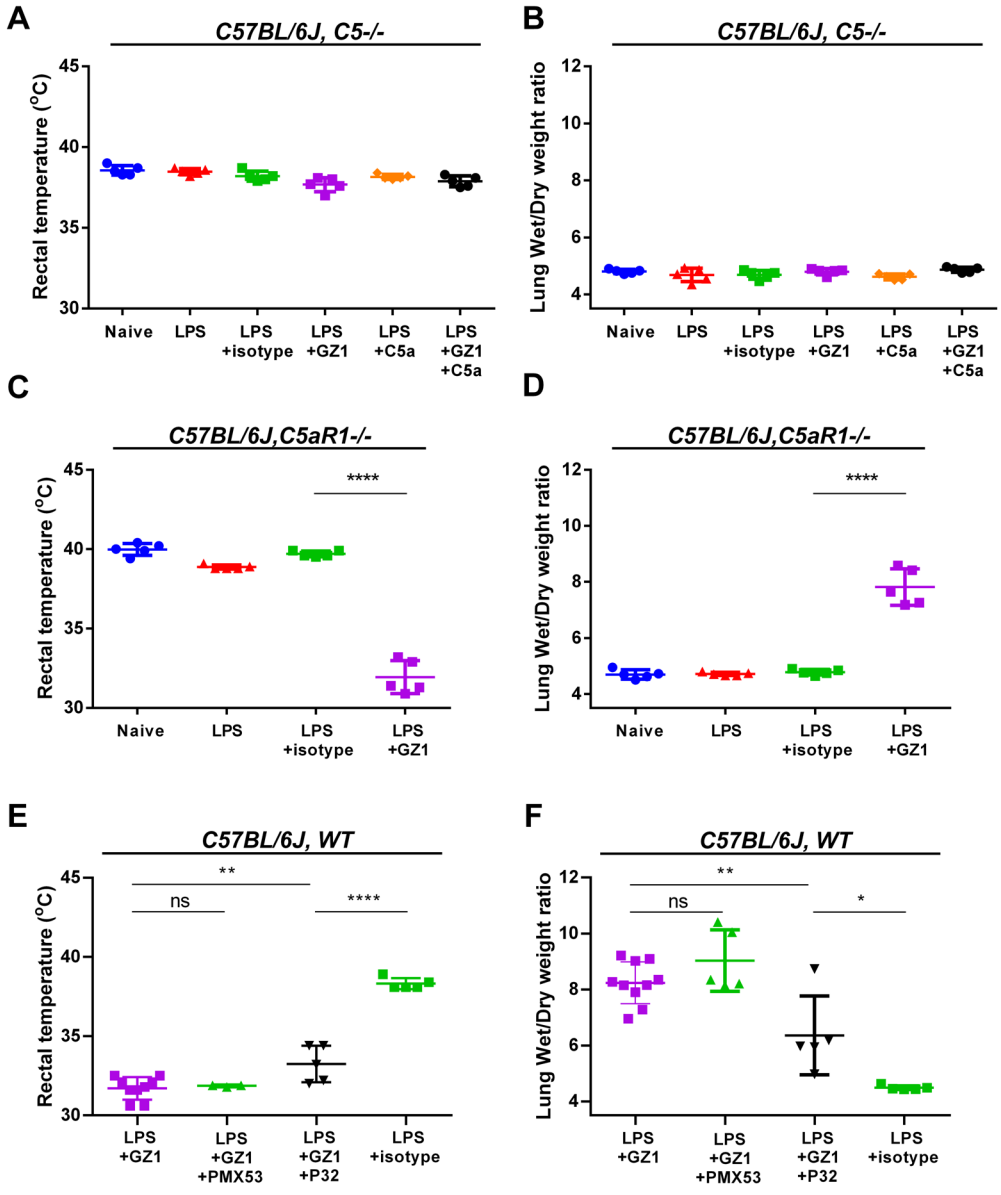

Figure 8. Analysis of anti-CD36–mediated TRALI in *C5*$^{-/-}$, *C5aR1*$^{-/-}$, and wild-type male mice receiving C5aR1 or C5aR2 agonist.

C5$^{-/-}$ and *C5aR1*$^{-/-}$ C57BL/6J male mice were treated with the indicated reagents. The signs of TRALI, including changes in rectal temperature and lung Wet/Dry weight ratios, in *C5*$^{-/-}$ mice (A, B), *C5aR1*$^{-/-}$ mice (C, D), and wild-type mice receiving C5aR1 agonist (PMX53) or C5aR2 agonist (P32) (E, F) are presented. For *C5*$^{-/-}$ mice (A, B), untreated wild-type mice (naïve) or those treated with lipopolysaccharide (LPS), LPS alone, or LPS and isotype control or mAb

GZ1 (0.4 mg/kg) were shown (n = 5 in each cohort).The rectal temperatures and lung Wet/Dry weight ratios of *C5*$^{-/-}$ mice supplemented with C5a (100 ng) and C5a together with mAb GZ1 (0.4 mg/kg) are shown (n = 5 in each cohort). Similar experiments to those performed for *C5*$^{-/-}$ mice (see above) were performed using *C5aR1*$^{-/-}$ mice (C, D). E and F show the rectal temperatures and lung wet/dry weight ratios of LPS-treated wild-type mice receiving either GZ1 mAb (n = 10), GZ1 and PMX53 (10 mg/kg; n = 5), or (P32: 3 mg/kg; n = 5) or isotype control (n = 5). Please note that rectal temperatures could only be measured in 3/5 in LPS+GZ1+PMX53 treated mice (two mice died within 30 min). Statistical analysis was performed with 1-way ANOVA with Bonferroni's correction for multiple comparisons. Each dot represents one mouse and error bars represent the SD. **** P <0.0001, ** P < 0.01, * P < 0.05, ns: non-significant.

3.7 *C5b-9* complement complex is upregulated in the lung tissues of TRALI mice

Activation of the terminal pathway, as determined by deposition of C5b-9, was detected by diaminobenzidine immunocytochemical staining in mouse lung tissue and BALF. Compared to the isotype control, the BALF C5b-9 concentration was significantly higher in mice treated with GZ1 (GZ1 vs. isotype: 91.32 ± 14.84 vs. 13.13 ± 0.30, P < 0.0001; **Figure 9A**). This upregulation was abolished when anti-C7 (mAb 73D1) IgG was administered to mAb GZ1-treated mice (**Figure 9A**). Furthermore, higher MAC deposition was detected on the lung tissues of mAb GZ1-treated mice compared to LPS-primed mice treated with isotype control, and this upregulation was reversed in TRALI mice pretreated with anti-C7 (**Figure 9B**). Anti-C7 can prevent the formation of the MAC, and prophylactic injection of anti-C7 can prevent the occurrence of TRALI. Moreover, anti-C7 can cure TRALI. These results indicate that after the activation of complement by anti-CD36 antibody, endothelial cell damage is caused by the production of the MAC, leading to the development of pulmonary edema and, eventually, TRALI.

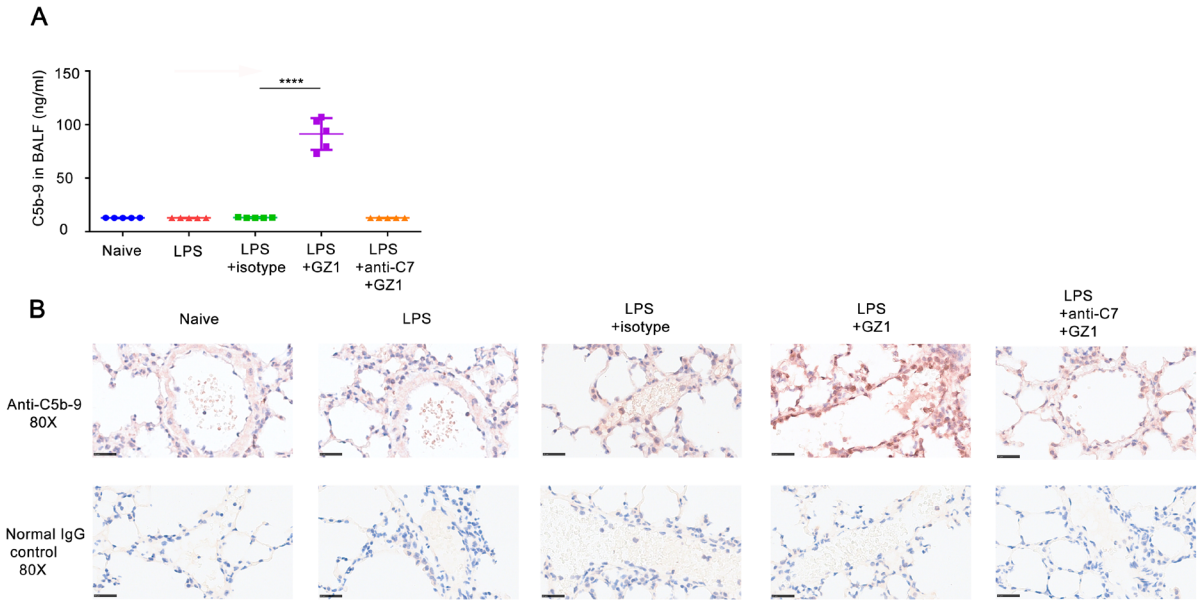

Figure 9. TRALI induced by anti-CD36 treatment led to the upregulation of C5b-9 in the lungs and could be inhibited by anti-C7.

(A) C5b-9 concentration in the BALF of untreated wild-type mice (naïve) compared to LPS pre-treated and received afterward mAb GZ1 (0.4 mg/kg), or isotype control, and pre-treated with anti-C7 before GZ1 (n = 5 in each group) were measured by ELISA. (B) Immunohistochemical detection of C5b-9 (MAC) in mice lung tissue from the indicated mouse groups. Lung tissue sections were stained with rabbit anti-C5b-9 (up panel) or normal rabbit IgG (normal IgG controls, down panel), and images were taken at x80 original magnification. Representative images from each indicated group are shown. Statistical analysis was performed with 1-way ANOVA with Bonferroni's correction for multiple comparisons. Each dot represents one mouse and error bars represent the SD. ****$P < 0.0001$.

3.8 Anti-CD36-induced TRALI can be prevented and cured using different inhibitors

3.8.1 Intravenous immunoglobulin (IVIG), anti-FcγRII/III antibodies and mAb GZ1 F(ab')$_2$ fragment

We previously showed that the F(ab')$_2$ fragment of GZ1 mAb did not induce anti-CD36-mediated TRALI, suggesting the involvement of the FcγR, and blockade of the activating FcγR by high-dose IVIG could silence the FcγR function (98). Compared to the control cohorts that

received HSA, intraperitoneal injection of IVIG (2 g/kg) prevented TRALI, as shown by the decrease in rectal temperature (37.68 ± 0.43 vs. 31.56 ± 0.65°C, $P < 0.0001$; **Figure 10A**) and the increase in lung wet/dry weight ratio (4.80 ± 0.11 vs. 8.26 ± 0.57, $P < 0.0001$; **Figure 10B**). We also examined the use of mAb 2.4G2 against FcγRII/III to block TRALI. Administration of mAb 2.4G2 (25 mg/kg) prior to TRALI induction did not show significant changes in rectal temperature (38.38 ± 0.30 vs. 32.52 ± 0.65°C, $P < 0.0001$; **Figure 10A**) or lung wet/dry weight ratio (4.84 ± 0.06 vs. 8.13 ± 0.33, $P < 0.0001$; **Figure 10B**) compared to the isotype control. High-dosed IVIG could silence the TRALI reaction, indicating the important role of FcγR in anti-CD36-mediated TRALI. In addition, mAb 2.4G2 against FcγRII/III could block the TRALI reaction, declared that anti-CD36 induced TRALI by interacting with FcγRII/III, but exactly how this works needs further investigation.

Typically, the removal of the Fc segment of an antibody eliminates the downstream reaction mediated by the Fc of the antibody (99). A previous study revealed that the $F(ab')_2$ of antibodies causes eliminates of the corresponding antigens from the circulation by homo-reactive antibodies (100). In this study, we tried a high concentration of GZ1 $F(ab')_2$ to silence GZ1-induced TRALI. Specifically, 200 µL of mAb GZ1 $F(ab')_2$ (5 mg/kg in PBS) was administered 30 minutes before TRALI was induced (prophylactic treatment).Additionally, the mAb GZ1 $F(ab')_2$ (5 mg/kg in PBS) was injected at the dose required after TRALI was induced (therapeutic treatment).

In prophylactic treatment, GZ1 $F(ab')_2$ completely prevented anti-CD36-induced TRALI. No change in rectal temperature (38.38 ± 0.30 vs. 32.12 ± 0.89°C, $P < 0.0001$; **Figure 11A**) and lung Wet/Dry weight ratio (4.28 ± 0.19 vs. 8.10 ± 1.00, $P < 0.0001$; **Figure 11B**) were observed compared to mice that did not receive any inhibitors (NT).

After TRALI induction, therapeutic treatment was initiated. The mice suffered serious TRALI compared to the mice that did not receive any inhibitors. A significant decrease in rectal temperature (32.70 ± 0.58 vs. 32.12 ± 0.89°C, $P > 0.05$; **Figure 11A**) and increase in lung Wet/Dry weight ratio (7.88 ± 0.65 vs. 8.10 ± 1.00, $P > 0.05$; **Figure 11B**) were observed, although the SR was not significantly higher compared to untreated TRALI mice (70 vs. 45%, $P > 0.05$; **Figure 11C**).

During CD36 antibody-mediated TRALI, we observed a significant drop in the rectal temperature of mice 3 min after the injection of anti-CD36 antibody (0.18 ± 0.13 vs. -0.63 ± 0.49°C, $P < 0.01$; **Figure 11D**), which we considered as the beginning of TRALI.

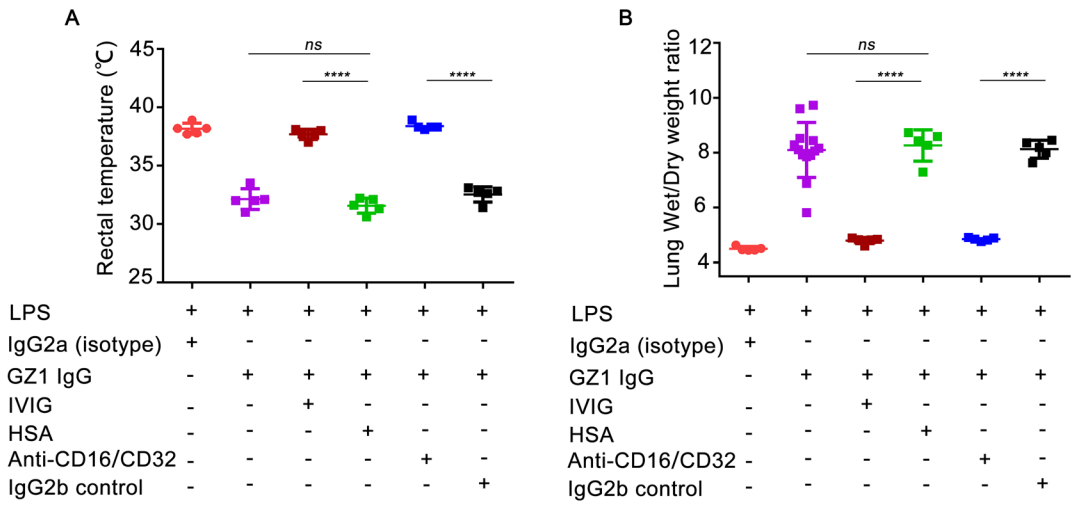

Figure 10. Anti-CD16/CD32 or IVIG prophylactic treatment prevents anti-CD36-induced TRALI in mice. (A) Rectal temperatures and (B) lung Wet/Dry weight ratios of LPS pre-treated male mice were first prophylactically treated with anti-CD16/CD32 or IVIG before administering mAb GZ1 IgG. Isotype IgG2b or HSA was used as a control. Statistical analysis was performed using 1-way ANOVA with Bonferroni's correction for multiple comparisons. Each dot represents one mouse (n = 5 in each group) and error bars represent the SD. ****$P <$ 0.0001, ns: non-significant.

3.8.2 NAC antioxidant

NAC is recommended as a potential treatment option for different disorders resulting from the generation of free oxygen radicals (92). Our previous in vitro assay showed that NAC prevented anti-CD36-activated monocytes from generating ROS (**Figure 6C**). In this study, we attempted to prevent and treat anti-CD36-mediated TRALI in vivo. Specifically, 200 µL of NAC solution (10 mg in saline; Sigma) was administered 5 min before TRALI was induced (prophylactic treatment). For therapeutic treatment, NAC was injected at the required dose after TRALI was induced 3 min after the rectal temperature dropped by 0.5°C, which we considered the onset of TRALI (**Figure 11D**). In addition, aerosolized NAC was administered for 20 min after NAC injection into the inhalation chamber.

In prophylactic treatment, NAC completely prevented anti-CD36-induced TRALI with no significant decrease in rectal temperature (38.06 ± 0.41 vs. 32.12 ± 0.89°C, $P < 0.0001$; **Figure 11A**) or increase in lung Wet/Dry weight ratio (4.17 ± 0.17 vs. 8.10 ± 1.00, $P < 0.0001$; **Figure 11B**) compared to the mice that did not receive any inhibitors.

In therapeutic treatment, the mice did not exhibit significant decrease in rectal temperature (31.90 ± 0.33 vs. 32.12 ± 0.89°C, $P > 0.05$; **Figure 11A**) and increase in lung Wet/Dry weight ratio (7.16 ± 0.97 vs. 8.10 ± 1.00, $P > 0.05$; **Figure 11B**) compared to the typical TRALI in the mice that did not receive any inhibitors. Although NAC treatment did not significantly improve the rectal temperature and lung Wet/Dry weight ratio, it significantly increased the survival rate of mice (85 vs. 45%, $P < 0.01$; **Figure 11C**), indicating that NAC is effective in treating TRALI.

3.8.3 Anti-C5 antibody (mAb BB5.1)

Based on our previous research and literature reports on the pathogenesis of TRALI, complement plays a pivotal role in anti-CD36-mediated TRALI, while complement depletion prevents mice from developing anti-CD36-induced TRALI. Among complement proteins, C5 plays a major role in complement-mediated inflammation (86). Therefore, research on drugs for complement therapy has mainly focused on complement C5 (101).

Specifically, 200 µL of mAb BB5.1 (anti-C5, 1 mg/200 µL in PBS) was administered 30 min before TRALI was induced (prophylactic treatment). In addition, the mAb BB5.1 (1 mg/200 µL in PBS) was injected at the dose required after TRALI induction (therapeutic treatment).

In prophylactic treatment, there was no significant decrease in rectal temperature (38.02± 0.22 vs. 32.12 ± 0.89°C, respectively, $P < 0.0001$; **Figure 11A**) or increase in lung wet/dry weight ratios (4.67 ± 0.20 vs. 8.10 ± 1.00, $P < 0.0001$; **Figure 11B**) compared to mice that did not receive any inhibitors.

In therapeutic treatment, the improvement in lung wet/dry weight ratios was more significant when the BB5.1 mAb was administered post-TRALI compared to those in the untreated TRALI group (5.33 ± 1.04 vs. 8.10 ± 1.00, $P < 0.0001$; **Figure 11B**). As a result, all mice survived post-induction treatment with the BB5.1 mAb (SR 100%), whereas only 85 and 70% of the mice survived after treatment with NAC and GZ1 $F(ab')_2$, respectively (**Figure 11C**).

Relevant complement levels were measured in serum collected from male TRALI mice, and significantly higher plasma C5a levels (15.35 ± 3.56 ng/mL) were detected after TRALI induction with the GZ1 mAb compared to those treated with LPS alone (5.11 ± 0.66 ng/mL, $P < 0.0001$) and naïve controls (4.02 ± 0.37 ng/mL, $P < 0.0001$; **Figure 11E**). The C5a levels remained unchanged following pre-treatment of mice with the neutralizing BB5.1 mAb against C5 before TRALI induction with the GZ1 mAb (5.51 ± 1.03 vs. 5.11 ± 0.66 ng/mL, $P > 0.05$;

Figure 11E). Previous studies have shown that anti-C5 can inhibit the activation of complement C5 and decrease the production of complement C5a (86).

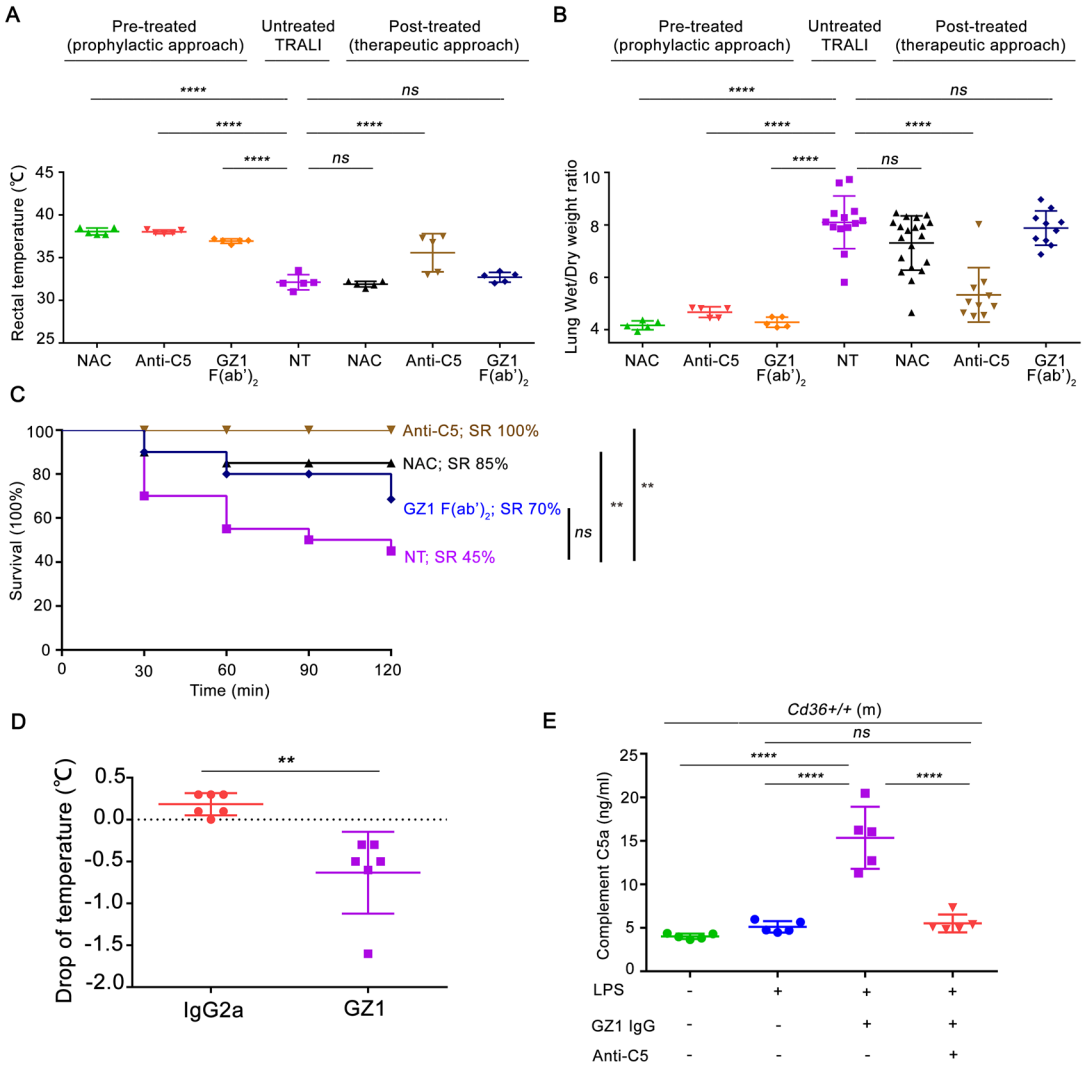

Figure 11. Anti-C5 not only prevents, but also completely rescues mice from anti–CD36–mediated TRALI.

In the prophylactic approach, GZ1 F(ab')$_2$ (n = 5), NAC (n = 5), or anti-C5 (n = 5) was used as pretreatment before TRALI induction with the mAb GZ1. In the therapeutic approach, TRALI was first induced using the mAb GZ1. The mice were treated with GZ1 F(ab')$_2$ (n = 10), NAC (n = 20), or anti-C5 (n = 10) after TRALI. Untreated TRALI mice (NT) were treated as controls (Ctrl). (A) Rectal temperatures and (B) lung Wet/Dry weight ratios were measured as described above. (C) SRs of *Cd36*$^{+/+}$ male mice treated with different inhibitors after TRALI induction were analyzed. (D) The drop of rectal temperature in three min after TRALI induction. LPS pre-treated *Cd36*$^{+/+}$ male mice were treated with mAb GZ1 (0.4 mg/kg) or isotype IgG2a (0.4 mg/kg), respectively. Rectal temperatures were measured three min after antibody injection. (E) Concentrations of C5a in untreated, LPS-treated, LPS plus GZ1-treated, and LPS-pretreated

GZ1 plus anti-C5-treated *Cd36*$^{+/+}$ male mice. Statistical analysis was performed with 1-way ANOVA with Bonferroni's correction for multiple comparisons (A, B, and E) or with a log-rank test (C), or with a two-tailed unpaired Student's *t*-test (D). Each dot represents one mouse and error bars represent the SD. ****$P < 0.0001$, **$P < 0.01$, ns: non-significant.

3.8.4 Anti-C7 (mAb 73D1)

Previous studies have shown that the TRALI-induced anti-CD36 antibody is dependent on complement C5 activation, and that anti-C5 (BB5.1) can prevent and treat TRALI induced by anti-CD36 antibody. BB5.1 has been reported to prevent C5 cleavage and C5a generation in vivo (86). The absence of complement C5a in anti-CD36 antibody-induced TRALI was confirmed through *C5aR1*$^{-/-}$ mouse, C5a reinfusion into *C5*$^{-/-}$ mouse, and C5aR antagonist experiments. The activation of complement by the CP triggers an enzymatic cascade reaction that leads to the formation of C3 cleavage enzymes (convertases) and subsequently C5 convertases. These cleave C5 into C5a, a potent anaphylatoxin, and initiates the formation of the anaphylatoxin, and C5b, which initiates the formation of the MAC by sequentially binding C6 and C7. The C5b67 complex then binds membranes and sequentially recruits C8 and C9 to complete the MAC (86). Therefore, TRALI induced by anti-CD36 antibody is most likely caused by the MAC formed by C5b, which is generated by complement C5 activation along with other terminal complexes of complement. Previous studies have reported that anti-C7 antibody (73D1) can inhibit complement for more than 48 h in vivo (87). Therefore, in the study of anti-CD36 antibody-mediated TRALI, 73D1 was used to prevent and treat TRALI. For prophylactic treatment, 73D1 was administered 0.5 h before anti-CD36 administration. For therapeutic treatment, 73D1 was injected 3 min after anti-CD36 infusion, as described previously for anti-C5.

TRALI was completely prevented when the anti-C7 IgG or F(ab')$_2$ fragment was administered before the induction of TRALI with GZ1 mAb. The rectal temperature of mice treated with GZ1 + anti-C7 IgG (37.30 ± 0.27°C) or GZ1 + anti-C7 F(ab')$_2$ (37.66 ± 0.18°C) was significantly higher than that of mice treated with GZ1 + PBS (34.44 ± 1.56°C, $P < 0.001$; **Figure 12A**). Accordingly, a significantly higher lung W/D weight ratio was found in the GZ1 + PBS group than in the GZ1 + anti-C7 IgG or F(ab')$_2$ treatment group (8.03 ± 1.42 vs. 4.78 ± 0.30 and 4.75 ± 0.17, $P < 0.0001$, respectively; **Figure 12B**). SR analysis using Kaplan–Meier curves showed that only 60% (6/10) of the GZ1+PBS-treated mice survived beyond 2 h after

TRALI induction with mAb GZ1 compared to 100% survival in the anti-C7 IgG and F(ab')$_2$ treatment group (**Table 5**). Similar results were obtained in LPS-primed mice after TRALI induction with mAb GZ1 when anti-C7 IgG or F(ab')$_2$ was administered. A significant decrease in the lung W/D weight ratio was observed in mice treated with GZ1 + anti-C7 (IgG or F(ab')$_2$: 6.36 ± 1.64 or 6.54 ± 1.53, respectively) compared to mice treated with GZ1 + PBS (9.28 ± 0.64, $P < 0.0001$; **Figure 12B**). Additionally, 90% (9/10) and 100% (10/10) of the anti-C7 IgG and F(ab')$_2$, treated mice, respectively survived severe TRALI, whereas the survival rate was only 20% (2/10) in the PBS treatment group (**Table 5**).

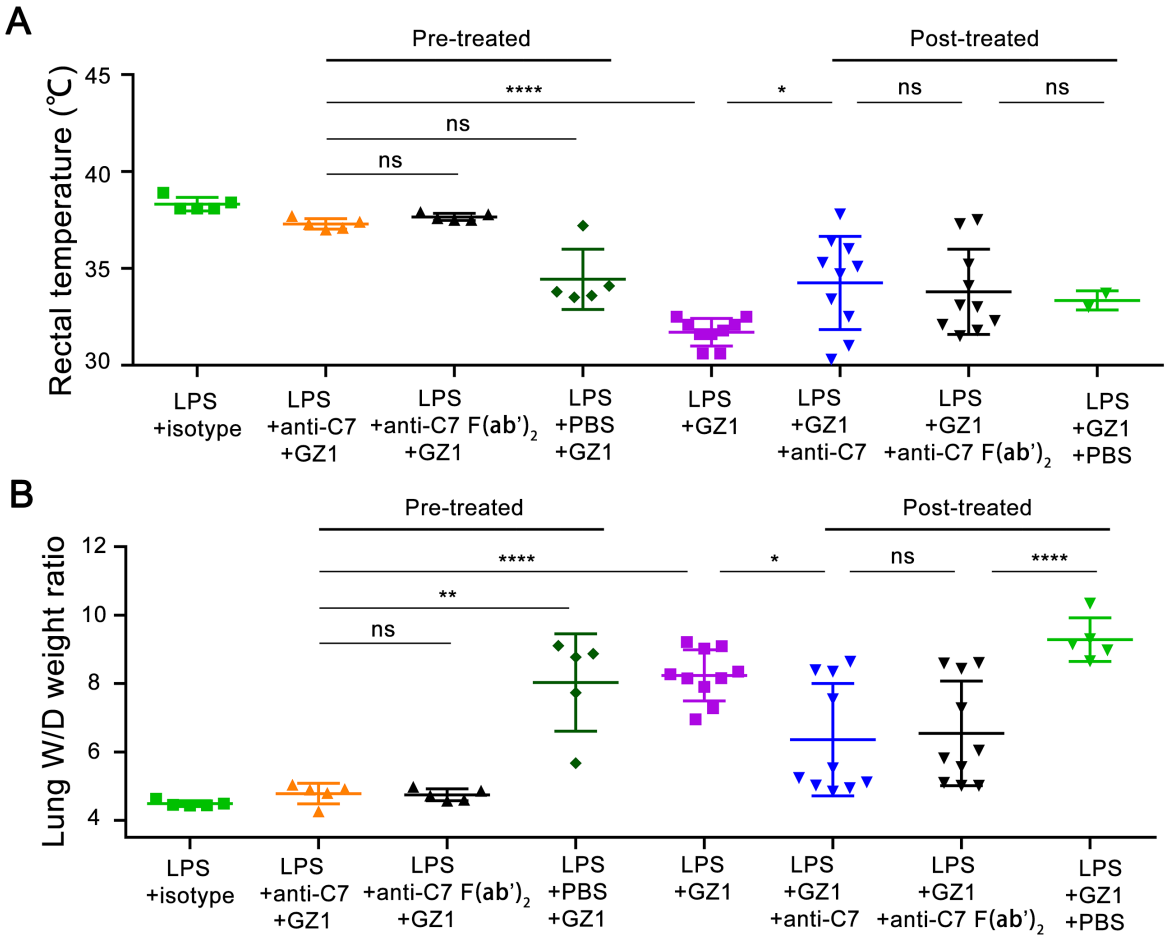

Figure 12. Anti-C7 prevents and rescues mice from anti-CD36-mediated TRALI. In the prophylactic approach, anti-C7 (dose: 1 mg/200 µL in PBS; n = 5), or anti-C7 F(ab')$_2$ (dose: 1 mg/200 µL in PBS; n = 5) was administered before TRALI induction with mAb GZ1 (0.4 mg/kg). In the therapeutic approach, TRALI was first induced with mAb GZ1 (0.4 mg/kg), then mice were treated with anti-C7 (dose: 1 mg/200 µL in PBS; n = 10), or anti-C7 F(ab')$_2$ (dose: 1 mg/200 µL in PBS; n = 10) after TRALI. PBS was treated as a control. (A) Rectal temperatures and (B) lung Wet/Dry weight ratios were measured as described above. (C) SRs of mice were analyzed in different groups. Statistical analysis was performed with 1-way

ANOVA with Bonferroni's correction for multiple comparisons (A and B) or with a log-rank test (C). Each dot represents 1 mouse and error bars represent the SD. *$P < 0.05$, **$P < 0.01$, ***$P < 0.001$, ****$P < 0.0001$, NS: non-significant.

Table 5. Survival rates of anti-CD36–mediated TRALI mice that recieved prophylactic and therapeutic treatments with anti-C7 IgG or F(ab')$_2$

			pre-treatment[1)]			post-treatment[2)]		
Time (min)	**Isotype**	**GZ1**	**anti-C7 IgG + GZ1**	**anti-C7 F(ab')$_2$ + GZ1**	**PBS + GZ1**	**GZ1 + anti-C7 IgG**	**GZ1 + anti-C7 F(ab')$_2$**	**GZ1 +PBS**
0	5	10	5	5	5	10	10	5
30	5	9	5	5	5	10	10	2
60	5	7	5	5	4	9	10	1
90	5	5	5	5	3	9	10	1
120	5	5	5	5	3	9	10	1
Survival rate of 2h	**100%**	**50%**	**100%**	**100%**	**60%**	**90%**	**100%**	**20%**

1) Anti-C7 or PBS was administered before TRALI induction with mAb GZ1; 2) Anti-C7 or PBS was administered after TRALI induction with mAb GZ1.

4. DISCUSSION

In this study, we developed a murine model of anti-CD36-induced TRALI and found that murine mAbs and human antibodies against CD36 induced severe TRALI in *Cd36*$^{+/+}$ male mice, but not in *Cd36*$^{+/+}$ female and *Cd36*$^{-/-}$ male mice. This TRALI response was only observed in the presence of a low dose of LPS (2-hit model) and was characterized by increased lung Wet/Dry weight ratios; decreased rectal temperatures; decreased PaO_2 and SaO_2; and increased protein, chemokine (KC, MIP-2), and cytokine (TNF-α) concentrations in BALF. This reaction depends not only on the sex of the mice but also on the Fc part of the antibodies, the presence of monocytes, ROS generation by monocytes, TNF-α production, complement C5 and C7 activation and complement C5b-9 deposition in lung tissues.

4.1 Mouse and human anti-CD36 antibodies induce severe TRALI in a 2-hit mouse model

A 1997 retrospective study found that PMN-priming activity was significantly higher in human patients with TRALI who had an underlying infection, cytokine administration, recent surgery, or massive transfusion than in transfused controls who did not develop TRALI (28). Therefore, it is proposed that TRALI may be a 2-hit model. The first event triggers an inflammatory response, which activates the pulmonary endothelium. This promotes the priming and emigration of PMNs into the lung vasculature, followed by their adherence to activated endothelial cells. The second hit is induced by biologic response modifiers or passively transferred antibodies via transfusion induce. This primes/adheres PMNs to release cytokines and ROS, leading to pulmonary endothelial damage, capillary leakage, and lung injury (42). Looney et.al developed a TRALI mouse model with anti-MHC class I for the first time using the 2-hit model theory. The model successfully induced TRALI symptoms, such as rectal temperature reduction and pulmonary edema, in mice through a low-dose LPS intraperitoneal injection as the first hit and tail vein injection of anti-MHC class I as the second hit (76).

In our anti-CD36-mediated TRALI mouse model, we revealed that, without LPS as the first hit, anti-CD36 antibody injection alone did not decrease the rectal temperature or increase the lung Wet/Dry weight ratio in *Cd36*$^{+/+}$ male mice. Based on the 2-hit TRALI model (76), intraperitoneal injection of LPS was administered to *Cd36*$^{+/+}$ male mice at a low dose (0.1 mg/kg) as the first hit, followed by the administration of anti-CD36. Subsequently, a drop in rectal temperature and

increase in lung Wet/Dry weight ratio were observed, which were treated as the parameters of a typical TRALI response (60, 76, 80, 102). Studies have found that the second-hit principle of TRALI may be related to the gut microbiota (103). Untreated barrier-free (BF) mice suffer from severe antibody-mediated ALI, whereas more sterile-housed SPF mice and gut flora-depleted BF mice were both protected from lung injury. Moreover, BF fecal matter transferred into SPF mice significantly restored TRALI susceptibility. In this anti-CD36-mediated TRALI model, all mice were housed under SPR conditions, which may have decreased their sensitivities to TRALI. Given that anti-CD36 from human sera could also induce TRALI in our murine model is likely due to the high degree of homology (around 85%) between the human and mouse CD36 protein (89) and the fact that most CD36 antibodies have been shown to react with immunodominant epitopes (69, 104). Therefore, the mouse model of TRALI mediated by anti-CD36 antibodies may be more similar to the human situation and better reflect the pathological process of TRALI.

4.2 Anti-CD36-induced TRALI is dependent on monocytes but not neutrophils

The contributions of different cell types to TRALI pathogenesis have become increasingly clear (1). It is commonly believed that antibody-mediated TRALI results from pulmonary damage caused by neutrophils. Interestingly, neutrophil-deficient patients have also been described as developing TRALI (105), and histochemical staining of lung sections from patients who died of TRALI does not always show neutrophil influx into the alveolar space (106). However, the pathogenic roles of other cells, including monocytes, macrophages, endothelial cells, and platelets have been well studied (1, 75, 81, 90, 107-109). Nevertheless, these cellular pathways remain complex and somehow depend on antibody specificities (1).

We found that anti-CD36 could still induce TRALI in the absence of neutrophils. In other TRALI models, neutrophil depletion completely protected mice against anti-MHC class I–mediated TRALI (74). This discrepancy is most likely due to the fact that neutrophils do not express CD36 antigens (91). A previous study demonstrated that HLA-DR is inducible in human neutrophils both in vitro and in vivo by IFN-γ or GM-CSF (110), suggesting that neutrophils play a more important role in anti-HLA class II-mediated TRALI (111). However, whether this is also true for CD36 is currently unknown. To study the role of neutrophils in TRALI, neutrophils are usually depleted in mice by injection of neutrophil antibodies, most

commonly Rb68c5 (anti-GR-1/Ly6G/C) (47, 60). However, previous studies have shown that anti-GR-1 not only recognizes neutrophils but also binds to Gr-1^+ monocytes (112). To remove neutrophils more specifically without affecting monocytes, we used another neutrophil-specific antibody, 1A8 (Anti-Ly6G mAb), which reduced blood neutrophils but not Gr-1^+ monocytes (112). As expected, when combined with hydroxyurea, 1A8 removed more than 90% of neutrophils, with little effect on the number of monocytes (Figure 13). After neutrophil depletion, anti-CD36-induced TRALI was observed in mice. However, the SR of neutrophil-depleted mice was higher than that of non-depleted mice (SR 65 vs. 45%), indicating that neutrophils may contribute to the severity of TRALI. Further studies are required to determine the role of neutrophils in anti-CD36-mediated TRALI.

Several studies have shown that monocytes are indispensable for the mechanism of antibody-mediated TRALI (47, 75, 80). Sachs et al. showed that antibodies against MHC class II antigens, which are expressed on monocytes, but not on neutrophils, triggered TRALI in an ex-vivo rat model (113). It was found that monocytes could be activated when incubated with matched HLA class II antibodies, and that matched monocyte supernatants can activate neutrophils to produce ROS, which may disturb endothelial permeability. However, anti-HLA class II-mediated TRALI was still induced in the ex vivo rat lung model in the absence of neutrophils.

In anti-MHC class I murine models, depletion/inactivation of monocytes/macrophages completely suppressed TRALI (47, 48, 75, 80). McKenzie et al. found that anti-MHC class I first binds to its cognate on blood monocytes, which generates MIP-2 chemokine production (80). TRALI induction by the intact antibody was completely abrogated by in vivo peripheral blood monocyte depletion or chemokine blockade with a MIP-2 receptor antagonist. In another study, macrophages were identified as the cellular source of Osteopontin (OPN), and OPN knockout (KO) mice were resistant to anti-MHC class I antibody-mediated TRALI induction (75). Strait et al. found that anti-MHC class I bonding to nonhematopoietic cells drives complement activation by Fc receptors to produce complement C5a, which stimulates macrophages to secrete reactive oxygen intermediate ROIs resulting in anti-MHC class I-mediated TRALI that could be prevented by ROI inhibition (47).

In this study, we demonstrated that depletion of monocytes abolished anti-CD36-induced TRALI. Normal lung Wet/Dry weight ratios and rectal temperatures were detected in monocyte-depleted mice, and no pulmonary edema or inflammatory cell aggregation was found in pathological sections. All mice survived (SR 100%), indicating a pivotal role for monocytes in anti-CD36-mediated murine TRALI. It has been demonstrated that gp91phox knock-out

mice were completely protected from TRALI induced by anti-MHC class I antibodies, suggesting that the formation of ROS is important for the development of TRALI (74). We found that anti-CD36 could induce ROS production, which could be inhibited by the antioxidant NAC, both in vitro and in vivo. This suggests that ROS also plays a key role in anti-CD36-induced TRALI.

4.3 Platelets are dispensable for the development of anti-CD36-induced TRALI

The role of platelets in TRALI has been less well-defined (108, 109). Platelets are traditionally recognized for their role in blood clotting, and hemostasis. However, over the past decade, it has become increasingly evident that platelets also fulfill non-hemostatic immune functions, particularly during inflammatory conditions. These immune functions include targeting pathogens via surface immune receptors, such as Toll-like receptors, and triggering the formation of neutrophil extracellular traps (NETs). Additionally, platelets communicate with various immune cells by secreting cytokines or shedding platelet microparticles (114-116). In light of the established correlation between inflammation and the development of TRALI, and given the recognized functionality of platelets in immune sensing, researchers have proposed the potentially significant role of platelets in the pathogenesis of TRALI. This assumption is based on two observations. First, mild thrombocytopenia is frequently observed in patients with TRALI (1). Second, a similar phenomenon has been observed in a mouse model of TRALI (76, 102). In our anti-CD36-mediated TRALI mouse model, we also observed a decrease in platelets in the peripheral blood of mice with TRALI (data not shown). However, the platelet counts may be related to hemostatic function and is not necessarily involved in TRALI development.

Some studies have found that recipient platelets are pathogenic (76, 117), whereas others have found that they are dispensable for the onset of TRALI (47, 118). This discrepancy may be caused by different factors, including different experimental methodologies. Looney et al. initially depleted platelets with rabbit anti-mouse platelet serum, and aspirin was shown to protect mice against anti-MHC class I-mediated TRALI (76). However, another research team found that this anti-platelet serum approach only lasted for 4 h and did not prevent TRALI after more than 24 h. It was also found that TRALI still develops after using neuraminidase therapy to deplete platelets through non-immune mechanisms (47). The researchers concluded that platelets are not involved in TRALI pathogenesis. In another study, platelets were found to be

a predisposing factor for NET formation, suggesting that platelets are essential for TRALI (117). However, platelet depletion does not prevent the expression of NET biomarkers in the lungs of TRALI mice (118). Furthermore, Hechler et al. depleted platelets with diphtheria toxin (DT) in PLT factor 4-Cre/inducible DT receptor mice or by infusion of anti-glycoprotein (GP)Ibα antibody. TRALI was still induced with these two methods of platelet depletion, indicating that platelets are not required in the development of TRALI (119). However, the authors identified a requirement for PLTs in preventing lung hemorrhage, suggesting that the hemostatic function of platelets may also reduce the severity of TRALI. Cognasse et al. also confirmed that neither inhibition of platelet activity after antiplatelet depletion nor inhibition of platelet activity by protease receptor 4 pathway inhibitors prevented the development of TRALI, but that platelet depletion did reduce its severity (81).

In our murine model, platelet depletion was performed by anti-GPIbα 24 h before anti-CD36 administration, and this depletion aggravated the severity of anti-CD36-induced TRALI. The SR of the mice in this cohort (SR 10%) was much lower than that of the controls. Moreover, massive hemorrhage was observed in the histopathological sections of the lungs of TRALI mice depleted of platelets. In addition to the signs of TRALI, a bleeding tendency was observed in our mice, indicating that platelets may maintain vascular integrity in anti-CD36-mediated TRALI (120).

4.4 Anti-CD36-induced TRALI depends on Fcγ receptors

The role of Fc receptors in mouse TRALI was first investigated by Loony et al. who found that FcRγ$^{-/-}$ mice are protected against anti-MHC class I–induced TRALI (60), indicating the crucial role of the FcγR in anti-MHC class I-induced murine TRALI. However, in another study, the role of Fc receptors was found to be limited. Strait et al. reported that BALB/c background FcRγ-deficient mice developed slightly less severe disease than WT mice (47). Moreover, mice deficient in the stimulatory FcγRs FcγRIII, FcγRI, or both FcγRI and FcγRIII still developed severe mTRALI, as did FcγRI/FcγRIII double-deficient mice treated with a blocking anti-FcγRIV mAb, demonstrating the trivial effect of deleting or blocking all stimulatory FcγRs on mTRALI. However, Fc-blocking mAb 2.4G2 against CD16/CD32, which cross-links both the stimulatory receptor FcγRIII and the inhibitory receptor FcγRIIb (121), completely prevented anti-MHC class I-induced TRALI (47). This suggested that 2.4G2 inhibits mTRALI by activating the inhibitor receptor, FcγRIIb, rather than by blocking FcγRIII. Since the discovery,

more than 30 years ago, that IVIG therapy can improve immune thrombocytopenia, the use of IVIG preparations has been extended to various autoimmune and inflammatory diseases (122). Along this line, prophylactic injection of IVIG also prevented TRALI, and treatment with IVIG after TRALI induced by anti-MHC class I also reduced lung damage and mortality (77). In addition, the protective effects of IVIG against lung damage were Fc-dependent as $F(ab')_2$ fragments prepared from IVIG were not effective in reversing lung damage. Fc-dependent mechanisms play a role in the activity of IVIG in both mice and humans. These mechanisms may involve blocking activating Fcγ receptors (FcγRs) or the neonatal Fc receptor (FcRn), expanding regulatory T cell populations, increasing the expression of the inhibitory receptor FcγRIIb, and modulating dendritic cell activity (122).

In our anti-CD36-mediated TRALI mouse model, we found that the $F(ab')_2$ fragment of anti-CD36 could not induce TRALI indicating the role of FcγRs. Moreover, pretreatment with mAb 2.4G2 and IVIG prevented the development of TRALI in our mice, strengthening the role of FcγR in anti-CD36-mediated TRALI. The question of whether activating or inhibitory FcγR is involved in our anti-CD36-mediated TRALI is intriguing and requires further investigation (123). The Fc segment of the antibody not only binds to the Fc receptor but also activates complement (124), the TRALI depends on the ability of the antibody Fc domain to induce activates complement (125).

A previous study demonstrated that anti-HNA-3a could bind to CTL-2 expressed on endothelial cells and induce endothelial barrier disturbance (126). In contrast, our in vitro experiments revealed a minor role for endothelial CD36 in anti-CD36-mediated TRALI. First, we observed low CD36 expression on the surface of HLMVECs. Second, direct priming with anti-CD36 serum did not alter the permeability and resistance of HLMVECs. However, we found that priming monocytes with anti-CD36 antibodies caused TNF-α secretion in the supernatant and upregulation of CD36 expression in monocytes when they interacted with TNF-α-activated endothelial cells. Incubation of HLMVECs with TNF-α-rich supernatants from anti-CD36 primed monocytes increased endothelial permeability and decreased endothelial resistance, supporting an important pathogenic role for monocytes.

4.5 Anti-CD36-induced TRALI is caused by complement C5b-9, not C5a

Although increasing evidence indicates that complement is an important mediator of lung injury in TRALI, this has not yet been systematically investigated (127). In human studies, Ambruso

et al. reported complement activation in two anti-HLA class II-mediated TRALI patient samples that were absent in pre-transfusion samples (58). Currently, the role of complement in TRALI is primarily studied using animal models. Müller et al. conducted a study using a murine model of TRALI, induced by LPS priming and infusion of an anti-MHC class I antibody (128). In the present study, we found increased levels of C3a and C5a in BALF. The pulmonary levels of C3a were attenuated by C1-INH treatment, which was associated with improved lung injury scores. However, there was no significant effect on C5a levels in BALF. Strait et al. found that anti-MHC class I antibodies bound to nonhematopoietic cells activated complement, leading to C5a production and monocyte recruitment to the lungs of mice, resulting in endothelial cell damage (47). Mice deficient in C3, C5, or C5a receptor (C5aR) were protected from TRALI. The requirement for C5a for TRALI induction was suggested to be related to the fact that only adult male mice were susceptible to anti-MHC class I-mediated TRALI, whereas adult female mice were resistant. Female mice have approximately 25% less plasma C5 than male mice. In addition, the C5 subtype is present in male mice but absent in females, which may partially explain the varying susceptibility of sexes to TRALI between sexes (47). It has been demonstrated that female BALB/c mice injected with anti-MHC class I mAb developed mTRALI if they were first administered plasma from male WT or C3-deficient mice, but not if they were first administered plasma from female WT mice or C5-deficient males (47). One recent study demonstrated complement activation on the surface of endothelial cells as shown in the murine model of anti–MHC class I-mediated TRALI (62). MHC class I proteins were selectively removed from the surface of endothelial cells, megakaryocyte-platelet lineage, neutrophils and monocytes, and $Ly6C^{lo}$ monocytes, and only removal of MHC class I from the endothelium was found to be protective in anti–MHC class I–mediated lung injury. Collective analysis of the available data indicates that the engagement of antibodies directed towards platelets, neutrophils, or $Ly6C^{lo}$ monocyte MHC class I is not a prerequisite for the initiation of TRALI. Detection of complement C3 deposits in lung tissue indicates complement fixation onto pulmonary endothelial cells, resulting in lung platelet retention and edema in anti-MHC class I-mediated lung injury. Furthermore, complement activation was investigated in patients with TRALI, with the findings revealing that the plasma C4d levels and C4d/C4 ratios were higher in patients with TRALI than in transfused controls without TRALI. Recently, the same research team found that anti-MHC class I recognizes the MHC class I antigen on endothelial cells, which facilitates IgG Fc-Fc interactions and IgG hexamer assembly, and that the IgG hexamer activates C1 complexes to trigger complement-dependent TRALI (63). Antibody

carbamylation, the K439E Fc mutation, and treatment with domain B from staphylococcal protein A were used to block alloantibody hexamerization, all of which were found to reduce lung injury. A recent study confirmed that complement activation is necessary for TRALI (61). It was found that TRALI was related to an increase in the transport of macrophages from lung tissue to the blood induced by complement C5a and the formation of NET (61), and that complement C5a levels were elevated in the plasma of patients with TRALI.

Accordingly, in our anti-CD36-mediated TRALI model, we found that the $F(ab')_2$ fragments of mAb GZ1 did not induce TRALI, and that depletion of complement or inhibition of C5 with anti-C5 (BB5.1) completely prevented the occurrence of anti-CD36-mediated TRALI (129). BB5.1 efficiently inhibited C5 in mouse serum and prevented C5 cleavage and C5a generation (86). The role of C5 may explain the observation that anti-CD36 antibodies did not cause TRALI in female mice, in agreement with the literature (93), C57BL/6J female mice had much lower plasma C5 levels than male mice. Furthermore, we found that anti-CD36 treatment could trigger the generation of C5a, which is involved in the recruitment of several inflammatory leukocyte types (130). C5a enhanced TNF-α release by LPS-stimulated monocytes and macrophages (131, 132), and recent data showed that binding of C5a to C5aR on monocytes could lead to ROS generation and secretion of inflammatory cytokines such as IL-1β (133). In this regard, our in vitro experiments showed that anti-CD36 antibodies generated ROS production in monocytes. To investigate the role of complement C5a in TRALI, we used LPS-primed $C5aR1^{-/-}$ mice, which revealed significant decreases in rectal temperature and an increase in the lung Wet/Dry weight ratio. Accordingly, administration of the C5aR1 antagonist PMX53 did not change the rectal temperature or the lung Wet/Dry weight ratio of mice treated with mAb GZ1 and PMX53 compared with those treated with mAb GZ1 alone. This suggests that the C5aR1-C5a axis does not play a significant role in anti-CD36-induced murine TRALI. Because C5a can interact with C5aR1 and C5aR2, whcih exhibit similar binding affinities (94), we next tested the contribution of C5aR2 to the occurrence of anti-CD36-induced TRALI in LPS-primed mice using the C5aR2 selective functional ligand, P32 (96). Compared to GZ1-only treatment, P32 administration decreased the severity of TRALI but did not prevent its occurrence. Previous research has confirmed the proinflammatory effects of C5aR1, but the function of C5aR2 is not fully understood (94, 134). Although C5aR2 can exacerbate sepsis-induced intestinal injury through cytokine production (135), it protects against ischemia-mediated intestinal injury through neutrophil modulation (136). A recent study showed that the C5a-C5aR2 interaction could drive cytokine induction in vivo, presumably through

monocytes/macrophages (137). The question of whether this interaction could induce ROS production leading to NET production and worsening of TRALI is intriguing (61).

The anti-CD36–mediated TRALI model showed that the selective C5aR2 ligand decreased the severity of TRALI, together with the result of C5aR1, indicating the limited role of C5a in anti-CD36-mediated TRALI. However, in a previous study, both $C5aR2^{-/-}$ and WT mice suffered TRALI caused by anti-MHC class I (47). Nevertheless, the role of C5aR2 in anti-CD36-induced TRALI required further investigation.

We further explored the role of C5b-9 in TRALI and found that the concentration of C5b-9 was significantly higher in the BALF of LPS-primed mice treated with GZ1 than in the BALF of LPS-primed mice in the isotype control group. This upregulation was abolished by administration of anti-C7 (mAb 73D1) IgG to mAb GZ1-treated mice. Furthermore, higher C5b-9 deposition was detected in the lung tissues of LPS-primed mice treated with mAb GZ1, but not in those treated with the isotype control, and this was reversed in TRALI mice pretreated with anti-C7. Zelek et al. found that blocking mAbs targeting C7 and/or the C5b-7 complex mAb, 73D1 showed strong binding to mouse C7 with a very slow off rate. The capacity of 73D1 to inhibit complement in vivo was similar to that of BB5.1, which could effectively inhibit complement up to the endpoint at 48 h (87). Dr. Kulkarni hypothesized that MAC lysed cells play an important role in the progression of TRALI based on previous studies (138), but no prior study has directly confirmed this theory. Based on the results of the in vivo experiments, we believe that anti-CD36 binds to the CD36 antigen expressed on endothelial cells, initiating the proteolytic cascade of complement activation by binding to and activating the C1 complex, which is known as the CP of complement activation. Finally, this leads to the formation of MAC that can perturb membranes and result in endothelial cell lysis, ultimately leading to pulmonary edema.

4.6 Blocking complement activation can prevent and treat TRALI

To date, no specific treatment for TRALI has been reported (73). In this study, we examined several inhibitors and revealed that the competitive inhibitor GZ1 $F(ab')_2$ was only effective in preventing TRALI, not as a post-TRALI remedy. This condition seemed different from FNAIT, in which deglycosylated GZ1 has been shown to prevent fetal death caused by anti-CD36 antibodies (69). However, significant inhibition was observed before and after TRALI when NAC was administered intravenously together with inhalation of atomized NAC.

Among the complement proteins, C5 plays a major role in complement-mediated inflammation (86). Therefore, anti-C5 treatments represent a favorable target for developing anti-complement drugs for different diseases (101, 139-141). Recently, Zelek et al. demonstrated that mAb BB5.1, which is specific for mouse C5, could effectively inhibit C5 activation and prevent C5a accumulation in mice (86). Compared to untreated mice, we found that administration of the mAb BB5.1 was not only prevented, but could also therapeutically treat anti-CD36 murine TRALI. C5b-9 is involved in the development of anti-CD36–mediated murine TRALI, which can be alleviated through the administration of anti-C7. Next, we examined the efficacy of anti-C7 in preventing and ameliorating anti-CD36 antibody–induced TRALI, in LPS-primed mice. When the anti-C7 IgG or F(ab')$_2$ fragment was administered before the induction of TRALI with mAb GZ1, TRALI was completely prevented. Similar results were obtained in LPS-primed mice after TRALI induction with mAb GZ1 when anti-C7 IgG or F(ab')$_2$ was administered.

Overall, our observations suggested that the interaction between monocytes and TNF-α-activate lung endothelial cells, leading to the upregulation of CD36 expression in monocytes, resulting in increased antibody binding, triggering complement activation, ROS generation, and cytokine production, all of which are responsible for severe endothelial dysfunction in TRALI (**Figure 13**).

In conclusion, we shed light on the pathomechanism of anti-CD36-mediated TRALI using a 2-hit murine model, in which we prevented the occurrence of TRALI by prophylactic injection of GZ1 F(ab')$_2$, NAC, anti-C5, anti-C7, or anti-C7 F(ab')$_2$. More interestingly, we also achieved a good therapeutic effect of anti-C5 and anti-C7/F(ab')$_2$ on established anti-CD36-mediated TRALI. The potential for effective therapy reinforces the need for increased awareness of anti-CD36-induced TRALI, particularly among Asian populations. These findings strengthen the feasibility and further exploration of inhibiting complement activation in treating TRALI in humans (101, 142, 143). Although some therapeutic approaches are suggested by our work, further research on the detailed mechanism using sera from TRALI cases should be performed to expand the relevance of these findings.

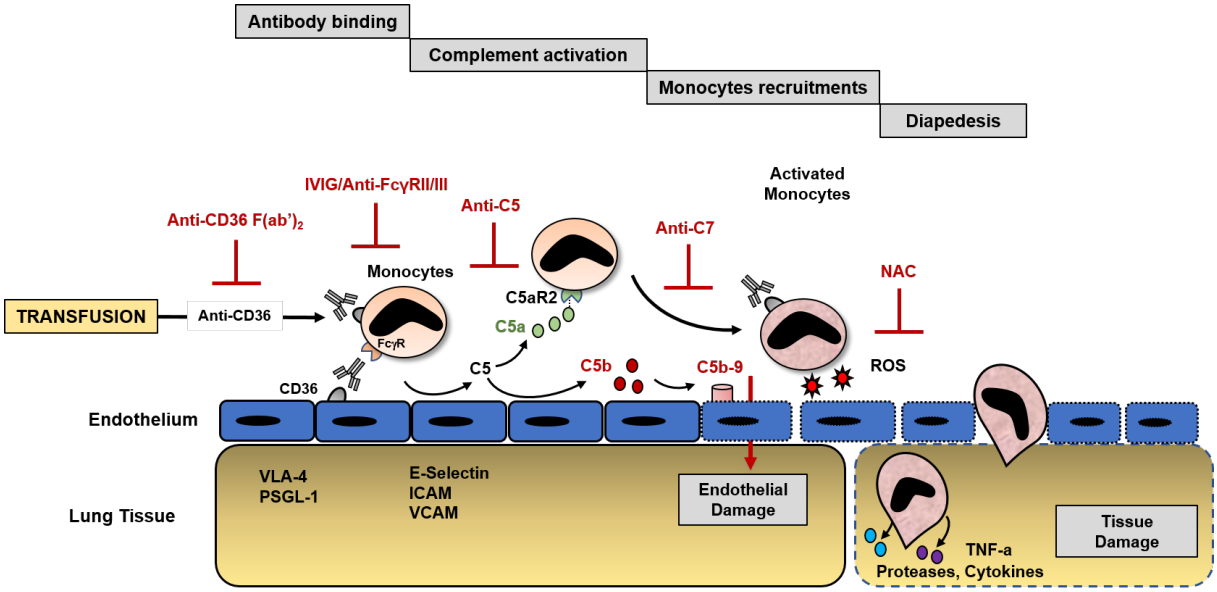

Figure 13. Proposed 2-hit mechanism of anti-CD36–mediated TRALI.

A state of inflammation induced by a first hit (e.g., LPS) triggers the upregulation of adhesion molecules on endothelial cells (E-selectin, ICAM-1, and VCAM) and monocytes (PSGL-1 or VLA-4), leading to the rolling and firm adhesion of monocytes on an endothelial surface. Cytokine (e.g., TNF-α), which may upregulate CD36 expression on monocytes. The second hit consists of anti-CD36 Abs bound to endothelial cells and monocytes. Upregulation of CD36 on monocytes enhances Ab binding and monocyte activation. This reaction triggers complement activation (accumulation of C5b-9 on endothelial cells), ROS generation, and cytokine secretion (e.g., TNF-α). This reaction cascade causes lung endothelial disturbance, strengthened by the recruitment of other blood cells (neutrophils or platelets) (not shown), and monocyte extravasation (diapedesis), resulting in severe TRALI symptoms. The potential targets for possible inhibitors — anti-CD36 F(ab')$_2$, IVIG, anti-FcγRII/III, NAC, anti-C5, and anti-C7 — are indicated.

5. SUMMARY

Individuals lacking CD36 on both platelets and monocytes (type I) are at risk of developing anti-CD36 antibodies after receiving a platelet transfusion or during pregnancy. Anti-CD36 antibodies have been suggested to induce transfusion-related acute lung injury (TRALI) upon blood transfusion, particularly in Asian populations. However, little is known about the pathological mechanism of anti-CD36-mediated TRALI, and potential therapies haven't yet been identified. Here, we developed a murine model of anti-CD36-mediated TRALI to address these questions. We found that administration of mouse monoclonal antibody against CD36 (mAb GZ1) or human anti-CD36 IgG, but not GZ1 F(ab')$_2$ fragments, induced severe TRALI in *Cd36*$^{+/+}$ male mice. Pre-depletion of recipient monocytes or complement, but not neutrophils or platelets, prevented the development of murine TRALI. Moreover, plasma C5a levels after TRALI induction by anti-CD36 were increased more than 3-fold, implying a critical role of complement C5 activation in the mechanism of Fc-dependent anti-CD36-mediated TRALI. Furthermore, *C5*$^{-/-}$ mice were protected from anti-CD36–mediated TRALI, not *C5aR1*$^{-/-}$ mice. C5aR1 and C5aR2 antagonists' administration did not inhibit TRALI, implying a possible role of C5b-9 (membrane attack complex [MAC]). Accordingly, elevated levels of MAC were detected in bronchoalveolar lavage fluid and lung tissue of mice with anti-CD36 induced TRALI. Administration of GZ1 F(ab')$_2$, antioxidant (NAC), IVIG, anti- FcγRII/III (mAb 2.4G2), anti-C5 (mAb BB5.1), anti-C7 (mAb 73D1) or anti-C7 F(ab')$_2$ before TRALI induction completely protected mice from anti-CD36-mediated TRALI. Inhibition of MAC formation by administration of anti-C7 alleviated TRALI in mice, suggesting the critical role of the MAC in the pathology of anti-CD36-mediated TRALI. Although no significant amelioration in TRALI was observed when mice were injected with GZ1 F(ab')$_2$ after TRALI induction, significant improvement was achieved when mice were treated post-induction with NAC or anti-C5. Importantly, anti-C5, anti-C7 and anti-C7 F(ab')$_2$ treatment completely rescued mice from TRALI, suggesting the potential role of existing anti-complement drugs in the treatment of patients with TRALI caused by anti-CD36 antibodies. The activation of complement is a rapid cascade reaction, which results in CD36 antibody-mediated TRALI being an acute response. Therefore, monoclonal antibodies directed against complement activation may be the best treatment.

6. ZUSAMMENFASSUNG

Personen, denen CD36 sowohl auf der Oberfläche der Blutplättchen als auch der Monozyten (Typ I) fehlt, haben das Risiko, nach einer Thrombozytentransfusion oder während der Schwangerschaft Antikörper gegen das CD36 Antigen zu entwickeln. Kürzlich wurde berichtet, dass Anti-CD36-Antikörper eine akute transfusionsassozierte Lungeninsuffizienz (TRALI) nach Bluttransfusionen induzieren können, insbesondere in asiatischen Populationen. Über den pathologischen Mechanismus der Anti-CD36-vermittelten TRALI ist jedoch wenig bekannt, und potenzielle Therapien wurden noch nicht identifiziert. Hier haben wir ein Mausmodell der Anti-CD36-vermittelten TRALI entwickelt, um diese Fragen zu beantworten.

Wir zeigten, dass die Verabreichung von monoklonalen Mausantikörpern gegen CD36 (mAb GZ1) oder humane Anti-CD36-IgG-Antikörper, aber nicht mAb GZ1 F(ab')2-Fragmente, eine schwere TRALI bei männlichen *Cd36*+/+ Mäusen induzierte. Die Depletion von Empfängermonozyten oder Komplementfaktoren, aber nicht von Neutrophilen oder Blutplättchen, verhinderte die Entwicklung der murinen TRALI. Darüber hinaus wurden die Plasma-C5a-Spiegel nach TRALI-Induktion durch Anti-CD36-Antikörper um mehr als das Dreifache erhöht, was eine kritische Rolle der Komplement-C5-Aktivierung im Mechanismus der Fc-abhängigen Anti-CD36-vermittelten TRALI impliziert. Darüber hinaus waren *C5-/-*, nicht aber *C5aR1-/-* Mäuse vor anti-CD36-vermittelter TRALI geschützt. Die Verabreichung von C5aR1- und C5aR2-Antagonisten hemmte TRALI nicht, was auf eine mögliche Rolle von C5b-9 (Membranangriffskomplex [MAC]) hindeutet. Dementsprechend wurden erhöhte MAC-Spiegel in bronchoalveolärer Flüssigkeit und Lungengewebe von Mäusen mit anti-CD36-induziertem TRALI nachgewiesen.

Die Verabreichung von mAb GZ1 F(ab')2, Antioxidans (NAC), IVIG, Anti-FcγRII/III (mAb 2.4G2), Anti-C5 (mAb BB5.1), Anti-C7 (mAb 73D1) vor der TRALI-Induktion schützte Mäuse vollständig vor Anti-CD36-vermittelter TRALI. Die Hemmung der MAC-Bildung durch Verabreichung von Anti-C7 linderte TRALI bei Mäusen, was auf die kritische Rolle des MAC bei der Pathologie der Anti-CD36-vermittelten TRALI hindeutet. Keine signifikante Verbesserung der TRALI wurde beobachtet wurde, wenn Mäuse nach TRALI-Induktion mit GZ1 F(ab')2 injiziert wurden. Eine signifikante Verbesserung wurde aber erreicht, wenn Mäuse nach der TRALI-Induktion mit NAC oder Anti-C5 behandelt wurden. Anti-C5-, Anti-C7- und Anti-C7 F(ab')2-Behandlung rettete die Mäuse vollständig nach TRALI-Induktion, was auf die potenzielle Rolle zugelassener Anti-Komplement-Medikamente bei der Behandlung von

Patienten mit TRALI hindeutet, die durch Anti-CD36-Antikörper verursacht wurde. Die Komplementaktivierung ist eine schnelle Kaskadenreaktion, die dazu führt, dass CD36-Antikörper-vermittelte TRALI eine akute Transfusionsreaktion ist. Daher könnten monoklonale Antikörper, die gegen die Komplementaktivierung gerichtet sind, der beste Kandidat zur Behandlung von TRALI sein.

7. REFERENCE

1. Semple JW, Rebetz J, and Kapur R. Transfusion-associated circulatory overload and transfusion-related acute lung injury. *Blood.* 2019;133(17):1840-53.
2. Tung JP, Chiaretti S, Dean MM, Sultana AJ, Reade MC, and Fung YL. Transfusion-related acute lung injury (TRALI): Potential pathways of development, strategies for prevention and treatment, and future research directions. *Blood Rev.* 2022:100926.
3. Vlaar APJ, Toy P, Fung M, Looney MR, Juffermans NP, Bux J, et al. A consensus redefinition of transfusion-related acute lung injury. *Transfusion.* 2019;59(7):2465-76.
4. Bux J. Antibody-mediated (immune) transfusion-related acute lung injury. *Vox Sang.* 2011;100(1):122-8.
5. Barnard RD. Indiscriminate transfusion: a critique of case reports illustrating hypersensitivity reactions. *N Y State J Med.* 1951;51(20):2399-402.
6. Popovsky MA, Abel MD, and Moore SB. Transfusion-related acute lung injury associated with passive transfer of antileukocyte antibodies. *Am Rev Respir Dis.* 1983;128(1):185-9.
7. Popovsky MA, and Moore SB. Diagnostic and pathogenetic considerations in transfusion-related acute lung injury. *Transfusion.* 1985;25(6):573-7.
8. Williamson LM, Lowe S, Love EM, Cohen H, Soldan K, McClelland DB, et al. Serious hazards of transfusion (SHOT) initiative: analysis of the first two annual reports. *Bmj.* 1999;319(7201):16-9.
9. Kleinman S, Caulfield T, Chan P, Davenport R, McFarland J, McPhedran S, et al. Toward an understanding of transfusion-related acute lung injury: statement of a consensus panel. *Transfusion.* 2004;44(12):1774-89.
10. Ranieri VM, Rubenfeld GD, Thompson BT, Ferguson ND, Caldwell E, Fan E, et al. Acute respiratory distress syndrome: the Berlin Definition. *Jama.* 2012;307(23):2526-33.
11. White SK, Walker BS, Schmidt RL, and Metcalf RA. The incidence of transfusion-related acute lung injury using active surveillance: A systematic review and meta-analysis. *Transfusion.* 2024;64(2):289-300.
12. Chapman CE, Stainsby D, Jones H, Love E, Massey E, Win N, et al. Ten years of hemovigilance reports of transfusion-related acute lung injury in the United Kingdom and the impact of preferential use of male donor plasma. *Transfusion.* 2009;49(3):440-52.
13. Keller-Stanislawski B, Reil A, Günay S, and Funk MB. Frequency and severity of transfusion-related acute lung injury--German haemovigilance data (2006-2007). *Vox Sang.* 2010;98(1):70-7.
14. Vossoughi S, Gorlin J, Kessler DA, Hillyer CD, Van Buren NL, Jimenez A, et al. Ten years of TRALI mitigation: measuring our progress. *Transfusion.* 2019;59(8):2567-74.
15. Bolton-Taylor C CH, Jones H, et al., editors. A. *Annual SHOT report, 2007 London, United Kingdom: Royal College of Pathologists, Serious Hazards of Transfusion Steering Group*. 2008.
16. Politis C, Wiersum JC, Richardson C, Robillard P, Jorgensen J, Renaudier P, et al. The International Haemovigilance Network Database for the Surveillance of Adverse Reactions and Events in Donors and Recipients of Blood Components: technical issues and results. *Vox Sang.* 2016;111(4):409-17.
17. BE. RCf. Transfusion/donation fatalities. FDA.2021. https://www.fda.gov/vaccines-blood-biologics/report-problem-center-biologics-evaluation-research/transfusiondonation-fatalities.

18. McVey MJ, Kapur R, Cserti-Gazdewich C, Semple JW, Karkouti K, and Kuebler WM. Transfusion-related Acute Lung Injury in the Perioperative Patient. *Anesthesiology.* 2019;131(3):693-715.
19. Vamvakas EC, and Blajchman MA. Transfusion-related mortality: the ongoing risks of allogeneic blood transfusion and the available strategies for their prevention. *Blood.* 2009;113(15):3406-17.
20. Dykes A, Smallwood D, Kotsimbos T, and Street A. Transfusion-related acute lung injury (Trali) in a patient with a single lung transplant. *Br J Haematol.* 2000;109(3):674-6.
21. Palfi M, Berg S, Ernerudh J, and Berlin G. A randomized controlled trial oftransfusion-related acute lung injury: is plasma from multiparous blood donors dangerous? *Transfusion.* 2001;41(3):317-22.
22. Reil A, Keller-Stanislawski B, Gunay S, and Bux J. Specificities of leucocyte alloantibodies in transfusion-related acute lung injury and results of leucocyte antibody screening of blood donors. *Vox Sang.* 2008;95(4):313-7.
23. Davoren A, Curtis BR, Shulman IA, Mohrbacher AF, Bux J, Kwiatkowska BJ, et al. TRALI due to granulocyte-agglutinating human neutrophil antigen-3a (5b) alloantibodies in donor plasma: a report of 2 fatalities. *Transfusion.* 2003;43(5):641-5.
24. Densmore TL, Goodnough LT, Ali S, Dynis M, and Chaplin H. Prevalence of HLA sensitization in female apheresis donors. *Transfusion.* 1999;39(1):103-6.
25. Xia W, Ye X, Xu X, Chen D, Deng J, Chen Y, et al. The prevalence of leucocyte alloantibodies in blood donors from South China. *Transfus Med.* 2015;25(6):385-92.
26. Nakajima F, Nishimura M, Hashimoto S, Okazaki H, and Tadokoro K. Role of anti-Nak(a) antibody, monocytes and platelets in the development of transfusion-related acute lung injury. *Vox Sang.* 2008;95(4):318-23.
27. Ando M, Nakajima F, Kamada H, Nakamura J, Shimizu M, Nagai T, et al. Defective CD36 mutations in anti-Naka antibody-positive subjects associated with transfusion-related acute lung injury (TRALI). *Japanese Journal of Transfusion and Cell Therapy.* 2016;62:587-91.
28. Silliman CC, Paterson AJ, Dickey WO, Stroneck DF, Popovsky MA, Caldwell SA, et al. The association of biologically active lipids with the development of transfusion-related acute lung injury: a retrospective study. *Transfusion.* 1997;37(7):719-26.
29. Toy P, Hollis-Perry KM, Jun J, and Nakagawa M. Recipients of blood from a donor with multiple HLA antibodies: a lookback study of transfusion-related acute lung injury. *Transfusion.* 2004;44(12):1683-8.
30. Kopko PM, Marshall CS, MacKenzie MR, Holland PV, and Popovsky MA. Transfusion-related acute lung injury: report of a clinical look-back investigation. *Jama.* 2002;287(15):1968-71.
31. Peters AL, van Hezel ME, Juffermans NP, and Vlaar AP. Pathogenesis of non-antibody mediated transfusion-related acute lung injury from bench to bedside. *Blood Rev.* 2015;29(1):51-61.
32. Silliman CC, Bjornsen AJ, Wyman TH, Kelher M, Allard J, Bieber S, et al. Plasma and lipids from stored platelets cause acute lung injury in an animal model. *Transfusion.* 2003;43(5):633-40.
33. Kelher MR, Masuno T, Moore EE, Damle S, Meng X, Song Y, et al. Plasma from stored packed red blood cells and MHC class I antibodies causes acute lung injury in a 2-event in vivo rat model. *Blood.* 2009;113(9):2079-87.
34. Silliman CC, Kelher MR, Khan SY, LaSarre M, West FB, Land KJ, et al. Experimental prestorage filtration removes antibodies and decreases lipids in RBC supernatants mitigating TRALI in vivo. *Blood.* 2014;123(22):3488-95.

35. Silliman CC, Voelkel NF, Allard JD, Elzi DJ, Tuder RM, Johnson JL, et al. Plasma and lipids from stored packed red blood cells cause acute lung injury in an animal model. *J Clin Invest.* 1998;101(7):1458-67.
36. Vlaar AP, Hofstra JJ, Kulik W, van Lenthe H, Nieuwland R, Schultz MJ, et al. Supernatant of stored platelets causes lung inflammation and coagulopathy in a novel in vivo transfusion model. *Blood.* 2010;116(8):1360-8.
37. Vlaar AP, Hofstra JJ, Levi M, Kulik W, Nieuwland R, Tool AT, et al. Supernatant of aged erythrocytes causes lung inflammation and coagulopathy in a "two-hit" in vivo syngeneic transfusion model. *Anesthesiology.* 2010;113(1):92-103.
38. Hashimoto N, Kawabe T, Imaizumi K, Hara T, Okamoto M, Kojima K, et al. CD40 plays a crucial role in lipopolysaccharide-induced acute lung injury. *Am J Respir Cell Mol Biol.* 2004;30(6):808-15.
39. McVey MJ, Weidenfeld S, Maishan M, Spring C, Kim M, Tabuchi A, et al. Platelet extracellular vesicles mediate transfusion-related acute lung injury by imbalancing the sphingolipid rheostat. *Blood.* 2021;137(5):690-701.
40. Silliman CC, Boshkov LK, Mehdizadehkashi Z, Elzi DJ, Dickey WO, Podlosky L, et al. Transfusion-related acute lung injury: epidemiology and a prospective analysis of etiologic factors. *Blood.* 2003;101(2):454-62.
41. Bux J, and Sachs UJ. The pathogenesis of transfusion-related acute lung injury (TRALI). *Br J Haematol.* 2007;136(6):788-99.
42. Kuldanek SA, Kelher M, and Silliman CC. Risk factors, management and prevention of transfusion-related acute lung injury: a comprehensive update. *Expert Rev Hematol.* 2019;12(9):773-85.
43. Toy P, Gajic O, Bacchetti P, Looney MR, Gropper MA, Hubmayr R, et al. Transfusion-related acute lung injury: incidence and risk factors. *Blood.* 2012;119(7):1757-67.
44. Benson AB, Austin GL, Berg M, McFann KK, Thomas S, Ramirez G, et al. Transfusion-related acute lung injury in ICU patients admitted with gastrointestinal bleeding. *Intensive Care Med.* 2010;36(10):1710-7.
45. Wyman TH, Bjornsen AJ, Elzi DJ, Smith CW, England KM, Kelher M, et al. A two-insult in vitro model of PMN-mediated pulmonary endothelial damage: requirements for adherence and chemokine release. *Am J Physiol Cell Physiol.* 2002;283(6):C1592-603.
46. Kopko PM, Paglieroni TG, Popovsky MA, Muto KN, MacKenzie MR, and Holland PV. TRALI: correlation of antigen-antibody and monocyte activation in donor-recipient pairs. *Transfusion.* 2003;43(2):177-84.
47. Strait RT, Hicks W, Barasa N, Mahler A, Khodoun M, Köhl J, et al. MHC class I-specific antibody binding to nonhematopoietic cells drives complement activation to induce transfusion-related acute lung injury in mice. *J Exp Med.* 2011;208(12):2525-44.
48. El Mdawar MB, Maître B, Magnenat S, Gachet C, Hechler B, and de la Salle H. The ATP-gated P2X(1) ion channel contributes to the severity of antibody-mediated Transfusion-Related Acute Lung Injury in mice. *Sci Rep.* 2019;9(1):5159.
49. Ricklin D, Hajishengallis G, Yang K, and Lambris JD. Complement: a key system for immune surveillance and homeostasis. *Nat Immunol.* 2010;11(9):785-97.
50. Noris M, Mescia F, and Remuzzi G. STEC-HUS, atypical HUS and TTP are all diseases of complement activation. *Nat Rev Nephrol.* 2012;8(11):622-33.
51. Bohlson SS, Garred P, Kemper C, and Tenner AJ. Complement Nomenclature-Deconvoluted. *Front Immunol.* 2019;10:1308.

52. Nauta AJ, Daha MR, van Kooten C, and Roos A. Recognition and clearance of apoptotic cells: a role for complement and pentraxins. *Trends Immunol.* 2003;24(3):148-54.
53. Noris M, and Remuzzi G. Overview of complement activation and regulation. *Semin Nephrol.* 2013;33(6):479-92.
54. Fayyazi A, Sandau R, Duong LQ, Götze O, Radzun HJ, Schweyer S, et al. C5a receptor and interleukin-6 are expressed in tissue macrophages and stimulated keratinocytes but not in pulmonary and intestinal epithelial cells. *Am J Pathol.* 1999;154(2):495-501.
55. Peng Q, Li K, Sacks SH, and Zhou W. The role of anaphylatoxins C3a and C5a in regulating innate and adaptive immune responses. *Inflamm Allergy Drug Targets.* 2009;8(3):236-46.
56. Gutzmer R, Köther B, Zwirner J, Dijkstra D, Purwar R, Wittmann M, et al. Human plasmacytoid dendritic cells express receptors for anaphylatoxins C3a and C5a and are chemoattracted to C3a and C5a. *J Invest Dermatol.* 2006;126(11):2422-9.
57. Chen NJ, Mirtsos C, Suh D, Lu YC, Lin WJ, McKerlie C, et al. C5L2 is critical for the biological activities of the anaphylatoxins C5a and C3a. *Nature.* 2007;446(7132):203-7.
58. Ambruso DR, Silliman CC, Kelher M, Thurman G, and Giclas P. Complement Activation in Transfusion Related Acute Lung Injury (TRALI). *Blood.* 2006;108(11):954-.
59. Lucas G, Rogers S, Evans R, Hambley H, and Win N. Transfusion-related acute lung injury associated with interdonor incompatibility for the neutrophil-specific antigen HNA-1a. *Vox Sang.* 2000;79(2):112-5.
60. Looney MR, Su X, Van Ziffle JA, Lowell CA, and Matthay MA. Neutrophils and their Fc gamma receptors are essential in a mouse model of transfusion-related acute lung injury. *J Clin Invest.* 2006;116(6):1615-23.
61. van der Velden S, van Osch TLJ, Seghier A, Bentlage AEH, Mok JY, Geerdes DM, et al. Complement activation drives antibody-mediated transfusion-related acute lung injury via macrophage trafficking and formation of NETs. *Blood.* 2024;143(1):79-91.
62. Cleary SJ, Kwaan N, Tian JJ, Calabrese DR, Mallavia B, Magnen M, et al. Complement activation on endothelium initiates antibody-mediated acute lung injury. *J Clin Invest.* 2020;130(11):5909-23.
63. Cleary SJ, Seo Y, Tian JJ, Kwaan N, Bulkley DP, Bentlage AE, et al. IgG hexamers initiate complement-dependent acute lung injury. *J Clin Invest.* 2024;134(11).
64. Febbraio M, Hajjar DP, and Silverstein RL. CD36: a class B scavenger receptor involved in angiogenesis, atherosclerosis, inflammation, and lipid metabolism. *J Clin Invest.* 2001;108(6):785-91.
65. Podrez EA, Schmitt D, Hoff HF, and Hazen SL. Myeloperoxidase-generated reactive nitrogen species convert LDL into an atherogenic form in vitro. *J Clin Invest.* 1999;103(11):1547-60.
66. Yamamoto N, Ikeda H, Tandon NN, Herman J, Tomiyama Y, Mitani T, et al. A platelet membrane glycoprotein (GP) deficiency in healthy blood donors: Naka-platelets lack detectable GPIV (CD36). *Blood.* 1990;76(9):1698-703.
67. Yamamoto N, Akamatsu N, Sakuraba H, Yamazaki H, and Tanoue K. Platelet glycoprotein IV (CD36) deficiency is associated with the absence (type I) or the presence (type II) of glycoprotein IV on monocytes. *Blood.* 1994;83(2):392-7.
68. Wakamoto S, Fujihara M, Urushibara N, Morishita K, Kaneko S, Yasuda H, et al. Heterogeneity of platelet responsiveness to anti-CD36 in plasma associated with adverse transfusion reactions. *Vox Sang.* 2005;88(1):41-51.

69. Xu X, Chen D, Ye X, Xia W, Xu Y, Chen Y, et al. Successful prenatal therapy for anti-CD36-mediated severe FNAIT by deglycosylated antibodies in a novel murine model. *Blood.* 2021;138(18):1757-67.
70. Xu X, Ye X, Xia W, Liu J, Ding H, Deng J, et al. Studies on CD36 deficiency in South China: Two cases demonstrating the clinical impact of anti-CD36 antibodies. *Thromb Haemost.* 2013;110(6):1199-206.
71. Xu X, Li L, Xia W, Ding H, Chen D, Liu J, et al. Successful management of a hydropic fetus with severe anemia and thrombocytopenia caused by anti-CD36 antibody. *Int J Hematol.* 2018;107(2):251-6.
72. Xia W, Ye X, Xu X, Ding H, Liu J, Deng J, et al. Two cases of platelet transfusion refractoriness and one case of possible FNAIT caused by antibodies against CD36 in China. *Transfus Med.* 2014;24(4):254-6.
73. Semple JW, McVey MJ, Kim M, Rebetz J, Kuebler WM, and Kapur R. Targeting Transfusion-Related Acute Lung Injury: The Journey From Basic Science to Novel Therapies. *Crit Care Med.* 2018;46(5):e452-e8.
74. Kapur R, Kim M, Aslam R, McVey MJ, Tabuchi A, Luo A, et al. T regulatory cells and dendritic cells protect against transfusion-related acute lung injury via IL-10. *Blood.* 2017;129(18):2557-69.
75. Kapur R, Kasetty G, Rebetz J, Egesten A, and Semple JW. Osteopontin mediates murine transfusion-related acute lung injury via stimulation of pulmonary neutrophil accumulation. *Blood.* 2019;134(1):74-84.
76. Looney MR, Nguyen JX, Hu Y, Van Ziffle JA, Lowell CA, and Matthay MA. Platelet depletion and aspirin treatment protect mice in a two-event model of transfusion-related acute lung injury. *J Clin Invest.* 2009;119(11):3450-61.
77. Semple JW, Kim M, Hou J, McVey M, Lee YJ, Tabuchi A, et al. Intravenous immunoglobulin prevents murine antibody-mediated acute lung injury at the level of neutrophil reactive oxygen species (ROS) production. *PLoS One.* 2012;7(2):e31357.
78. Boyer JF, Balard P, Authier H, Faucon B, Bernad J, Mazières B, et al. Tumor necrosis factor alpha and adalimumab differentially regulate CD36 expression in human monocytes. *Arthritis Res Ther.* 2007;9(2):R22.
79. Holzlöhner P, and Hanack K. Generation of Murine Monoclonal Antibodies by Hybridoma Technology. *J Vis Exp.* 2017(119).
80. McKenzie CG, Kim M, Singh TK, Milev Y, Freedman J, and Semple JW. Peripheral blood monocyte-derived chemokine blockade prevents murine transfusion-related acute lung injury (TRALI). *Blood.* 2014;123(22):3496-503.
81. Cognasse F, Tariket S, Hamzeh-Cognasse H, Arthaud CA, Eyraud MA, Bourlet T, et al. Platelet depletion limits the severity but does not prevent the occurrence of experimental transfusion-related acute lung injury. *Transfusion.* 2020;60(4):713-23.
82. Sakagawa H, Miyazaki T, Fujihara M, Sato S, Yamaguchi M, Fukai K, et al. Generation of inflammatory cytokines and chemokines from peripheral blood mononuclear cells by HLA Class II antibody-containing plasma unit that was associated with severe nonhemolytic transfusion reactions. *Transfusion.* 2007;47(1):154-61.
83. Wakamoto S, Fujihara M, Sakagawa H, Takahashi D, Niwa K, Morioka M, et al. Endothelial permeability is increased by the supernatant of peripheral blood mononuclear cells stimulated with HLA Class II antibody. *Transfusion.* 2008;48(10):2060-8.
84. Huh HY, Lo SK, Yesner LM, and Silverstein RL. CD36 induction on human monocytes upon adhesion to tumor necrosis factor-activated endothelial cells. *J Biol Chem.* 1995;270(11):6267-71.

85. Bayat B, Traum A, Berghöfer H, Werth S, Zhu J, Bein G, et al. Current Anti-HPA-1a Standard Antibodies React with the β3 Integrin Subunit but not with αIIbβ3 and αvβ3 Complexes. *Thromb Haemost.* 2019;119(11):1807-15.
86. Zelek WM, Menzies GE, Brancale A, Stockinger B, and Morgan BP. Characterizing the original anti-C5 function-blocking antibody, BB5.1, for species specificity, mode of action and interactions with C5. *Immunology.* 2020;161(2):103-13.
87. Zelek WM, and Morgan BP. Monoclonal Antibodies Capable of Inhibiting Complement Downstream of C5 in Multiple Species. *Front Immunol.* 2020;11:612402.
88. Wang F, Huang M, Wang Y, Hong Y, Zang D, Yang C, et al. Membrane Attack Complex C5b-9 Promotes Renal Tubular Epithelial Cell Pyroptosis in Trichloroethylene-Sensitized Mice. *Front Pharmacol.* 2022;13:877988.
89. Holmes RS. Comparative Studies of Vertebrate Platelet Glycoprotein 4 (CD36). *Biomolecules.* 2012;2(3):389-414.
90. Rebetz J, Semple JW, and Kapur R. The Pathogenic Involvement of Neutrophils in Acute Respiratory Distress Syndrome and Transfusion-Related Acute Lung Injury. *Transfus Med Hemother.* 2018;45(5):290-8.
91. Ericson JA, Duffau P, Yasuda K, Ortiz-Lopez A, Rothamel K, Rifkin IR, et al. Gene expression during the generation and activation of mouse neutrophils: implication of novel functional and regulatory pathways. *PLoS One.* 2014;9(10):e108553.
92. Mokhtari V, Afsharian P, Shahhoseini M, Kalantar SM, and Moini A. A Review on Various Uses of N-Acetyl Cysteine. *Cell J.* 2017;19(1):11-7.
93. Baba A, Fujita T, and Tamura N. Sexual dimorphism of the fifth component of mouse complement. *J Exp Med.* 1984;160(2):411-9.
94. Li XX, Lee JD, Kemper C, and Woodruff TM. The Complement Receptor C5aR2: A Powerful Modulator of Innate and Adaptive Immunity. *J Immunol.* 2019;202(12):3339-48.
95. Lillegard KE, Loeks-Johnson AC, Opacich JW, Peterson JM, Bauer AJ, Elmquist BJ, et al. Differential effects of complement activation products c3a and c5a on cardiovascular function in hypertensive pregnant rats. *J Pharmacol Exp Ther.* 2014;351(2):344-51.
96. Croker DE, Monk PN, Halai R, Kaeslin G, Schofield Z, Wu MC, et al. Discovery of functionally selective C5aR2 ligands: novel modulators of C5a signalling. *Immunol Cell Biol.* 2016;94(8):787-95.
97. Morgan BP, and Harris CL. Complement, a target for therapy in inflammatory and degenerative diseases. *Nat Rev Drug Discov.* 2015;14(12):857-77.
98. Nagelkerke SQ, and Kuijpers TW. Immunomodulation by IVIg and the Role of Fc-Gamma Receptors: Classic Mechanisms of Action after all? *Front Immunol.* 2014;5:674.
99. Kang TH, and Jung ST. Boosting therapeutic potency of antibodies by taming Fc domain functions. *Exp Mol Med.* 2019;51(11):1-9.
100. Yano S, Kaku S, Suzuki K, Terazaki C, Sakayori T, Kawasaki T, et al. Natural antibodies against the immunoglobulin F(ab')2 fragment cause elimination of antigens recognized by the F(ab')2 from the circulation. *Eur J Immunol.* 1995;25(11):3128-33.
101. Harris CL, Pouw RB, Kavanagh D, Sun R, and Ricklin D. Developments in anti-complement therapy; from disease to clinical trial. *Mol Immunol.* 2018;102:89-119.
102. Kapur R, Kim M, Shanmugabhavananthan S, Liu J, Li Y, and Semple JW. C-reactive protein enhances murine antibody-mediated transfusion-related acute lung injury. *Blood.* 2015;126(25):2747-51.

103. Kapur R, Kim M, Rebetz J, Hallström B, Björkman JT, Takabe-French A, et al. Gastrointestinal microbiota contributes to the development of murine transfusion-related acute lung injury. *Blood Adv.* 2018;2(13):1651-63.
104. Daviet L, Morel-Kopp MC, Kaplan C, and McGregor JL. A structural/functional domain on human CD36 is involved in the binding of anti-Nak(a) antibodies. *Thromb Haemost.* 1995;73(3):543-5.
105. Finlayson J, Grey D, Kavanagh L, and Witt C. Transfusion-related acute lung injury in a neutropenic patient. *Intern Med J.* 2011;41(8):638-41.
106. Danielson C, Benjamin RJ, Mangano MM, Mills CJ, and Waxman DA. Pulmonary pathology of rapidly fatal transfusion-related acute lung injury reveals minimal evidence of diffuse alveolar damage or alveolar granulocyte infiltration. *Transfusion.* 2008;48(11):2401-8.
107. Zeeuw van der Laan EAN, van der Velden S, Porcelijn L, Semple JW, van der Schoot CE, and Kapur R. Update on the pathophysiology of transfusion-related acute lung injury. *Curr Opin Hematol.* 2020;27(6):386-91.
108. Semple JW, and Kapur R. The contribution of recipient platelets in TRALI: has the jury reached a verdict? *Transfusion.* 2020;60(5):886-8.
109. Zeeuw van der Laan EAN, van der Velden S, Porcelijn L, Semple JW, van der Schoot CE, and Kapur R. Evaluation of Platelet Responses in Transfusion-Related Acute Lung Injury (TRALI). *Transfus Med Rev.* 2020;34(4):227-33.
110. Reinisch W, Lichtenberger C, Steger G, Tillinger W, Scheiner O, Gangl A, et al. Donor dependent, interferon-gamma induced HLA-DR expression on human neutrophils in vivo. *Clin Exp Immunol.* 2003;133(3):476-84.
111. Kelher MR, Banerjee A, Gamboni F, Anderson C, and Silliman CC. Antibodies to major histocompatibility complex class II antigens directly prime neutrophils and cause acute lung injury in a two-event in vivo rat model. *Transfusion.* 2016;56(12):3004-11.
112. Daley JM, Thomay AA, Connolly MD, Reichner JS, and Albina JE. Use of Ly6G-specific monoclonal antibody to deplete neutrophils in mice. *J Leukoc Biol.* 2008;83(1):64-70.
113. Sachs UJ, Wasel W, Bayat B, Bohle RM, Hattar K, Berghöfer H, et al. Mechanism of transfusion-related acute lung injury induced by HLA class II antibodies. *Blood.* 2011;117(2):669-77.
114. Kapur R, Zufferey A, Boilard E, and Semple JW. Nouvelle cuisine: platelets served with inflammation. *J Immunol.* 2015;194(12):5579-87.
115. Kapur R, and Semple JW. Platelets as immune-sensing cells. *Blood Adv.* 2016;1(1):10-4.
116. Kapur R, and Semple JW. The nonhemostatic immune functions of platelets. *Semin Hematol.* 2016;53 Suppl 1:S2-6.
117. Caudrillier A, Kessenbrock K, Gilliss BM, Nguyen JX, Marques MB, Monestier M, et al. Platelets induce neutrophil extracellular traps in transfusion-related acute lung injury. *J Clin Invest.* 2012;122(7):2661-71.
118. Thomas GM, Carbo C, Curtis BR, Martinod K, Mazo IB, Schatzberg D, et al. Extracellular DNA traps are associated with the pathogenesis of TRALI in humans and mice. *Blood.* 2012;119(26):6335-43.
119. Hechler B, Maître B, Magnenat S, Heim V, El Mdawar MB, Gachet C, et al. Platelets are dispensable for antibody-mediated transfusion-related acute lung injury in the mouse. *J Thromb Haemost.* 2016;14(6):1255-67.

120. Goerge T, Ho-Tin-Noe B, Carbo C, Benarafa C, Remold-O'Donnell E, Zhao BQ, et al. Inflammation induces hemorrhage in thrombocytopenia. *Blood.* 2008;111(10):4958-64.
121. Strait RT, Morris SC, Yang M, Qu XW, and Finkelman FD. Pathways of anaphylaxis in the mouse. *J Allergy Clin Immunol.* 2002;109(4):658-68.
122. Schwab I, and Nimmerjahn F. Intravenous immunoglobulin therapy: how does IgG modulate the immune system? *Nat Rev Immunol.* 2013;13(3):176-89.
123. Nimmerjahn F, and Ravetch JV. Fcgamma receptors as regulators of immune responses. *Nat Rev Immunol.* 2008;8(1):34-47.
124. Sörman A, Zhang L, Ding Z, and Heyman B. How antibodies use complement to regulate antibody responses. *Mol Immunol.* 2014;61(2):79-88.
125. Zeeuw van der Laan EAN, van der Velden S, Bentlage AEH, Larsen MD, van Osch TLJ, Mok JY, et al. Biological and structural characterization of murine TRALI antibody reveals increased Fc-mediated complement activation. *Blood Adv.* 2020;4(16):3875-85.
126. Bayat B, Tjahjono Y, Sydykov A, Werth S, Hippenstiel S, Weissmann N, et al. Anti-human neutrophil antigen-3a induced transfusion-related acute lung injury in mice by direct disturbance of lung endothelial cells. *Arterioscler Thromb Vasc Biol.* 2013;33(11):2538-48.
127. Jongerius I, Porcelijn L, van Beek AE, Semple JW, van der Schoot CE, Vlaar APJ, et al. The Role of Complement in Transfusion-Related Acute Lung Injury. *Transfus Med Rev.* 2019;33(4):236-42.
128. Müller MC, Stroo I, Wouters D, Zeerleder SS, Roelofs JJ, Boon L, et al. The effect of C1-inhibitor in a murine model of transfusion-related acute lung injury. *Vox Sang.* 2014;107(1):71-5.
129. Chen DW, Kang T, Xu XZ, Xia WJ, Ye X, Wu YB, et al. Mechanism and intervention of murine transfusion-related acute lung injury caused by anti-CD36 antibodies. *JCI Insight.* 2023;8(6).
130. Guo RF, and Ward PA. Role of C5a in inflammatory responses. *Annu Rev Immunol.* 2005;23:821-52.
131. Cavaillon JM, Fitting C, and Haeffner-Cavaillon N. Recombinant C5a enhances interleukin 1 and tumor necrosis factor release by lipopolysaccharide-stimulated monocytes and macrophages. *Eur J Immunol.* 1990;20(2):253-7.
132. Schaeffer V, Cuschieri J, Garcia I, Knoll M, Billgren J, Jelacic S, et al. The priming effect of C5a on monocytes is predominantly mediated by the p38 MAPK pathway. *Shock.* 2007;27(6):623-30.
133. Khameneh HJ, Ho AW, Laudisi F, Derks H, Kandasamy M, Sivasankar B, et al. C5a Regulates IL-1β Production and Leukocyte Recruitment in a Murine Model of Monosodium Urate Crystal-Induced Peritonitis. *Front Pharmacol.* 2017;8:10.
134. Li R, Coulthard LG, Wu MC, Taylor SM, and Woodruff TM. C5L2: a controversial receptor of complement anaphylatoxin, C5a. *Faseb j.* 2013;27(3):855-64.
135. Rittirsch D, Flierl MA, Nadeau BA, Day DE, Huber-Lang M, Mackay CR, et al. Functional roles for C5a receptors in sepsis. *Nat Med.* 2008;14(5):551-7.
136. Wu MCL, Lee JD, Ruitenberg MJ, and Woodruff TM. Absence of the C5a Receptor C5aR2 Worsens Ischemic Tissue Injury by Increasing C5aR1-Mediated Neutrophil Infiltration. *J Immunol.* 2020;205(10):2834-9.
137. Li XX, Clark RJ, and Woodruff TM. C5aR2 Activation Broadly Modulates the Signaling and Function of Primary Human Macrophages. *J Immunol.* 2020;205(4):1102-12.

138. Kulkarni HS. Hexamerization: explaining the original sin of IgG-mediated complement activation in acute lung injury. *J Clin Invest.* 2024;134(11).
139. Copland DA, Hussain K, Baalasubramanian S, Hughes TR, Morgan BP, Xu H, et al. Systemic and local anti-C5 therapy reduces the disease severity in experimental autoimmune uveoretinitis. *Clin Exp Immunol.* 2010;159(3):303-14.
140. Raedler H, Vieyra MB, Leisman S, Lakhani P, Kwan W, Yang M, et al. Anti-complement component C5 mAb synergizes with CTLA4Ig to inhibit alloreactive T cells and prolong cardiac allograft survival in mice. *Am J Transplant.* 2011;11(7):1397-406.
141. Huugen D, van Esch A, Xiao H, Peutz-Kootstra CJ, Buurman WA, Tervaert JW, et al. Inhibition of complement factor C5 protects against anti-myeloperoxidase antibody-mediated glomerulonephritis in mice. *Kidney Int.* 2007;71(7):646-54.
142. Kapur R, Semple JW, and Vlaar APJ. The importance of disrupting complement activation in acute lung injury. *The Journal of Clinical Investigation.* 2024;134(12):e182251.
143. Lekova E, Zelek WM, Gower D, Spitzfaden C, Osuch IH, John-Morris E, et al. Discovery of functionally distinct anti-C7 monoclonal antibodies and stratification of anti-nicotinic AChR positive Myasthenia Gravis patients. *Front Immunol.* 2022;13:968206.

8 ACKNOWLEDGEMENTS

The *in vitro* and the *in vivo* study in mice (study approval: SYSU-IACUC-2020-000185, HTSW-IACUC-2021-211123) of this dissertation were performed at the Institute for Clinical Immunology, Transfusion Medicine, and Hemostasis at Justus-Liebig-University of Giessen, Germany, and in Guangzhou Blood Center, respectively under the supervision of Prof. Dr. Gregor Bein and Dr. Santoso Sentot.

First and foremost, I would like to thank Prof. Dr. Gregor Bein and Dr. Santoso Sentot for providing me with this precious opportunity to work on this project within their outstanding team under their supervision. I truly appreciate the confidence, patience and geniality my supervisor has always shown to me during these years. Their advice, ideas, moral support and guidance through this project, were vital for me to grow as an independent researcher. Particularly, I would like to express my deepest gratitude to Dr. Santoso Sentot for his constant scientific and technical assistance and guidance. His enthusiasm about this work and his wealth of knowledge in the field of transfusion medicine and immunology has always inspired me.

I would like to sincerely thank Prof. Dr. Yongshui Fu and Dr. Huaqin Liang in Guangzhou Blood Center for supporting me to finish the doctoral thesis in Germany. I am extremely thankful to Dr. Xiuzhang Xu for her essential help in animal surgery, which made my project go deeper. I would like to thank Dr. Wenjie Xia for her guidance and help in my work, as well as her encouragement in life. I sincerely appreciate the kind help from all my colleges: Xin Ye, Jing Liu, Yaori Xu, Jiansen He, Jing Deng, Yangkai Chen, Haoqing Ding, Silke Werth, Behnaz Bayat for extending their unstinted support, timely motivation, sympathetic attitude and unfailing help while the course of my entire study

I am extremely thankful to Prof. Dr. B. Paul Morgan and Dr. Wioleta M. Zelek for supporting me with the precious anti-C5 and anti-C7 monoclonal antibodies, which constitute an important component of the overall study. I also thank Prof. Dr. Trent M. Woodruff for supporting me with the C5aR2 agonist. Moreover, I want to thank Dr. Fumiaki Nakajima at the Japanese Red Cross in Tokyo, Japan, for the generous gift of human anti-CD36 sera. It is also my pleasure to thank Prof. Dr. Rick Kapur for guiding my animal experiments and reviewing the manuscript.

This is a great opportunity to express my deepest gratitude to my parents, my wife and my sister, who were always supporting me and encouraged me with their best wishes.

In the end, I owe my thanks to Guangzhou Blood Center, which has provided me with the great opportunity and financial support to study in Germany for two years.

9. LIST OF PUBLICATION

1. **Dawei Chen (first author)**, Huaqin Liang, Xiuzhang Xu, Wenjie Xia, Xin Ye, Yalin Luo, Jiansen He, Yaori Xu, Jing Liu, Hui Ren, Shengxue Luo, Trent M. Woodruff, Wioleta M. Zelek, B. Paul Morgan, Rick Kapur, Sentot Santoso, and Yongshui Fu. Inhibition of terminal complement complex formation alleviates murine antibody-mediated TRALI. Blood. 2025; 146(6):759-764.

2. **Dawei Chen (first author)**, Tian Kang, Xiuzhang Xu, Wenjie Xia, Xin Ye, Yongbin Wu, Yaori Xu, Jing Liu, Hui Ren, Jing Deng, Yangkai Chen, Haoqiang Ding, Muhammad Aslam, Wioleta M. Zelek, B. Paul Morgan, Rick Kapur, Sentot Santoso, and Yongshui Fu. Mechanism and intervention of murine transfusion-related acute lung injury caused by anti-CD36 antibodies. JCI Insight. 2023; 8(6): e165142.

3. Xiuzhang Xu, **Dawei Chen (co-first author)**, Xin Ye, Wenjie Xia, Yaori Xu, Yangkai Chen, Yuan Shao, Jing Deng, Haoqiang Ding, Jing Liu, Jiali Wang, Heyu Ni, Yongshui Fu, Sentot Santoso. Successful prenatal therapy of anti-CD36-mediated severe FNAIT by deglycosylated antibodies in a novel murine model**.** Blood. 2021; 138(18):1757-1767.

4. **Dawei Chen (first author)**, Tao Wang, Xin Ye, Xiuzhang Xu, Wenjie Xia, Yongshui Fu. Generation of induced pluripotent stem cell line derived from FNAIT patients with CD36 deficiency mutation. Stem Cell Research. 2022; 61:102749.

5. Yongbin Wu, **Dawei Chen (co-first author)**, Xiuzhang Xu, Mingqin Mai, Xin Ye, Chengyao Li, Sentot Santoso, Wenjie Xia,Yongshui Fu. Hydrops fetalis associated with anti-CD36 antibodies in fetal and neonatal alloimmune thrombocytopenia: Possible underlying mechanism. Transfus Med. 2020; 30(5):361-368.

6. Wenjie Xia , **Dawei Chen (co-first author)**, Xinnian Li, Jing Liu, Xiuzhang Xu, Xin Ye, Jing Deng, Haoqiang Ding, Hui Ren, Yangkai Chen, Huaqin Liang, Xingqiang Lai, Yongshui Fu. Haplotypes analysis reveals the genetic basis of type I CD36 deficiency. Sci Rep. 2024; 14(1):23977.

7. Xiuzhang Xu, **Dawei Chen**, Xin Ye, Wenjie Xia, Yuan Shao, Jing Deng, Yangkai Chen, Haoqiang Ding, Jing Liu, Yaori Xu, Sentot Santoso, Yongshui Fu**.** Improvement of anti-CD36 antibody detection via monoclonal antibody immobilization of platelet antigens assay by using selected monoclonal antibodies. Ann Lab Med. 2023; 43(1):86-91.

8. Xiuzhang Xu, Lin Li, Wenjie Xia, Haoqiang Ding, **Dawei Chen**, Jing Liu, Jing Deng, Yangkai Chen, Zhiming He, Jiali Wang, Yuan Shao, Sentot Santoso, Xin Ye, Qun Fang.

Successful management of a hydropic fetus with severe anemia and thrombocytopenia caused by anti-CD36 antibody. Int J Hematol. 2018; 107(2):251-256.

9. Ying Liu, Yufan Zhang, **Dawei Chen**, Yongshui Fu. Current status of and global trends in platelet transfusion refractoriness from 2004 to 2021: a bibliometric analysis. Front Med (Lausanne). 2022; 9: 873500.

10. **Dawei Chen (first author),** Xiuzhang Xu, Wenjie Xia, Yuan Shao, Jiali Wang, Jing Liu, Jing Deng, Yangkai Chen, Haoqiang Ding, Xin Ye. Preparation and application of a mouse monoclonal antibody against human CD36. Chinese journal of Guangzhou Yi Yao. 2020; 51(4):28-31+42.

11. Romain Duval, Alissa Soudry, Jonathan De Oliveira Rios, Sarah Liane Linguet, Miguel Taillepierre, Graziella Matesic, Alexandre Raneri, Guy Laiguillon, Emilie Le Toriellec, Emilie-Fleur Gautier, Damien Vainqueur, Jérôme Babinet, Cécile Masson, jean Christophe Gelly, Caroline Le Van Kim, Marc Romana, **Dawei Chen,** Sentot Santoso, Berengere Koehl, Thierry Peyrard, Slim Azouzi. The neutrophil antigen 3a/b polymorphism in SLC44A2 unexpectedly encodes Csa/Csb red cell antigens. Blood. 2025; 146(2):247-253.

Other publication:

1. **Dawei Chen (first author)**, Xiuzhang Xu, Wenjie Xia, Xin Ye, Behnaz Bayat, Gregor Bein, Yongshui Fu, Sentot Santoso. Anti-CD36 antibodies induced endothelial disturbance via activation of PBMC: evidence of crucial epitope(s)? (ISBT oral presentation) Vox Sanguinis. 2020, 115 (Supplement 1). The 36th International Congress of the ISBT, Barcelona, Spain, 12.-16. December 2020.

2. **Dawei Chen (first author)**, Xin Ye, Wenjie Xia, and Xiuzhang Xu. The immunological analysis for one case of foetus with anaemia and thrombocytopenia caused by anti-CD36 antibodies. (ISBT poster) Vox Sanguinis. 2017, 112 (Supplement 2). The 28th Regional Congress of the ISBT, Guangzhou, China, 25.-28. November 2017.

10. EHRENWÖRTLICHE ERKLÄRUNG

“I hereby declare that I have completed this work independently and without inadmissible assistance or the use of other than the resources quoted. All texts that have been quoted verbatim or by analogy from published and non-published writings and all details based on verbal information have been identified as such. In the analyses that I have conducted and to which I refer in this thesis, I have followed the principles of good scientific practice, as stated in the Statute of Justus Liebig University Giessen for Ensuring Good Scientific Practice, as well as ethical principles and those governing data protection and animal welfare. I give my assurance that third parties have not received from me, either directly or indirectly, any financial remuneration for work in connection with the content of this doctoral thesis and that the work presented has not been submitted in the same or a similar form to another assessment authority in Germany or elsewhere for the purpose of being awarded a doctorate or another assessment procedure. All material taken from other sources and other persons and used in this thesis or to which direct reference is made has been identified as such. In particular, all those who took part directly and indirectly in the production of this study have been named. I agree to my thesis being subjected to scrutiny by plagiarism detection software or by an internet-based software programme.”

Giessen, den

_____

Dawei Chen